Title
The Transcriptional Response to Tumorigenic Polarity Loss in Drosophila melanogaster

Author
Bunker, Brandon

Publication Date
2013

Peer reviewed|Thesis/dissertation

The Transcriptional Response to Tumorigenic Polarity Loss in *Drosophila melanogaster*

by

Brandon David Bunker

A dissertation submitted in partial satisfaction of the

requirements for the degree of

Doctor of Philosophy

in

Molecular and Cell Biology

in the

Graduate Division

of the

University of California, Berkeley

Committee in charge:

Professor David Bilder, Chair
Professor Iswar Hariharan
Professor Gary Karpen
Professor Zinmay Sung

Fall 2013

The Transcriptional Response to Tumorigenic Polarity Loss in *Drosophila melanogaster*

by

Brandon David Bunker

Abstract

The Transcriptional Response to Tumorigenic Polarity Loss in *Drosophila melanogaster*

by

Brandon David Bunker

Doctor of Philosophy in Molecular and Cell Biology

University of California, Berkeley

Professor David Bilder, Chair

Epithelia provide the fundamental building block for nearly all Eumetazoan organs. These tissues provide a barrier between the organism and its surroundings, facilitating absorption and secretion of necessary macromolecules, while protecting the animal from harm. To perform these functions, epithelia polarize along their apicobasal axis, forming an apical domain that faces the environment or lumen, and a basal domain that attaches to the extracellular matrix. Maintenance of apicobasal polarity is critical for normal organ function, and defective architecture has been linked to disease. Most importantly, loss of tissue polarity is associated with increased malignancy of human tumors. However, the mechanisms coupling epithelial polarity to the suppression of tumor formation are unknown.

The identification of regulators of epithelial architecture revealed that the core apical and basolateral determinants are evolutionarily conserved. Thus, the epithelial tissues of Drosophila provide a genetically tractable model for studying the relationship between polarity and tumor suppression. In Drosophila epithelia, disruption of apical membrane regulators leads to cell death, while mutation of basolateral determinants gives rise to the strikingly opposite phenotype: the formation of massively overproliferating apolar tumors that fail to differentiate and exhibit increased metastatic potential. Due to these cancer-like phenotypes, genes encoding the basolateral regulators have been termed neoplastic tumor suppressor genes (nTSGs). Although these data demonstrate an intimate link between polarity and proliferation control, it remains mysterious how disorganization at the plasma membrane leads to the downstream transcriptional changes required for neoplastic tumor formation.

Studies of nTSG mutant tissue have identified several signaling pathways activated upon polarity loss. In Chapter 1, I review the recent findings implicating these pathways and their known downstream transcriptional targets to tumor formation. Specifically, I highlight the roles of the stress-activated Jun kinase (JNK) cascade, the apical regulator, atypical Protein Kinase C (aPKC), and the tumor suppressive Hippo (Hpo) pathway in neoplastic overgrowth. In addition, I discuss the controversies surrounding how these pathways interact to modulate downstream transcription.

A key unanswered question that follows from these findings is: how is polarity status at the plasma membrane transduced into expression alterations of oncogenic target genes in the nucleus? To address this outstanding issue, in Chapter 2, I analyze the gene expression profile of

neoplastic tumors and identify transcriptional signatures of neoplasia as well as specific functional targets mediating overproliferation. To assess the interactions of downstream pathways driving transcription, I isolate a polarity-responsive enhancer element at a functionally important locus and evaluate its response to aPKC, JNK and Hpo signaling. My results demonstrate that, although JNK is necessary for neoplastic tumor formation, aPKC is a key mediator of gene expression alterations, via the Hpo pathway transcription factor Yorkie. These findings provide a model for how polarity-sensitive signaling pathways synergize to activate mitogenic target genes, leading to tumor formation.

In Chapter 3, I demonstrate additional regulation of polarity-responsive enhancer elements by the chromatin-modifying Polycomb Group genes, a recently identified TSG class. Further, I use molecular, genetic, and genomic approaches to evaluate the inter-relationship between the polarity-regulating and chromatin-modifying TSGs in modulating downstream target expression. Based upon my findings, I propose a model where misregulation of chromatin-modifying TSGs upon polarity loss potentiates target enhancers for activation by the polarity-responsive signaling pathways.

Taken together, my thesis work reveals that polarity loss triggers architecture disruption, the activation of stress signaling, dedifferentiation, and mitogenic gene expression. Interestingly, these responses, including PcG-mediated transcriptional derepression, are similarly elicited upon epithelial damage, such as wounding. After a wound response, however, the epithelium is repaired, and these signals are abrogated to maintain homeostasis. In contrast, epithelial integrity is never restored in polarity-deficient tissues and these signals persist, leading to the formation of a neoplastic tumor. These data suggest that Drosophila tumors behave like ‘wounds that never heal’, paralleling previously described models of human tumors.

Table of Contents

List of Figures

List of Tables

Acknowledgements

First, I would like to thank my advisor, David Bilder, for all of his support during my thesis research. His excitement about my work was truly motivating, and I am especially appreciative of his willingness to make time for me. He has always been a patient and kind teacher, molding me into a better writer and scientist. I am grateful to have worked with such a passionate mentor. I would also like to recognize my committee members—Iswar Hariharan, Gary Karpen, and Renee Sung—for asking insightful questions, challenging my assumptions, and providing valuable feedback during each committee meeting.

Thanks to all of my wonderful collaborators, especially Tittu Nellimoottil, Justin Dalton, and Michelle Arbeitmann for help with the transcriptome experiments and data analysis. Your thoughtfulness and genuine care regarding my project was truly appreciated, and was critical for its success. I am also grateful to Carl Thummel and Huiqi Jiang for sharing valuable advice and reagents.

To all of the members of the Bilder lab past and present- Saori Haigo, Sarah Windler, Holly Morrison, Thomas Vaccari, Lin Yuan, Josh Schoenfeld, Xinghua Li, Lucy O'Brien, Katherine Smith, Dong-Yuan Chen, Justin Crest, Lupe Coy- thanks for making the lab such a fun and stimulating place to do science. It was truly great to work with such a smart and motivated group of researchers. I want to extend a special thanks to Alejandra Figueroa-Clarevega, Geert de Vreede, and Lara Skwarek- the 'tumor team'- for all of their thoughtful advice on my project during many, many group meetings. I am especially grateful to Anne Classen for being such a great mentor during my first few years in the lab. Her support was invaluable during those early days- I appreciate everything she taught me about becoming a successful scientist.

To Charles Rock, for taking a chance and giving me my first job in a research lab as a college freshman. To Jean Cook, for inspiring me about basic research and encouraging me to pursue a PhD at Berkeley. To the members of the Cook lab, especially Elizabeth Dorn, Jonathan Hall, and Kathleen Nevis, thanks for being such amazing co-workers and teaching me what graduate school is all about.

Finally, I want to thank all of my friends, especially Elena Bekerman, John Young, and Jakob von Moltke, for reminding me there is a life outside of the lab. Thanks also to my family for always providing prospective and support. You guys are the best and I love you very much. And most importantly, I want to thank Lara- meeting you has made this whole thing worth it.

Chapter 1

Introduction

Epithelial tissues and apicobasal polarity

Epithelial tissues

To support life, organs and tissues must develop to an appropriate size and a distinctive organization. How individual cells coordinate their architecture and proliferation in order to form a functional tissue is a central unresolved question in biology. The relationship between these processes has been explored most thoroughly in epithelia, a simple tissue type that serves as the foundation for nearly all animal organs. An epithelium consists of a tightly packed arrangement of cells whose main function is to provide a barrier between an organism and its surroundings. This barrier role allows the epithelium to protect the animal from environmental insults, while facilitating absorption and secretion of nutrients and other products in the surrounding milieu. Epithelial cells are categorized based on their morphology as cuboidal, columnar, or squamous, and form tissues comprised of a monolayered sheet ("simple epithelia"), or multiple layers ("stratified epithelia"). By combining these distinct cell architectures and tissue configurations, epithelia perform the essential functions necessary for the development of multicellular organisms, including the ability to take on various shapes and execute specialized tasks [1]. For example, epithelia make up the body of Cnidarians and the skin, lungs, and intestines of mammals. Because this ancient tissue type provides the fundamental building block of Eumetazoan body plans, epithelia provide a model in which to investigate the basic mechanisms that cells use to generate the myriad organs found throughout the animal kingdom.

Apicobasal polarity

One of the defining features of epithelia is their ability to polarize [2]. Specifically, epithelial cells display an anisotropic organization of macromolecules (lipids and proteins) and cellular components (cytoskeleton and organelles) along their apicobasal axis, perpendicular to the plane of the tissue. The apical domain typically faces outwardly towards the environment or lumen, while the basal domain is attached to a secreted extra-cellular matrix (ECM). The ability of epithelial cells to organize into functional tissues is dependent on the establishment and maintenance of apicobasal polarity: the apical domain is often specialized for absorption or secretion, while the basal domain regulates cell-ECM interactions [3]. Interestingly, elaboration on apicobasal polarity is seen in several cell types. For instance, neurons polarize to form an axon and cell body, which are optimized for sending and receiving signals, respectively [4].

To polarize, cells respond to cues typically mediated through cell-cell or cell-ECM contacts to distinguish 'contacting' versus 'free' surfaces [5]. Upon receiving these signals, cells produce an asymmetric distribution of different protein complexes along their apicobasal axis, creating distinct membrane domains [6]. At the sub-apical region, cell-cell contacts generate a band of adherens junctions, known as the zonula adherens (ZA), which generates a mechanical attachment between cells and provides a partition between the apical and basolateral membrane domains [7]. To inhibit paracellular transport, vertebrate epithelia create tight junctions, localized apically to the ZA, while the analogous structure in invertebrates, the septate junction (SJ), is basal to the ZA [8]. Apicobasal polarity is subsequently propagated throughout the cell via polarization of the cytoskeletal machinery and the regulation of protein trafficking [9, 10]. Through these inter-dependent signaling events, the entire cell, from proteins, mRNAs and lipids to cytoplasmic organelles becomes polarized. While this asymmetry is established and maintained within a single cell, it is also coordinated among neighboring cells to form a polarized epithelial sheet.

Apicobasal polarity regulators

The conserved and robust organization of epithelial tissue raises the question of how apicobasal polarity is controlled. To isolate the molecular regulators of apicobasal polarity, genetic screens were performed in Drosophila and *C. elegans* [11]. These studies identified two protein complexes, Par and Crumbs (Crb), necessary for the establishment of apical membrane identity. The Par complex consists of the scaffold proteins, Par3 (Bazooka (Baz) in Drosophila) and Par6, as well as atypical protein kinase C (aPKC) and the GTPase Cdc42. Both Baz and Par6 mediate protein-protein interactions through their PDZ domains, and primarily act to establish polarity by recruiting aPKC and its substrates to the apical membrane [12]. Once membrane-localized, aPKC kinase activity, stimulated by GTP-bound Cdc42, maintains apical domain identity in part by preventing accumulation of basal determinants [13]. In addition, aPKC activity ensures proper localization of the Crb complex, the second apical domain regulator. The Crb complex consists of the transmembrane protein, Crb, as well as the PDZ domain-containing scaffold proteins Stardust and PATJ [14]. Recruitment of the Crb complex to the apical domain reinforces Par complex activity and indirectly represses basolateral membrane regulators [8]. In the Drosophila embryonic epithelium, loss of either Crb or Par complex function leads to a dramatic reduction in apical domain size and defective AJ assembly, often followed by cell death [15, 16].

In order to form a polarized cell, the apical domain must be restricted to just a portion of the plasma membrane. That is the job of a diverse group of 'basolateral regulators'. The principal basolateral membrane determinant in epithelial cells is the Scribble (Scrib) module, which is composed of Scrib, Discs Large (Dlg), and Lethal Giant Larvae (Lgl). Like Sdt, PATJ, and Par3/6, the Scrib module components are scaffolds that mediate protein-protein interaction, albeit not only though PDZ domains (Dlg and Scrib), but also leucine-rich repeats (Scrib), as well as MAGUK (Dlg) and WD-40 domains (Lgl) [8]. In contrast to the Par complex members, none of the Scrib module proteins has discernable catalytic activity, and the mechanism through which they establish basal membrane identity is not entirely known. However, Scrib module components have been implicated in influencing protein transport. For example, Scrib module mutant epithelia have disrupted retromer trafficking, and mutations in the *S. cerevisiae* homologs of Lgl, *SRO7p* and *SRO77p*, display vesicle sorting defects [de Vreede and Bilder, unpublished], [17]. In addition, Lgl binding to aPKC has been shown to inhibit kinase activity [18]. Consistent with a role for the basolateral regulators in antagonizing apical identity, loss of Scrib module function leads to apical domain expansion at the expense of the basolateral membrane, and ectopic AJ formation [19].

Analysis of mammalian epithelial cells has revealed that the apical and basolateral membrane regulators are evolutionarily conserved, in both composition and polarized localization. Humans have homologous members of the Crb and Par membrane complexes at the apical domain, as well as orthologs of Dlg (DLG1-4), Scrib (hSCRIB1/DENSIN-180/ERBIN/ LANO), and Lgl (LGL1/2) at the basolateral membrane [8, 20]. Interestingly, though the functional redundancy of these genes has complicated analysis, their roles in polarity regulation are also conserved in mammals. Heterozygosity of SCRIB1 causes apical expansion and E-cadherin mislocalization in mouse prostate epithelia, though it has no effect on apicobasal polarity in intestine, lung, or bladder tissue [21]. The mammalian Crb complex is necessary for apical membrane establishment as well: Par complex components are required for apical domain formation in MDCK cells and loss of *CRB3* leads to polarity defects in mouse epithelia [22, 23]. Further

supporting a conserved function for these polarity regulators, expression of vertebrate orthologs of Dlg, Lgl, and Scrib can rescue the corresponding mutant phenotypes in Drosophila [24-26]. The high degree of conservation of apicobasal polarity regulators is consistent with their crucial role in maintaining proper tissue function.

Apicobasal polarity and tumorigenesis

Apicobasal polarity regulators and cancer

Intriguingly, studies of mammalian epithelial tumors have suggested a surprising additional role for apicobasal polarity regulators: the suppression of tumor formation. Though pathologists have long recognized the correlation between disorganized tissue architecture and increased malignancy in human epithelial tumors, recent work has shown that the molecular regulators of polarity are altered as well [27]. The Par complex component aPKC is overexpressed in breast, liver, and pancreatic tumors [28]. Strikingly, functional studies have implicated misregulation of aPKC in promoting Hedgehog signaling, which drives proliferation of basal cell carcinoma cells [29]. Consistent with their antagonistic roles in polarity regulation, apical and basolateral determinants appear to have opposite effects on tumorigenesis. For example, basolateral components are lost or mislocalized in several epithelial tumors, including breast, colon, and lung, and SCRIB and DLG are targeted for degradation by the human papillomavirus E6 oncoprotein [28, 30]. However, as yet, somatic mutations in any of the basolateral junctional scaffolds have not been identified in human tumor samples. Furthermore, given the complex nature of human tumors, which are driven by many factors, including genome instability and tumor-stromal interactions, the impact of polarity loss on tumorigenesis and the mechanisms coupling polarity defects to cancer progression remain unknown.

Apicobasal polarity and tumor formation in Drosophila

In light of the prevalence of architecture defects in human cancers, it is critical to understand the relationship between polarity loss and cell proliferation. Studying this connection in mammalian models is complicated due to the functional redundancy of mammalian polarity regulators. However, given the evolutionary conservation of both epithelial tissue and apicobasal polarity determinants, Drosophila provides a genetically tractable system to investigate these mechanisms. Interestingly, the role of polarity regulators in the control of cell proliferation is strikingly apparent in Drosophila epithelia: while disruption of apical determinants promotes cell death, mutation of any Scrib module component leads to the formation of tumors that harbor many characteristics of human cancers, including massive tissue overgrowth, apicobasal polarity loss, decreased cell differentiation, and increased invasive potential [8]. The analysis of these polarity-deficient tumors has revealed insights into the links between regulation of epithelial polarity and growth control.

Polarity and proliferation control in Drosophila

The tumor suppressive effects of Scrib module function are most unambiguous in the larval imaginal discs, epithelial tissues that act as the primordia of most adult structures, including the eye, legs and wings. During embryogenesis, imaginal discs are specified as groups of 20-50 cells. Throughout the larval stage, wild-type imaginal cells proliferate until reaching a population of ~50,000, in the wing disc for example, when they stop dividing as the larvae undergoes pupariation [8]. In contrast, Scrib module mutant imaginal disc cells overgrow as they lose polarity, eventually forming massive tumors comprised of over 5 times as many cells as

a wild-type disc [31]. Intriguingly, analysis of these tumorous imaginal discs revealed unexpected growth kinetics: polarity-deficient tumors do not arise due to increased growth or faster cell proliferation. In contrast, Scrib module mutant cells divide more slowly than wild-type; tumors form because these cells never stop proliferating [32]. This growth property results in the seemingly paradoxical behavior of homozygous Scrib tissues as compared to Scrib mutant clones generated in a wild-type background. Scrib module mutant tumors can be serially transplanted into the abdomen of adult flies and maintained indefinitely [8]. However, Scrib module mutant cells surrounded by wild-type tissue undergo apoptosis due to cell competition, a process that eliminates many types of slow-growing cells and may reflect an ancient tumor-suppressive mechanism [33].

In addition to polarity loss and overgrowth, Scrib module mutant tissues display dramatic architectural defects. Specifically, Scrib module mutant cells pile atop each other to generate round, multilayered tumors; by comparison, wild-type cells form a well-organized monolayered sheet. Recent work has attributed the multilayering phenotype to misorientation of the mitotic spindle upon polarity disruption [34]. Strikingly, cancerous breast epithelia in 3D culture display similar architecture defects [35].

During human cancer progression, tumor cells metastasize to neighboring tissues and seed secondary sites, which ultimately causes mortality. Scrib module mutant tumors display a similar malignant capacity. For example, polarity-deficient tumors transplanted into adult flies invade nearby organs, where they form secondary tumors and kill the animal [36]. Invasive behavior also is observed within Scrib module mutant larvae: adjacent tumorous thorasic imaginal discs (comprised of the wing, leg, and haltere tissues) often fuse into a single tumor. In addition to increased metastasis, Scrib module mutant tumors fail to undergo terminal differentiation; transcription factors involved in cell differentiation and segment specification are downregulated upon polarity loss [this work]. A recent report demonstrated that re-expression of differentiation-promoting genes suppressed the tumorigenic phenotype of *lgl* tissues, suggesting an oncogenic role for the de-differentiation of neoplastic cells [37].

Beyond the tissue-autonomous phenotypes described above, recent studies have demonstrated that Drosophila tumors elicit systemic alterations in the host, including metabolic changes and activation of the immune response. For example, Drosophila immune cells (hemocytes) are recruited to Scrib module mutant tumors upon degradation of the basement membrane [38]. Intriguingly, these tumor-localized hemocytes have been implicated in reducing tumor growth, an extrinsic tumor suppression mechanism that parallels the 'tumor immune surveillance' reported in mammals [39, 40]. Further work demonstrated that expression of Eiger, the Drosophila TNFα homolog, by the hemocytes promotes apoptosis of polarity-deficient cells, restricting tumor growth [41]. In mammalian systems, loss of TNFα increases the susceptibility of mice to chemical-induced carcinoma, suggesting that common regulators mediate tumor immune surveillance in Drosophila and humans [42]. In addition to stimulating an immune response, Scrib module mutant tumors transplanted into adult flies disrupt homeostatic metabolic processes, leading to a degradation of host tissues [Figueroa-Clarevega, A Bilder D, unpublished]. This response strongly resembles cachexia, a 'muscle-wasting' phenotype observed in human cancer patients [43].

Taken together, these 'malignant-like' phenotypes have led researchers to classify the genes encoding the basolateral junctional scaffolds as "neoplastic tumor suppressor genes" (nTSGs) [32]. Further supporting the relevance of Drosophila tumor models to human cancers, several

groups have performed cancer drug screenings using Drosophila tumor models [44, 45]. Interestingly, a recent study demonstrated that acivicin, a compound with known activity against human tumors, restricts the growth of polarity-deficient Drosophila tissues. This work also demonstrated that growth of Drosophila tumors is glutamine-dependent, a trait previously noted in many human cancers [44, 46]. Despite these similarities, it is also important to recognize that certain traits of human tumors cannot be modeled in Drosophila. For instance, Drosophila tumors arise from a single mutation and do not exhibit genome instability. Furthermore, Drosophila has an open circulatory system (and therefore does not undergo angiogenesis) and does not have a gene encoding telomerase [8].

Although the existence of nTSGs suggests that tissue polarity and proliferation control are linked, the causal relationships between these properties of epithelial cells and if they are uncoupled by the Scrib module have only recently been investigated. The discovery that Scrib module mutant embryonic tissues lose apicobasal polarity without altering proliferation, along with the conserved polarity roles in other animals, suggest that the core function of the Scrib module is to regulate polarity rather than proliferation [7, 13]. Moreover, studies of an allelic series of *scrib* mutations suggest that polarity and proliferation control are indeed coupled in the imaginal disc; *scrib* tissues with weaker polarity defects exhibited correspondingly milder overproliferation [31].

The question of whether polarity loss is a cause or consequence of overproliferation is also addressed by analyses of the hyperplastic TSGs, genes whose loss of function leads to massive overproliferation without affecting apicobasal polarity [32]. Included among this class of TSGs are Hippo pathway components. The Hippo pathway is an evolutionarily conserved signaling cascade activated by a variety of inputs, including the protocadherin *Fat*, leading to the phosphorylation of the Sterile20-kinase Hippo (Hpo), and subsequent activation of its substrate, the Nuclear Dbf2-related kinase Warts (Wts). Upon stimulation, Wts phosphorylates the transcription factor Yorkie (Yki), sequestering it in the cytoplasm. Downregulation of upstream pathway components, such as *hpo* or *wts*, allows Yki to translocate into the nucleus and stimulate the expression of pro-growth targets [47]. Intriguingly, ectopic Yki activity leads to the formation of tumors that overgrow dramatically, but retain apicobasal polarity, tissue integrity and the ability to differentiate [32]. The observation that hyperplastic TSG mutant tissues overproliferate, but retain proper architecture and cell fate demonstrates that polarity loss is not an inevitable consequence of overgrowth. Taken together, these data implicate polarity loss as the primary driver of the malignant phenotypes in Scrib module mutant tissues.

The fact that loss of a single apicobasal polarity regulator leads to such manifold tissue- and organism-level phenotypes suggests that polarity is intimately linked to cell signaling modules that impact transcription. Indeed, tissue growth, differentiation, and invasion involve alterations in gene expression. Given the evolutionary conservation of apicobasal polarity regulators, studies of Drosophila nTSGs and their links to cell signaling have potential to reveal mechanisms coupling polarity and tumorigenesis in human epithelia.

Polarity-responsive signaling pathways

With these all of these data in mind, there has been great interest in identifying effectors connecting polarity loss to oncogenic transcriptional changes. Below, I will review the data implicating two such signaling mediators: the Jun kinase (JNK) cascade and aPKC signaling.

Specifically, I will highlight their contributions to the neoplastic phenotype as well as controversies and open questions surrounding their respective roles.

Jun Kinase signaling

In Drosophila, loss of apicobasal polarity can trigger the stress-responsive JNK pathway, an evolutionarily conserved canonical MAP kinase cascade. In both mammalian and Drosophila tissues, JNK signaling is stimulated primarily by stress, such as tissue damage, as well as by pro-inflammatory cytokines such as TNFα (Eiger in Drosophila) [48, 49]. Although JNK phosphorylates several substrates, its effects are primarily mediated through the heterodimeric transcription factor AP-1 (c-Jun/Fos; Jra/Kayak, in Drosophila), which modifies expression of specific target genes [50]. JNK signaling has been implicated in many processes throughout mammalian development; however, the functional redundancy of the three genes encoding JNK has complicated analysis [51]. Conversely, Drosophila possesses a single JNK, Basket (Bsk), allowing for straightforward dissection of the physiological roles of pathway activity [52]. In Drosophila, JNK activity has been implicated in several tissue morphogenetic events, including dorsal closure of the embryo and imaginal disc eversion, as well as cell proliferation and apoptosis [49, 53]. The capacity of JNK signaling to promote proliferation, apoptosis, and cell migration- all of which are observed in polarity-deficient tissues- suggested that JNK is a key mediator of neoplasia upon Scrib module loss.

JNK signaling and proliferation of Scrib module mutant tissues

Intriguingly, studies of JNK activity in polarity-deficient tissues have demonstrated that it can have both growth-promoting and growth-suppressing functions, in a context-dependent manner. For example, activation of JNK in Scrib clones generated in a wild-type background promotes apoptosis and clone elimination by cell competition. In this context, blocking JNK activity prevents cell death, allowing clones to overgrow and ultimately kill the animal [33, 54, 55]. The ability of wild-type cells to use JNK to drive apoptosis of potentially tumorigenic Scrib module mutant cells has been suggested to be an intrinsic tumor suppressor mechanism in Drosophila epithelial tissue [53]. Interestingly, a similar role for JNK has been reported in mammalian tumors; JNK signaling suppresses chemical-induced hepatocellular carcinoma in a mice [56].

However, oncogenic roles for JNK activity have also been observed in both Drosophila and mammalian epithelia. For instance, in mice, JNK activation is required for *Ras*-induced lung adenoma formation [57]. In a similar model of oncogenic cooperativity in Drosophila, expression of an activated form of *Ras* (Ras^{V12}) in *scrib* clones prevents apoptotic elimination and leads to the formation of metastatic tumors [54, 58]. Interestingly, inhibiting JNK activity in these clones significantly reduces tumor growth, suggesting that the coordination of Ras^{V12} and *scrib* is mediated by JNK [54]. Indeed, co-activation of JNK and Ras drives overgrowth similar to that observed in *scrib*/Ras^{V12} clones [54]. Furthermore, subsequent reports have implicated JNK signaling in the oncogenic cooperation of activated Ras with different forms of cellular stress, including mitochondrial damage and tissue wounding [59, 60].

Strikingly, recent data have demonstrated that inhibiting JNK activity completely suppresses the overgrowth of homozygous Scrib module mutant tissues, restoring them to wild-type size [59]. However, the mechanism through which JNK promotes overproliferation remains controversial. Most recently, JNK signaling has been linked to downregulation of the Hpo pathway. According to these findings, direct phosphorylation of Ajuba LIM protein (Jub) by

JNK increases binding of Jub and Wts, facilitating nuclear import of Yki and tissue growth [61]. However, a separate report has implicated AP-1-driven transcriptional activity in the overproliferation of *lgl* tissues [62]. Clarifying the roles of AP-1 and Yki in the transcriptional upregulation of target genes downstream of JNK will elucidate mechanisms coupling polarity and proliferation control.

JNK signaling and additional neoplastic phenotypes

Beyond driving proliferation or cell death, JNK activation has been implicated in additional phenotypes of neoplastic tumors. The invasive phenotype of polarity-deficient tissues has been most robustly studied in *scrib/Ras^{V12}* clones in the eye imaginal disc [54, 58]. These clones form malignant tumors that have the ability to migrate into neighboring tissues, such as the brain lobes and ventral nerve cord. Blocking JNK in these clones completely suppresses this invasive behavior. Strikingly, co-activation of *Ras^{V12}* and the JNK kinase *hep* in eye discs clones is sufficient for metastasis [58]. Importantly, the invasion-promoting role of JNK is separable from its role in driving growth; reducing the size of *scrib/Ras^{V12}* tumors does not block invasion [54, 58]. Instead, JNK activity is necessary and sufficient for the transcriptional upregulation of the pro-invasion genes, *Matrix metalloprotease 1* (*Mmp1*) *and Paxillin* (*Pax*), upon polarity loss [33, 58].

In addition to promoting invasion, Mmp1-mediated degradation of the basement membrane attracts hemocytes to the tumor, generating a host immune response. Hemocyte recruitment restricts Scrib module mutant tumor growth at least in part by promoting the apoptotic elimination of polarity-deficient cells [41]. Inhibiting JNK (and upregulation of its downstream targets) in Scrib module mutant tissues prevents localization of hemocytes to the tumor, blocking the immune response [38, 41].

Activation of immune cells is not the only systemic response induced by Scrib module mutant tumors; larvae hosting neoplastic tissues also undergo a delay in developmental progression. Recent work demonstrated that the delay is mediated by upregulation of *insulin-like peptide 8* (*dilp8*), which encodes a secreted factor that acts in the brain to prevent synthesis of ecdysone, the hormone that signals developmental progression [63, 64]. JNK is required for *dilp8* expression upon polarity loss, suggesting that JNK activation promotes *dilp8* upregulation in Scrib module mutant tissues, extending larval development [63]. However, developmental delay is observed in larvae harboring tumors that do not upregulate JNK, and *dilp8* expression during normal larval progression in JNK-independent, indicating that there are multiple ways to activate *dilp8* expression [32, 63].

aPKC in Drosophila and mammals

Although JNK signaling is involved in many of the malignant properties of polarity-deficient tissues, activation of JNK is not sufficient to phenocopy loss of Scrib module function. In fact, JNK activation alone drives apoptosis [65]. These data suggest that additional growth-promoting factors are misregulated upon polarity loss. One such effector that is activated in polarity-deficient tissues, but not upon ectopic JNK signaling, is the apical determinant aPKC. Direct targets of aPKC activity include substrates implicated in polarity regulation, such as Crb and Baz [66]. Intriguingly, some evidence suggests that aPKC affects proliferation through its role as a polarity regulator. For example, aPKC promotes asymmetric cell division in Drosophila neuroblasts by directly phosphorylating the differentiation-promoting factors Numb and Miranda, removing them from the apical cortex [67, 68]. Ectopic aPKC activation leads to

symmetric division, and the formation of neuroblast tumors [69]. However, despite its potent effects, in contrast to JNK, aPKC has not yet been shown to impinge upon a specific transcription factor to activate genes involved in growth, differentiation, and invasion.

aPKC signaling and tissue growth

aPKC acts as a potent growth promoter in epithelial tissues as well; overexpression of an activated form of aPKC is sufficient to promote neoplastic tumor formation in imaginal discs, phenocopying loss of Scrib module function [70]. Further, overgrowth of Scrib module mutant tissue is aPKC-dependent [71]. Although aPKC misregulation is necessary and sufficient for overproliferation of Scrib module mutant imaginal discs, the mechanism through which aPKC triggers overgrowth remains controversial. Unlike the neuroblasts, Drosophila imaginal discs cells undergo symmetric divisions; each daughter cell has equal proliferative capacity [72]. Therefore, the improper segregation of differentiation factors is unlikely to mediate overgrowth downstream of aPKC.

Recent work has implicated JNK signaling in the proliferative response downstream of aPKC: inhibiting JNK rescues the overgrowth of wing discs expressing a wild-type, membrane-bound form of aPKC [73]. In contrast to these findings, however, other data suggest a JNK-independent role for aPKC in promoting growth. JNK inhibition is unable to suppress overproliferation of eye imaginal disc cells expressing a truncated, constitutively active form of aPKC [74]. In contrast, however, reducing Yki activity in these clones restores normal tissue size, supporting a role for aPKC misregulation in downregulating Hpo signaling. Intriguingly, many upstream Hpo pathway regulators are enriched along the apical membrane, suggesting that aPKC activation directly impinges upon Hpo components. In support of this possibility, ectopic aPKC activity in the eye disc leads to co-mislocalization of Hpo and its negative regulator RASSF, promoting Yki activation and overgrowth [75]. In addition, gain of Crb function increases Yki-mediated transcriptional activity via mislocalization of Expanded, a positive regulator of Hpo [76]. Taken together, these data demonstrate that aPKC misregulation affects Hpo signaling; however, how the integrated inputs of aPKC, JNK and Yki signaling mediate the downstream transcriptional changes leading to neoplasia upon polarity loss is unknown.

Determining how polarity loss triggers transcriptional changes driving neoplasia

Although much progress has been made in identifying the signaling modules coupling polarity disruption and tumorigenesis, the downstream targets of these regulators, and how these signaling pathways interact to generate a tumor remains unclear. In the following chapters, I address these questions, clarifying the mechanisms coupling polarity loss to the direct transcriptional targets driving neoplasia. In Chapter 2, I perform gene expression analysis on Scrib module mutant tissues to identify targets mediating tumor formation. To address how polarity-responsive pathways synergize to promote mitogenic gene expression, I assess the transcriptional activation of a growth-promoting target by JNK, aPKC, and Yki signaling. In Chapter 3, I evaluate the interaction between the Scrib module and the chromatin-modifying Polycomb Group (PcG) genes, a recently identified class of TSG. Functional and molecular analyses reveal coordination between the PcGs and the Scrib module in the transcriptional regulation of common targets. Taken together, the data presented here elucidate the mechanisms linking disruption of tissue polarity to oncogenic gene expression changes.

Chapter 2

Mechanisms linking apicobasal polarity and the transcriptional control of tissue growth

ABSTRACT

Loss of polarity correlates with disease progression in epithelial cancers, but how misorganization at the plasma membrane drives oncogenic transcriptional events remains unclear. The core apicobasal polarity regulators of the Drosophila Scribble (Scrib) module are potent tumor suppressors and provide a model to investigate these mechanisms. RNA profiling of Scrib module mutant tumors reveals multiple signatures of neoplasia, including increased oxidative stress and activated immune response. Prominent amongst these alterations is upregulation of the cytokine-like Unpaired (Upd) family of ligands, which drive JAK-STAT pathway activity and tumor overgrowth. To identify signaling events connecting polarity loss to gene expression changes, we analyzed *upd3 cis*-regulatory elements and uncovered a polarity-responsive enhancer, whose activation is Jun kinase (JNK)-dependent. Though JNK signaling alone weakly stimulates the enhancer, our data implicate aPKC misregulation in driving stronger enhancer activation and overgrowth upon Scrib module loss. Ectopic aPKC activity is sufficient for enhancer expression and neoplasia independently of JNK, but requires activated Yorkie. Taken together, our results identify polarity-responsive transcriptional targets and link JNK signaling and aPKC misregulation to activation of a polarity-responsive enhancer, elucidating a pathway coupling polarity loss to mitogenic gene expression.

INTRODUCTION

Maintenance of apicobasal polarity is essential for the proper function of epithelial tissues. To polarize, epithelial cells establish an anisotropic distribution of protein complexes along the apical and basolateral membrane domains in response to extracellular signals [77]. This asymmetry is not only coordinated throughout a cell, but also across neighboring cells to form a polarized tissue [3]. In an epithelium, the apical domain typically faces outwardly towards the environment or lumen, while the basal domain is attached to a secreted extracellular matrix. Specialization of the apical and basolateral membranes allows the tissue to perform specific tasks. For example, receptors for nutrient uptake localize preferentially to the apical surface of intestinal epithelia [78].

In human cancers, progressive deterioration of epithelial polarity is associated with increased malignancy [79], [80]. Polarity defects are reflected in the altered expression of apicobasal polarity regulators. For example, the apical determinant atypical protein kinase C (aPKC) is overexpressed in multiple cancers [81]. Further, basolateral factors such as Scribble (Scrib) and Discs Large (Dlg) are targeted for degradation by the E6 viral oncoprotein and lost or mislocalized in several tumor types [8, 81]. While polarity disruption correlates with poor clinical prognosis, it remains unclear how proper regulation of tissue polarity suppresses tumorigenesis.

The core regulators of epithelial polarity are well-conserved, facilitating study of mechanisms coupling polarity and growth control in genetically tractable organisms. In Drosophila, the basolateral domain is established by the Scrib module, a junctional scaffold consisting of Scrib, Dlg, and Lethal Giant Larvae (Lgl). At the apical membrane, aPKC interacts with Par6, and Par3 (Drosophila Bazooka; (Baz)) to form the Par complex, the principal apical membrane determinant [12]. Reciprocal antagonistic interactions between the apical and basolateral membrane regulators maintain tissue polarity [8, 82]. Decreased Par complex activity leads to apical membrane loss, while mutations in members of the Scrib module cause expansion of the apical domain at the expense of basolateral identity [15, 19].

Strikingly, disruption of apical and basolateral regulators not only has opposite effects on epithelial polarity, but also cell proliferation. Although mutations of Par complex members promote cell death, loss of Scrib module function leads to dramatic overgrowth and tumor formation [32]. The oncogenic effects of polarity disruption are most evident in the larval imaginal discs, epithelial tissues that serve as precursors to adult structures such as the eye, wing, and leg. Remarkably, the phenotypes of Scrib module mutant tissues strongly resemble those of human cancers. For example, while wild-type epithelia organize into a monolayered sheet, apolar Scrib module mutant tissues form a multilayered and rounded tumor. These polarity-deficient tissues exhibit massive overproliferation, comprising more than 5 times as many cells as wild-type discs. Furthermore, tissues lacking Scrib module function exhibit metastatic potential; tumors transplanted into adult flies invade surrounding tissues, killing the animal [8]. As observed in human cancers, Drosophila tumors elicit systemic responses in the host, including activation of the immune system and alterations of metabolic and developmental programs [38, 44, 63, 64]. Due to these malignant-like mutant phenotypes, the genes encoding basolateral determinants have been classified as neoplastic tumor suppressor genes (nTSGs).

What signaling pathways link polarity disruption to tumor formation? Recent work has implicated the Jun kinase (JNK) cascade in mediating neoplasia upon polarity loss [59, 73].

Activation of JNK signaling can drive transcriptional up-regulation of several tumor-promoting target genes, while blocking JNK signaling can ameliorate the phenotypes of neoplastic tumors [38, 58, 70, 73]. However, other observations indicate that the effect of JNK signaling on the growth of polarity-deficient cells is more complex. In Scrib module mutant clones generated in a wild-type background, JNK activation leads to apoptotic elimination, while inhibiting JNK activity causes tumor formation [33, 54]. Determining how JNK signaling acts as either a tumor-promoter or tumor-suppressor in a context-dependent manner remains unresolved.

Intriguingly, ectopic activation of JNK signaling drives apoptosis, rather than tumor formation, suggesting that additional polarity-responsive signaling effectors promote tumorigenesis upon polarity loss. Indeed, aPKC misregulation is necessary and sufficient for tumor formation upon Scrib module loss [70, 71]. However, the mechanism through which aPKC activity at the membrane precipitates downstream signaling events that drive tumor formation remains controversial. Although some reports have suggested that tumorigenic effects of aPKC are mediated by JNK, others indicate that aPKC acts independently [73, 74]. Overproliferation of polarity-deficient cells has also been attributed to downregulation of Hippo (Hpo) signaling, another Drosophila tumor suppressor pathway [73, 74]. Misregulation of the Hpo pathway leads to the formation of hyperplastic tumors: mutant tissues overgrow dramatically, but retain polarity, tissue integrity, and the ability to differentiate [32]. Strikingly, although the Hpo pathway is disrupted upon polarity loss, how its activity integrates with JNK signaling to effect gene expression changes that gives rise to a neoplastic tumor is unclear.

Thus, although several signaling cascades silenced by maintenance of epithelial polarity have been identified, the overall downstream transcriptional targets of these pathways whose misregulation leads to tumor formation remain unknown. Further, how these disparate effector pathways interact to drive transcriptional change at any of these targets remains unclear. Here we use RNA profiling to identify targets whose misregulation drives tumor formation downstream of polarity loss. We then use these data to untangle the signaling pathways connecting apicobasal polarity at the plasma membrane to gene expression changes in the nucleus.

RESULTS

Transcriptome analysis of neoplastic tumors

To identify genes that are transcriptionally misregulated upon loss of apicobasal polarity, we sequenced cDNA libraries generated from *white*^{1118}, *scrib*^{1}, and *dlg*$^{40\text{-}2}$ wing discs (Materials and Methods). To avoid influences of genetic background, we focused on genes that were differentially expressed in both *scrib* and *dlg* tumors. Our analysis revealed that 574 genes are misregulated at least twofold (FDR < 0.05), with 311 and 263 up- and downregulated, respectively (Figure 2.1A-B, Table 2.1-2.2).

Among the differentially expressed genes are tumor-promoting factors previously shown to be misregulated in neoplastic tissues. The highest upregulated gene, overexpressed >150-fold, is *dilp8*, which mediates the developmental delay of larvae hosting neoplastic tumors (Figure 2.2A). The invasion-promoting genes *Matrix Metalloprotease 1 (Mmp1)* and *Paxillin* are also upregulated. To further validate the sequencing data, we analyzed the expression of selected genes in *scrib* tissue by qRT-PCR and found close agreement with the RNA-Seq dataset (Figure 2.2B). From these results, we conclude that the transcriptome data accurately captures the expression profile of neoplastic tissues, and contains genes whose misregulation drives tumorigenesis upon polarity loss.

Stress response genes are upregulated upon polarity loss

We performed Gene Ontology (GO) analysis on the differentially expressed genes with GOstat (Figure 2.1 C,D) [83]. GO categories most prevalent in the downregulated genes are associated with organ and organism development, as well as cell differentiation, consistent with the known inability of *scrib* or *dlg* tissues to differentiate (Figure 2.1 D, Figure 2.2A) [8]. GO analysis of upregulated targets highlights genes involved in Response to Stimulus. Prominent amongst these genes are immune response factors, including the crystal cell determinant *lozenge* (*lz*) and *Serine protease 7* (*Sp7*), which promotes melanization after infection [84, 85]. The enrichment of immunity-related genes among the upregulated targets may be due to the presence of hemocytes, which are recruited to neoplastic tumors upon basement membrane degradation [38, 41].

Several additional genes within the Response to Stimulus cluster, including *Glutathione S transferase E1* (*GstE1)*, *CG7130*, and *virus induced RNA 1 (vir-1),* are known to be over-expressed upon oxidative stress. Further analysis revealed 19 polarity-sensitive targets that are also upregulated after hyperoxia treatment (Figure 2.3A) [86]. We treated *dlgIR*-expressing tissue with dihydroethidium (DHE), a fluorescent probe for superoxide anion (O_2^-), and found a distinctive positive signal, demonstrating increased oxidative stress (Figure 2.3B-C). To determine if oxidative stress contributes to the neoplastic phenotype, we co-expressed *dlgIR* with either *Superoxide dismutase 2* (*Sod2*), an O_2^- scavenger that transforms superoxide into hydrogen peroxide, or *Catalase (Cat)*, an antioxidant enzyme that converts hydrogen peroxide to water [87, 88]. However, neither *Sod2* nor *Cat* expression has a significant effect on tumor growth or architecture, relative to controls (Figure 2.3D-I). Taken together, these data demonstrate that polarity-deficient tissues have increased superoxide levels, but do not provide evidence for a functional role for oxidative stress in neoplastic overgrowth.

JAK-STAT pathway components are upregulated in neoplastic tumors

The only signaling pathway recognized among the top GO categories is the JAK-STAT cascade. Among the upregulated JAK-STAT genes are downstream targets, and a JAK-STAT reporter is strongly expressed in *scrib* and *dlg* discs, demonstrating high pathway activation (Figure 2.4A-C). Each of the three *unpaired* (*upd*) genes, which encode cytokine-like ligands for the JAK-STAT pathway, is also upregulated, ranging from ~3 fold (*upd)* to 20 fold (*upd3)* to 50 fold (*upd2)*. However, other JAK-STAT pathway components are normally expressed, suggesting that ectopic transcription of the *upd*s drives JAK-STAT activity downstream of polarity loss (Figure 2.4D). To assess the functional role of JAK-STAT activation in neoplastic overgrowth, we used *engrailed-GAL4* to express *SOCS36E*, a negative regulator of JAK-STAT activity, in the posterior compartment of tissue carrying a hypomorphic allele of *dlg* (*dlg*^{hf321}) [89, 90]. Reduction of JAK-STAT activity with SOCS36E decreases *dlg* tissue growth by 50%, while having no significant effect on normal growth (Figure 2.4E-I). Importantly, SOCS36E does not promote apoptosis in wild-type or *dlg* discs, indicating that the size decrease is not due to increased cell death (Figure 2.5). From these data, we conclude that the Scrib module regulates JAK-STAT signaling to suppress tumorous overgrowth.

A 1-kb fragment in the intron of *upd3* is responsive to polarity loss

A molecular mechanism linking polarity regulation to the transcriptional control of a growth target has not yet been defined. We therefore focused on transcription of *upd3*, a key growth regulator whose ectopic expression in several developmental contexts, including the adult midgut, can lead to increased cell proliferation [91]. To identify a *cis*-regulatory region responsive to polarity loss, we generated a LacZ reporter to analyze activation of a 3-kb *upd3* enhancer (*upd3LacZ*) in neoplastic tissue (Figure 2.6A). While *upd3LacZ* is not expressed in wild-type discs, as expected, it is distinctly upregulated in *dlg* tissue (Figure 2.6B-C). *upd3>GFP*, which contains an overlapping sequence, is highly expressed in *dlg* and *scrib* discs, confirming that this region is sensitive to the polarity status of the tissue (Figure 2.7C-E) [92].

To isolate the minimal polarity-responsive region in the *upd3* enhancer, we assayed 1-kb sub-fragments of *upd3LacZ* in *dlg* tissue (Figure 2.6A) [93]. Like *upd3LacZ*, none of the sub-fragments is expressed in wild-type wing discs (Figure 2.6D,F,H). However, though neither *upd3.1LacZ* nor *upd3.2LacZ* display consistent activation, *upd3.3LacZ* is significantly expressed in a patchy manner throughout *dlg* discs (Figure 2.6D-I). *Upd3.3LacZ* is similarly upregulated in *scrib* discs, demonstrating that this region is responsive to Scrib module function (Figure 2.10A,D) and thus identifying a *cis*-regulatory region through which Scrib module proteins suppress *upd3* transcription to prevent tumor formation.

JNK-dependent transcription is required for neoplasia

To identify molecular pathways linking Scrib module proteins to *upd3* expression, we scanned the *upd3.3* enhancer for transcription factor binding motifs using Vista Genome Browser [94]. This analysis identified two binding sites (TGANTCA) for AP-1, the Jun kinase (JNK) pathway transcription factor, which are evolutionarily conserved in *upd3* from other Drosophila species (Figure 2.8A-B) [95]. We tested whether JNK signaling is required for *upd3.3LacZ* activation. Expression of transgenic RNAi depleting *dlg* (*dlgIR)* in wing tissue causes overgrowth, loss of apicobasal polarity, and upregulation of the JNK target *Mmp1*, phenocopying loss of *dlg,* while co-expression of a dominant-negative form of Drosophila JNK,

basket (*bsk*^{DN}), blocks *dlgIR*-mediated overgrowth, polarity defects, and *Mmp1* expression, as previously reported (Figure 2.9, Figure 2.11A,B) [73]. Importantly, while *dlgIR* activates *upd3.3LacZ*, albeit with less penetrance than *dlg* null tissue, coexpression of *bsk*^{DN} completely abrogates reporter expression (Figure 2.9C,E). Mutation of the JNK kinase, *hemipterous* (*hep*) similarly prevents *upd3.3LacZ* upregulation in *scrib* tissue, confirming that canonical JNK signaling is necessary for *upd3* transcription downstream of polarity loss (Figure 2.10).

JNK has been suggested to regulate neoplastic tumor growth though phosphorylation of the downstream target, Ajuba LIM protein (Jub) [61]; however the presence of an AP-1 binding site within *upd3.3* suggests that JNK mediates *upd* transcriptional upregulation to promote overgrowth. To determine if the tumor-promoting effects of JNK signaling are driven by JNK kinase activity directly or alternatively, through activity of the AP-1 transcription regulator that it stimulates, we assayed discs co-expressing *dlgIR* and *fos*^{DN}, a dominant-negative form of the *fos* transcription factor [96]. Surprisingly, *fos*^{DN} expression phenocopies the tumor suppressive effects of *Bsk*^{DN}, including prevention of *upd3.3LacZ* expression (Figure 2.9, Figure 2.11A,C). From these results, we conclude that the mechanism through which polarity maintenance by the Scrib module suppresses tumor formation is JNK-dependent transcription.

JNK activation drives *upd3.3* activation and overgrowth but not polarity defects

Given that JNK activation is necessary for *upd3.3LacZ* expression and neoplastic overgrowth, is it sufficient? We expressed the JNK-activating ligand Eiger along with a microRNA targeting the pro-apoptotic genes *reaper*, *grim*, and *head involution defective* (*miRGH*) to block cell death [97]. When caspase activation is inhibited with *miRGH*, Eiger drives *upd3.3LacZ* expression, along with dramatic tissue overgrowth (Figure 2.12, Figure 2.11) [98]. However, polarity determinants aPKC and Dlg remain properly localized in *eiger/miRGH*-expressing tissues, indicating that JNK activation is not sufficient to promote neoplasia, in agreement with a previous observation (Figure 2.13) [73]. From these data, we conclude that ectopic JNK activity is sufficient to activate *upd3.3LacZ* expression and overgrowth, but not polarity defects.

aPKC drives *upd3.3* activation and neoplasia, independently of JNK

We noticed that, relative to *dlg* knockdown, expression of *eiger* and *miRGH* drives higher Mmp1 levels, but lower *upd3.3LacZ* expression (compare Figures 2.9F,J and 2.12F,I). This result suggests that Scrib module proteins regulate additional factors to suppress polarity-responsive transcription and tumor formation. Indeed, JNK activation alone promotes apoptosis; overgrowth is only observed when cell death is blocked, and cell death is not constitutively blocked in *dlg* mutant tissue (Figure 2.12, Figure 2.13). One factor misregulated upon loss of Scrib module function is aPKC. aPKC is not misregulated by JNK activation alone (compare Figure 2.9 and Figure 2.13), but is itself sufficient to drive neoplasia [70]. To investigate the role of aPKC in the transcriptional response to polarity loss, we expressed a constitutively active form of *aPKC* (*aPKC*$^{\Delta N}$) and found that it also activated *upd3.3LacZ* (Figure 2.14) [18]. *aPKC*$^{\Delta N}$ expression activates JNK targets (Figure 2.14D-E), raising the possibility that aPKC regulates *upd3* transcription through JNK. Strikingly, inhibiting JNK activity in *aPKC*$^{\Delta N}$-expressing tissues abrogates *Mmp1* expression, but does not prevent *upd3.3LacZ* activation, nor did it block overgrowth or polarity loss (Figure 2.14). Similar results were obtained upon co-expression of membrane-bound wild-type *aPKC* (*aPKC*^{CAAX}) along with its Par complex partner, *Par6*,

demonstrating that these results are not transgene-specific (Figure 2.15). From these data, we conclude that aPKC misregulation strongly promotes transcription of polarity-responsive targets and tumorigenesis, independently of JNK.

aPKC is required for overgrowth, but not *upd3.3* activation upon Scrib module loss

The above data suggest a pathway through which misregulation of aPKC downstream of JNK signaling triggers *upd3* transcription and tumor formation. To determine if aPKC mediates the downstream transcriptional response to polarity loss, we analyzed the effect of *aPKC* knockdown in *dlgIR*-expressing tissue. Reducing *aPKC* expression to levels that do not affect normal growth restores *dlgIR*-expressing discs nearly to wild-type size, as expected (Figure 2.14G-J, Figure 2.11D-I) [71]. Importantly, aPKC knockdown does not act by blocking JNK; Mmp1 is upregulated even upon *aPKCIR* expression (Figure 2.14I). Similar results were obtained upon *Baz* knockdown, showing that excess aPKC activity drives overgrowth upon loss of Scrib module function (Figure 2.16).

Strikingly, however, *aPKCIR* decreases, but does not completely eliminate, *upd3.3LacZ* expression (Figure 2.14H) in *dlgIR* tissue. Similarly, decreasing *aPKC* has no effect on *upd3.3LacZ* expression in discs co-expressing *eiger* and *miRGH* (Figure 2.17). These data suggest that JNK can drive aPKC-independent *upd3.3LacZ* upregulation, consistent with our previous data (Figure 2.12, Figure 2.13). We conclude that, while JNK signaling alone can activate *upd3.3*, aPKC misregulation downstream of JNK is the primary driver of *upd3.3* activation and overgrowth downstream of Scrib module loss.

Yki drives *upd3.3LacZ* activation and overgrowth downstream of aPKC

To determine how aPKC activity at the cell cortex drives transcriptional upregulation of *upd3*, we returned to our analysis of *upd3.3* enhancer sequences. Interestingly, we detected one partially conserved binding site (CATTCCA) for Scalloped (Sd), the DNA binding protein that recruits activated Yorkie (Yki) to downstream target genes (Figure 2.8A,C) [99]. To determine if activated Yki mediates the transcriptional response downstream of aPKC misregulation, we assessed *upd3.3LacZ* expression and tissue growth in discs co-expressing $aPKC^{\Delta N}$ and *ykiIR*. While *yki* knockdown under these conditions has a minimal effect on wild-type growth and survival, it completely abrogates both *upd3.3LacZ* expression and tumor formation upon ectopic *aPKC* activation (Figure 2.18, Figure 2.11N-O). Overexpression of *hpo* in *dlgIR*-expressing tissues also prevents *upd3.3LacZ* activation, indicating that aPKC acts through canonical Hpo signaling to stimulate Yki-dependent transcription (Figure 2.19). To determine if activated Yki is sufficient to stimulate the polarity-responsive *upd3.3* enhancer, we monitored *upd3.3LacZ* expression in wing discs expressing a constitutively active form of Yki (Yki^{S168A}). *upd3.3LacZ* expression is highly elevated in theYki^{S168A}-expressing tissues, which display massive overgrowth without affecting epithelial polarity [100]. These data support a model in which aPKC misregulation triggers Yki-medated *trans*-activation of the *upd3.3* enhancer, driving overgrowth downstream of Scrib module loss.

DISCUSSION

In this study, we use Scrib module mutant tissues to investigate the link between polarity misregulation and tumorigenesis. Expression profiling of Drosophila tumors reveals characteristic signatures of neoplasia, including failures of differentiation, increased oxidative stress, and activated immune response. Our data implicate the *upd* family of JAK-STAT pathway ligands as specific targets whose transcriptional upregulation triggers overgrowth upon polarity loss. To connect polarity defects to gene expression changes, we isolated a polarity-sensitive *cis*-regulatory region within the *upd3* enhancer, and interrogated its response to JNK and aPKC signaling. Although JNK-driven transcription is essential for enhancer upregulation, JNK alone only weakly stimulates the enhancer. Strikingly, our results implicate aPKC-mediated Yki activation in strong enhancer upregulation and overgrowth upon Scrib module loss. Taken together, our data demonstrate that polarity regulators modulate growth by suppressing JNK activation and aPKC signaling, which synergize upon polarity loss to drive high levels of *upd* transcription and tumor formation.

Transcriptional signatures of neoplasia

Transcriptome analysis of polarity-deficient tumors reveals distinct signs of cellular stress; genes involved in response to infection, hyperoxia, and starvation are differentially expressed. Several reports have shown that hemocytes are recruited to neoplastic tumors upon basement membrane degradation, where they proliferate upon exposure to tumor-secreted mitogens [38]. Consistent with these findings, we identify hemocyte-specific factors in the transcriptome. We attribute the presence of these factors to expression from tumor-associated hemocytes, rather than the tumor cells, though our data do not rule out the latter possibility. Interestingly, though plasmatocytes have been identified as the primary hemocyte population recruited to tumors, we also detect crystal cell markers in the gene expression dataset [38]. Although primarily involved in promoting melanization upon infection, crystal cells have also been implicated in wound repair, suggesting that the tumor triggers a tissue damage response within the host [101].

Recent work in Zebrafish and Drosophila embryos has demonstrated that recruitment of immune cells to epithelial wounds is promoted by greater production of the oxidizing agent, hydrogen peroxide (H_2O_2) [102, 103]. Although such a role for H_2O_2 has not yet been reported in the imaginal discs, genes involved in the oxidative stress response are highly upregulated in Scrib module tumors, and superoxide levels are dramatically increased. Further, we observe that JNK activity, which promotes hemocyte recruitment to the tumors, is essential for superoxide generation upon polarity loss (data not shown). Although our functional tests do not support a role for oxidative stress in tissue autonomous neoplastic phenotypes, these data hint at a possible role of oxidizing agents in driving the systemic responses to tumor formation, including hemocyte recruitment.

In addition to genes indicative of a wound response, the expression profile of polarity-deficient discs displays hallmarks of metabolic alterations, including starvation. For example, 28% of genes upregulated in Scrib module mutants are overexpressed in starved larvae (data not shown) [104]. Furthermore, Amino Acid transporters are among the top GO categories identified in the upregulated targets, suggestive of nutrient scavenging. Although the drivers of this starvation-like phenotype are unknown, one upregulated target gene that may contribute to this response is *ImpL2*, a secreted antagonist of insulin implicated in restricting tissue growth

[105]. Indeed, many starvation-response genes are under the control of FOXO, the transcriptional repressor downstream of insulin signaling [106]. Consistent with low insulin pathway activity in polarity-deficient tumors, the downstream FOXO target *Thor* is upregulated. Future work will assess the role of *ImpL2* in mediating nutrient-deprived gene expression signature and its overall effect on tumor growth.

Aside from starvation response genes, the Scrib module mutant transcriptome contains additional factors involved in altered metabolism. Most strikingly among these genes is *ImpL3*, the Drosophila *lactate dehydrogenase (LDH*) ortholog, which is upregulated >100-fold in *scrib* tissue. Previous work in mammalian tumors has implicated LDH in shunting pyrovate away from the Krebs cycle, leading to aerobic glycolysis and increased glucose import [107]. This metabolic alteration, known as the Warburg effect, contributes to macromolecule synthesis, promoting tumor growth [108]. Although no evidence of Warburg-like metabolism in Drosophila tumors has been reported, future work will investigate this possibility, as well as an understanding of the mechanisms linking tissue polarity to changes in cellular metabolism.

It is interesting to compare the Scrib module transcriptome that we have generated to the expression profiles of other types of Drosophila tumors. Interestingly, this analysis reveals that distinct tumor types display varying degrees of de-differentiation. For example, Hpo pathway mutant tumors do not exhibit differentiation defects; mutant tissues are capable of generating recognizable adult structures [32]. At the opposite extreme, *lethal (3) metastatic tumor* (*l(3)mbt*) brain tumors upregulate germline-specific genes and undergo a soma-to-germline transformation [32, 109]. Scrib module mutant tumors display a moderate degree of de-differentiation: they downregulate genes that specify positional cues, such as *vestigial* and *engrailed*, but do not acquire a new tissue identity. Taken together, these data demonstrate that, despite the phenotypic similarities of different tumors, in Drosophila, as in mammals, there is more than one route to malignancy.

Relationship of JNK and aPKC in promoting growth of Scrib module mutant tissue

Having identified downstream factors whose transcriptional misregulation drives tumor formation, we focused on determining the mechanisms through which these genes are activated upon polarity loss. Our analysis, along with others, points to the JNK pathway as a major mediator of polarity-responsive target activation. The RNA-Seq dataset includes many JNK-responsive target genes, such as *Mmp1*, the JNK phosphatase, *puckered* (*puc*) and *Ets at 21C* (*Ets21C*), and our data confirm previous work that suppression of JNK can revert almost all of the phenotypes associated with Scrib module loss. However, the mechanism through which JNK enacts its effects has been controversial. A recent report implicates JNK-mediated phosphorylation of Jub, a negative regulator of Hpo, in promoting overproliferation of *lgl* tissues [61]. In contrast, our data show that inhibiting AP-1 suppresses overgrowth, architecture defects, and activation of a polarity-responsive enhancer, consistent with observations in another report [62]. Therefore, though our data do not rule out a role for other targets of JNK kinase activity, we conclude that JNK signaling drives neoplasia upon Scrib module loss primarily through AP-1-dependent transcriptional activation.

Although JNK is necessary for neoplasia in Scrib module mutant tissues, our data suggest that aPKC acts downstream of JNK to promote tumor growth. This model is supported by three observations: 1) *aPKC* knockdown suppresses *dlg*-mediated overgrowth, even though JNK remains active, 2) ectopic aPKC activation promotes growth in a JNK-independent manner, and

3) inhibiting JNK restores normal apical localization of aPKC in *dlgIR*-expressing discs. Together, these data indicate that JNK activity promotes aPKC misregulation. The mechanism involved remains unknown, although the dependence of tumor growth on JNK-mediated transcription suggests that it is due to upregulation of an AP-1 target. Transcriptome analysis does not reveal overexpression of canonical apical polarity components; the relevant regulator lies amongst genes for future investigation using this dataset.

Our data demonstrate that aPKC misregulation drives overgrowth by impinging upon Hpo pathway activity, independently of JNK. These findings conflict with a recent report which suggested that aPKC modulates Yki activation through JNK [73]. Although our findings do not rule out a role for aPKC in stimulating JNK, the discrepancies between these results are likely due to the use of different aPKC activating constructs. Our study utilized $aPKC^{\Delta N}$, a truncated version of aPKC lacking the N-terminal regulatory domain, while the other work used $aPKC^{CAAX}$, a wild-type, membrane bound form of the protein [18, 73]. Significantly, we find that $aPKC^{CAAX}$ expression does not recapitulate Scrib module loss: $aPKC^{CAAX}$ leads to the formation of small tumors comprised primarily of apoptotic cells that fail to upregulate *upd3.3LacZ*. However, co-expression of $aPKC^{CAAX}$ and its Par complex partner *Par6* generate neoplastic tumors that activate *upd3.3LacZ*, phenocopying Scrib module mutations and $aPKC^{\Delta N}$ expression. Importantly, neoplasia and *upd3.3LacZ* upregulation downstream of both $aPKC^{\Delta N}$ and $aPKC^{CAAX}$/*Par6* are independent of JNK. These observations are consistent with previous results in $aPKC^{\Delta N}$-expressing clones, as well as data implicating aPKC misregulation in directly inhibiting Hpo activity [74, 75]. Taken together, these data clarify the relationship between JNK and aPKC, and elucidate a single pathway linking polarity loss to the transcriptional activation of a downstream target.

Role of Yki in Scrib module mutant tissues discs

Our data showing that Scrib mutant tissue growth is dependent upon Yki activity extend previous work linking two major Drosophila TSG pathways. However, they also highlight a major puzzle: the phenotypes of Scrib module and Hpo mutant tissues are quite distinct. Scrib module mutant tumors are characterized by slow, inexorable growth of apolar tissue, while Hpo pathway mutant epithelia proliferate more quickly than wild-type [32]. Significantly, nearly all transcriptional targets of the Hpo pathway, including *expanded* and *DIAP1*, are normally expressed in Scrib module mutants.

If Yki is activated in both tumorous tissues, why do they behave so differently? One possibility is that activation of Yki-independent pathways, such as JNK, upon polarity loss may have effects on growth kinetics and transcription that oppose Yki. According to this model, the pro-apoptotic role of JNK decreases the growth-promoting function of active Yki. Consistent with this possibility, inhibiting JNK in $aPKC^{\Delta N}$-expressing tissue qualitatively appears to increase tumor growth (see Figure 5). We tested this hypothesis directly but found that co-activation of Yki and JNK does not recapitulate Scrib module mutant growth kinetics (data not shown). Alternatively, Yki may upregulate targets in a context-dependent manner. In Scrib module mutant discs, for example, activation of Yki may preferentially promote transcription of the *upd*s at polarity-responsive enhancers, such as *upd3.3*, rather than loci such as *DIAP1*. The increased sensitivity of the *upd*s in polarity-deficient discs may be due to synergy with AP-1-mediated transcription, different chromatin environments, or perhaps the misregulation of additional polarity-sensitive effector pathways. These pathways and targets may not be

accessible or activated in Hpo pathway mutant tissues. Identifying these additional regulators is a ripe area for future investigation and is partially addressed in Chapter 3.

Neoplastic tumors as wounds that never heal

Why does disruption of tissue polarity lead to activation of stress response pathways and ultimately transcription of mitogenic targets? Interestingly, our transcriptome analysis reveals that disruption of apicobasal polarity elicits the same response as epithelial wounds: activation of stress signaling, de-differentiation, recruitment of hemocytes, and transcriptional upregulation of growth-promoting cytokines that stimulate cell proliferation and wound repair [110]. Upon tissue damage, restoration of tissue architecture and re-establishment of tissue integrity abrogates these wound-response signals. In contrast, in Scrib module mutant tissues, polarity is never repaired, and these pro-growth, de-differentiation cues remain active, leading to the formation of neoplastic tumors that ultimately kill the organism. Thus, our data provide support for the contention that tumors are wounds that never heal [111, 112].

MATERIALS AND METHODS

Fly Stocks

All flies were reared at 25°C. Full genotypes of the flies used are: *white*^{1118}, *scrib*^{1}*/TM6b*, *dlg*$^{40\text{-}2}$*/FM7GFP*, *eyeFLP; act>>GAL4,UAS-GFP*, *dlg*^{hf321}*/FM7 ; enGAL4,UAS-GFP*, *ms1096-GAL4*, *hep*^{R75}*/FM7c ; scrib*^{1}*/TM3, UAS-dlgIR* (*39035*, Bloomington), *UAS-Sod2* [113], *UAS-Catalase* [114], *UAS-SOCS36E* [115], *STAT-GFP* [116], *upd3-GAL4, UAS-GFP* [92], *upd3LacZ*, *upd3.1LacZ*, *upd3.2LacZ*, *upd3.3LacZ* [93], *UAS-Bsk*^{K53R}*/TM6b* (*UAS-Bsk*^{DN}) [117], *UAS-fos*^{panAla} (*UAS-fos*^{DN}) [96], *UAS-aPKCIR* (*25946,* Bloomingon), *UAS-BazIR* (*35002*, Bloomington), *UAS-miRNA*^{reapergrimhid} (*UAS-miRGH*) [97], *UAS-ykiIR* (*104523*, VDRC), *UAS-hippo* [118], *UAS-eiger* [65], *UAS-aPKC*$^{\Delta N}$ (*UAS-aPKC*^{CA}) [18], *UAS-aPKC*^{CAAX}*,UAS-Par6* [T Harris, unpublished], *UAS-yki*^{S168A} [100]

mRNA Purification, Sequencing, and Data Analysis

At least 50 wing imaginal discs were dissected from *white*^{1118}, *scrib*^{1}, and *dlg*$^{40\text{-}2}$*/Y* larvae for each biological replicate, and at least 2 biological replicates were sequenced per genotype. The *white* tissue was isolated 5-6 days after egg lay (AEL); *scrib* and *dlg/Y* discs were dissected 7-8 days AEL (to account for the developmental delay of tumor-bearing larvae) and stored in RNAlater (Qiagen) at 4 degrees prior to processing. After lysing the tissue, mRNA was purified via two rounds of poly-A RNA extraction using PolyAPurist columns (Ambion). The purified mRNA was prepared for sequencing using a standard protocol [119].

The libraries were sequenced by 50-bp single-end reads on either the GAIIX Genome Analyzer or HighSeq2000 platform (Illumina). The reads were aligned to the *Drosophila melanogaster* reference genome (version 5.25.62) using Bowtie, allowing a maximum of two mismatches [120]. The reads from each replicate were pooled into a single sample for each genotype, and the expression levels across all of samples were normalized such that the total expression of each sample was identical. Relative gene expression was calculated using DESeq, on UNION mode [121]. The normalized value for gene expression is reported in a single 'reads per kilobase gene length per million total reads' (RPKM) value for each gene, rather than using expression values for every isoform. Table 2.3 contains the sequencing and mapping statistics for each genotype, and Table 2.4 contains the number of differentially expressed genes. GOstat was used to perform Gene Ontology analysis [83].

Immunofluorescence and Microscopy

Imaginal discs were dissected, fixed, and stained using standard procedures. Unless otherwise noted, all transgenes were expressed using *ms1096GAL4*, and the wing discs were analyzed. The following primary antibodies and dilutions were used: rabbit anti-Bgal 1:100 (Abcam), mouse anti-Mmp1 1:100 (1:1:1 mix of 3 antibodies from DSHB), mouse anti-Dlg 1:100 (DSHB), rabbit anti-aPKC (Sigma), rat anti-Scrib (DSHB). To visualize cell outlines, we used TRITC-phalloidin 1:200 (Sigma); DAPI 1:1000 (Molecular Probes) was used to assess nucleus integrity. Secondary antibodies were obtained from Molecular Probes. Mutant and wild-type discs were stained in the same tube and imaged under identical confocal settings. Images were obtained on either a Leica TCS or a Zeiss LSM 700 and processed with Adobe Photoshop CS2 12.0.1.

qRT-PCR

Total RNA was isolated from at least 20 *white* and *scrib* wing discs using the RNeasy Mini Kit (Qiagen), and cDNA was prepared under standard procedures. Quantitative real-time PCR was performed using SYBR GreenER qPCR SuperMix for ABI Prism (Invitrogen) on a StepOnePlus ABI Machine (Applied Biosystems). Relative gene expression levels were quantified using the $\Delta\Delta C_T$ method, after normalization to three endogenous control genes (*GAPDH, CG12703*, *Cp1*). Average fold expression of at least 2 biological replicates is shown. Target primer sequences are available upon request.

Cloning *upd3* Enhancer Fragments

Genomic DNA was isolated from adult flies using standard procedures. Briefly, 30 *white*^{1118} flies were homogenized in Buffer A (100uM Tris-HCl pH 7.5, 100mM EDTA, 100mM NaCl, 1% SDS) and incubated at 60°C for 30 minutes. One part 5M KAc and 2.5 parts 6M KCl were added to the sample, the cuticle was spun down, and the DNA was cleaned by ethanol precipitation. The upd3 fragment was amplified from the genomic DNA using Phusion High Fidelity Polymerase (NEB) and the following primers: 5'-GGTGGTACCTCGTACAATGGTTTAAAAATAGCTCGGCCAA -3' and 5'-GGAAGGCCTCTCCTACACATCGAGCAGCATGGTCAACGAA -3'. The resulting 3-kb fragment was cut with *KpnI* and *StuI* and ligated into a pH-Pelican-attB vector cut with *KpnI* and *BamHI*. Klenow polymerase (NEB) was used to generate a blunt end on the 3' *BamHI* fragment on the vector so it would ligate with the blunt 5' end of the insert. The cloned vector was transformed into *DH5α* cells, and isolated by Midiprep kit (Qiagen). The sequence of the *upd3LacZ* fragment was confirmed by DNA sequencing and integrated into the *attP2* landing site on the third chromosome of *white*^{1118} flies by ϕC31-integrase mediated transformation. The injections and isolation of *miniwhite*$^{+}$ transformants were performed by BestGene, Inc.

Fluorescence Activated Cell Sorting Analysis

At least 10 wing discs were dissected from L3 larvae for each genotype, and washed to remove any fat body and trachea. The discs then were transferred to a 5mL polystyrene tube containing 500uL of Trypsin-EDTA (Sigma) and 1XPBS. The cells were dissociated by gentle rocking on a nutator at room temperature for 3 hours along with manual shaking every 30 minutes. After 3 hours, the samples were pipetted up and down briefly to break up any remaining clumps, and counted using an EPICS XL flow cytometer (Beckman-Coulter) in the Cancer Research Laboratory Flow Cytometry Facility at UC Berkeley. Cells were gated using side- and forward-scatter to isolate the live cell population and from that population, the GFP+ and GFP- cells were counted. The GFP+ and GFP- gates were generated based on a *white*^{1118} negative control sample. To calculate Posterior Compartment Size, the number of GFP+ cells was divided by the total number of live cells. A two-tailed Student's T-test was used to calculate the P-values based on at least 3 biological replicates for each genotype.

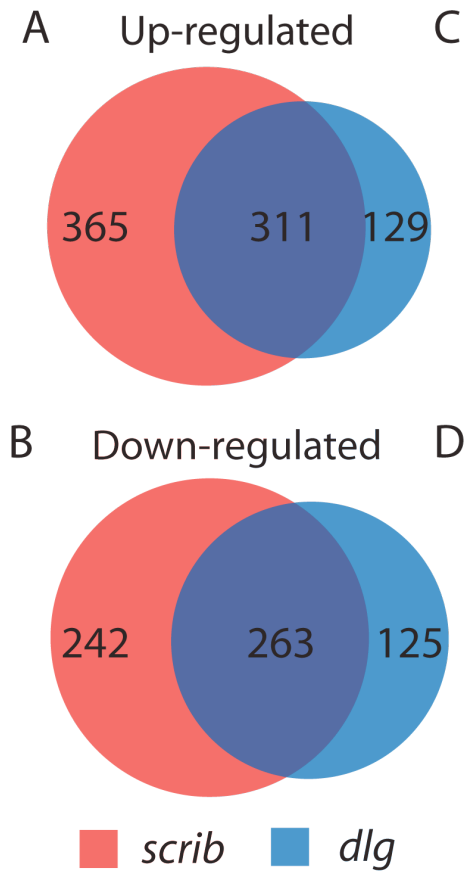

C

GO Categories: Upregulated Genes	P-value
Response to Stimulus	0.00505
Cytokine Activity	0.00798
Regulation of JAK-STAT Cascade	0.0271
Multicellular Organism Development	0.0338
Olfactory Learning	0.0404
Defense Response	0.0405
Phosphatidate Phosphatase Activity	0.0405
Amino Acid Transporter Activity	0.0434
Receptor Binding	0.0470

D

GO Categories: Downregulated Genes	P-value
Larval Development	4.00e-14
Metamorphosis	8.04e-14
Transcription Factor Activity	2.76e-12
Imaginal Disc Morphogenesis	2.76e-12
Nervous System Development	1.30e-5
Cell Differentiation	2.28e-5
Proximal/Distal Pattern Formation	8.82e-5
Regulation of Metabolic Process	0.000130

Figure 2.1: Transcriptome Analysis of Neoplastic Tumors
Overlap of genes upregulated (A) or downregulated (B) in *scrib* and *dlg* tissues; differentially expressed genes are misregulated at least 2-fold relative to wild-type (FDR < 0.05). We focused our analysis on genes within the overlap. GOstat was used to identify functional categories enriched in the upregulated (C) and downregulated (D) genes.

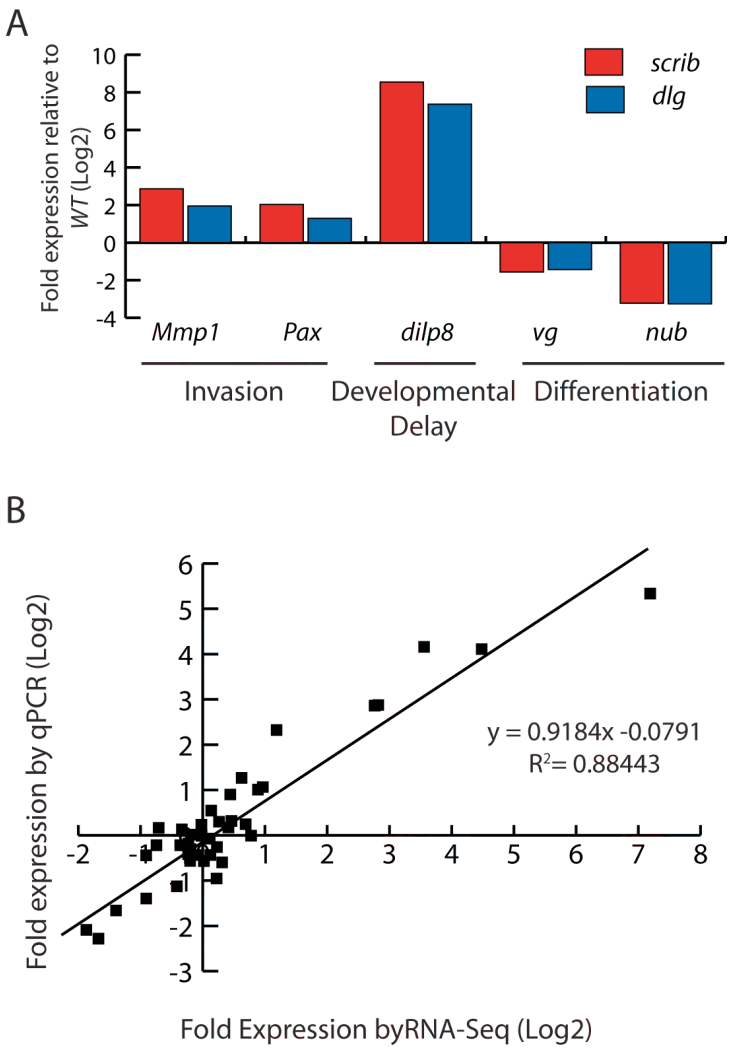

Figure 2.2: RNA-Seq Captures the Expression Profile of Polarity-Deficient Tissues
Genes whose misregulation contributes to invasion (*Mmp1* and *Paxillin*), developmental delay (*dilp8*), and de-differentiation (*vg* and *nub*) in Scrib module mutant tissues are significantly differentially expressed in the RNA-Seq dataset (A). RNA-Seq and qRT-PCR data of *scrib* tissue are in agreement (B).

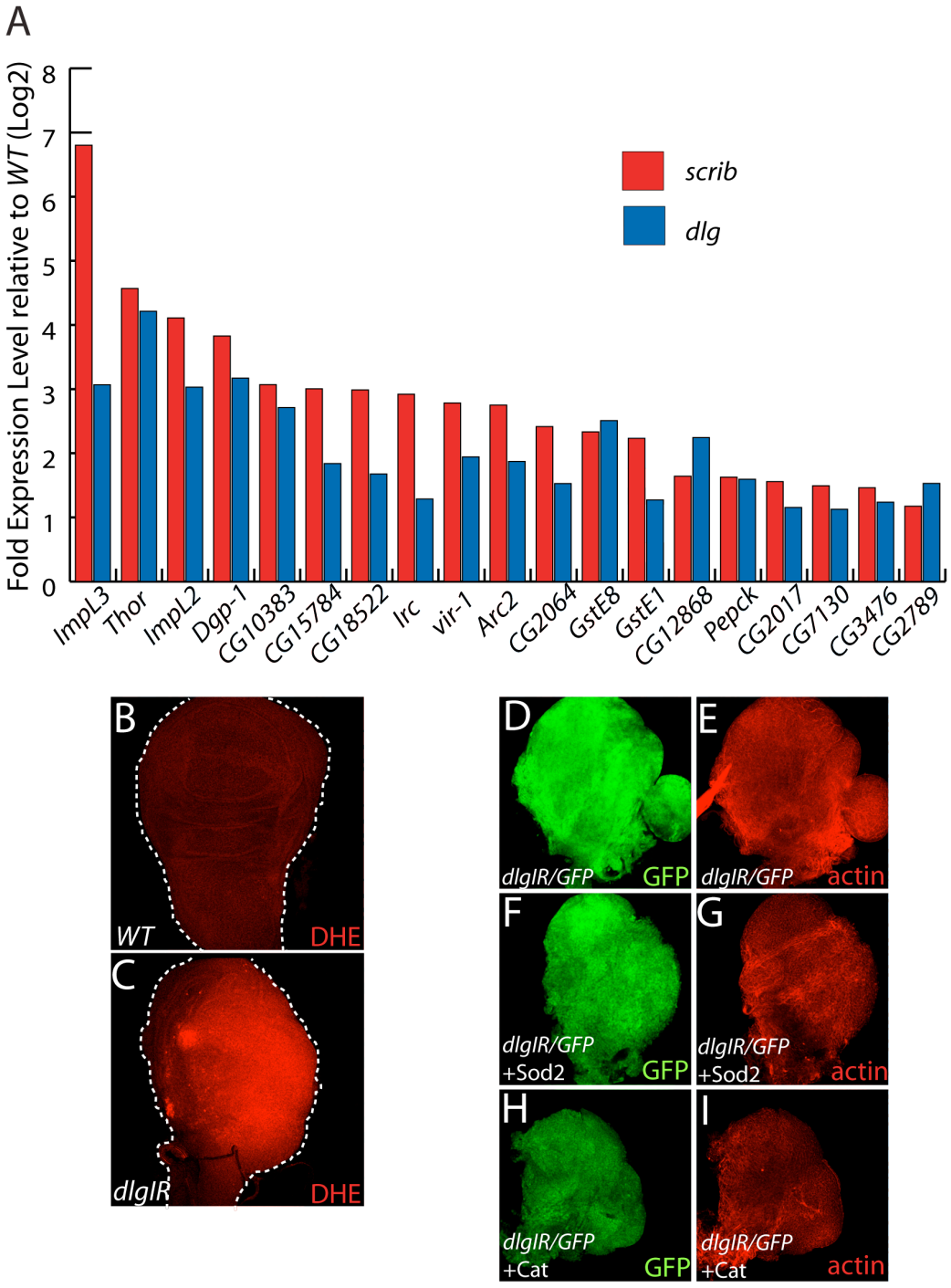

Figure 2.3: Loss of Polarity Leads to Increased Oxidative Stress
Nineteen genes activated in response to oxidative stress are significantly upregulated upon polarity loss (A). Knockdown of *dlg* leads to increased superoxide levels, as evidenced by increased DHE staining (C), relative to wild-type tissue (B). Over-expression of the superoxide scavenger, *Sod2* (F,G) or the antioxidant enzyme *Cat* (H,I) has no effect on the size or architecture defects of eye discs expressing *dlgIR* (D,E).

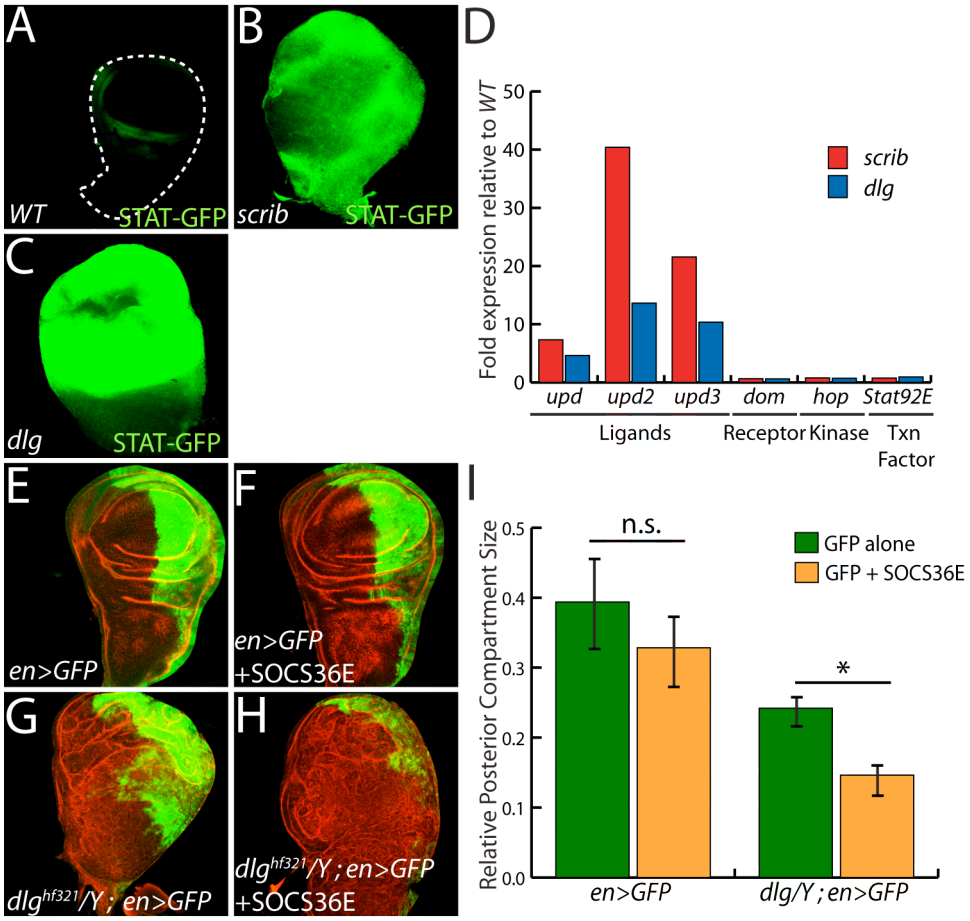

Figure 2.4: JAK-STAT Activation Drives Overgrowth upon Polarity Loss
The JAK-STAT pathway reporter *10XSTAT-GFP* is expressed in a ring around the pouch in wild-type wing discs (A). Reporter activity is highly elevated throughout *scrib* (B) and *dlg* (C) discs, indicative of strong pathway activation. The *upd*s, but not other JAK-STAT pathway components, are transcriptionally upregulated in *scrib* and *dlg* tissues (D). Reduction of JAK-STAT pathway activity has no effect on wild-type growth (E,F), but suppresses overgrowth of dlg^{hf321}/Y tissue (G,H). Quantification is shown in I (*p<0.001).

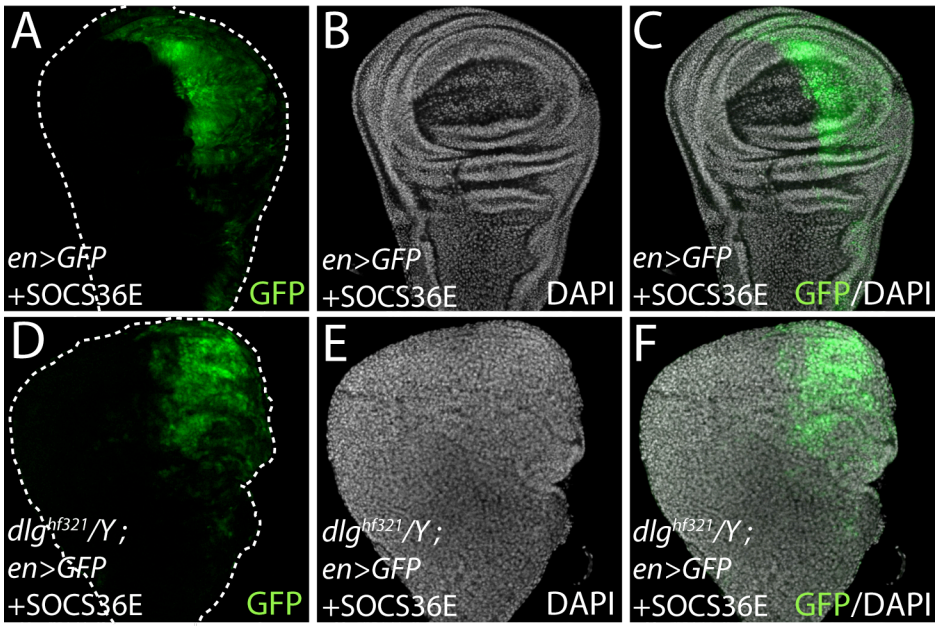

Figure 2.5: SOCS36E Expression Does Not Promote Apoptosis in Wild-Type or *dlg* Tissue
Expression of *SOCS36E* in the posterior compartment of wild-type (A-C) or dlg^{hf321}/Y (D-F) discs does not promote cell death, as assessed by DAPI staining for nuclear fragmentation.

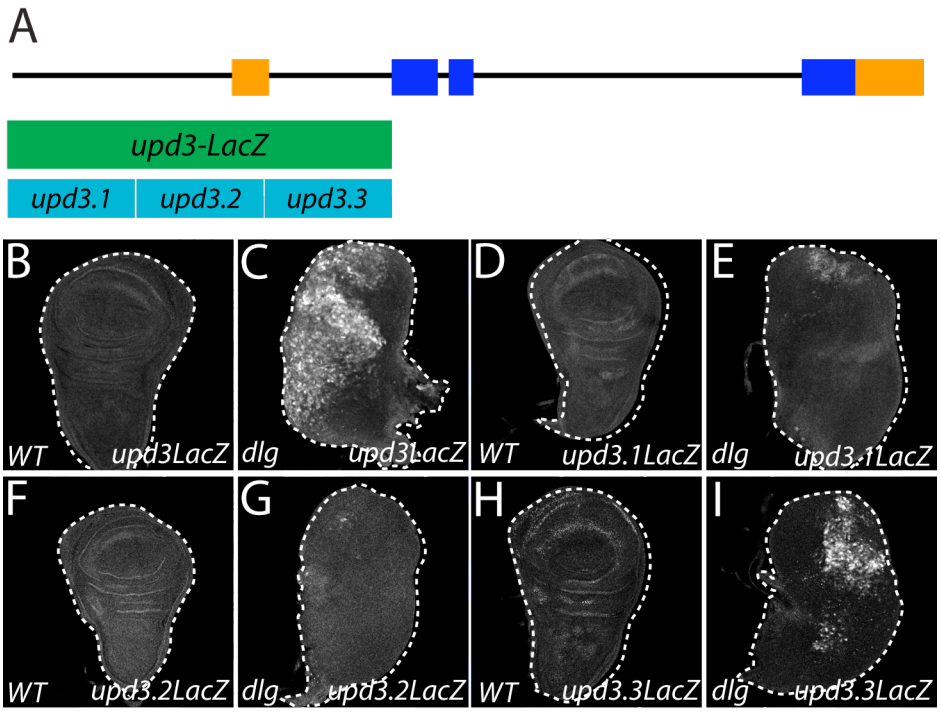

Figure 2.6: A 1-kb Region in the First Intron of *upd3* is Activated Upon Polarity Loss
A schematic of the *upd3* reporter constructs is depicted, along with the corresponding genomic region (A). Orange and blue boxes correspond to non-coding and coding exons, respectively. The 3-kb *upd3LacZ* reporter is not expressed in wild-type tissue (B), but is upregulated in scattered regions throughout *dlg* discs (C). *Upd3.1LacZ* and *upd3.2LacZ* are not expressed in wild-type discs (D,F), and elicit mild, inconsistent expression in *dlg* tissue (E,G). The *upd3.3* sub-fragment is also silent in wild-type tissue (H); however, in *dlg* tissue its expression pattern resembles that of *upd3LacZ* (I).

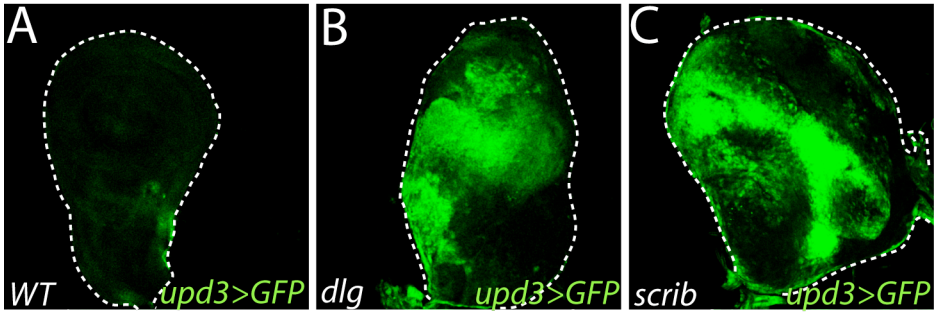

Figure 2.7: The *upd3* Enhancer is Responsive to Scrib Module Loss
The *upd3>GFP* reporter, which overlaps *upd3LacZ*, is strongly upregulated in *dlg* (B) and *scrib* (C) tissue relative to wild-type (A).

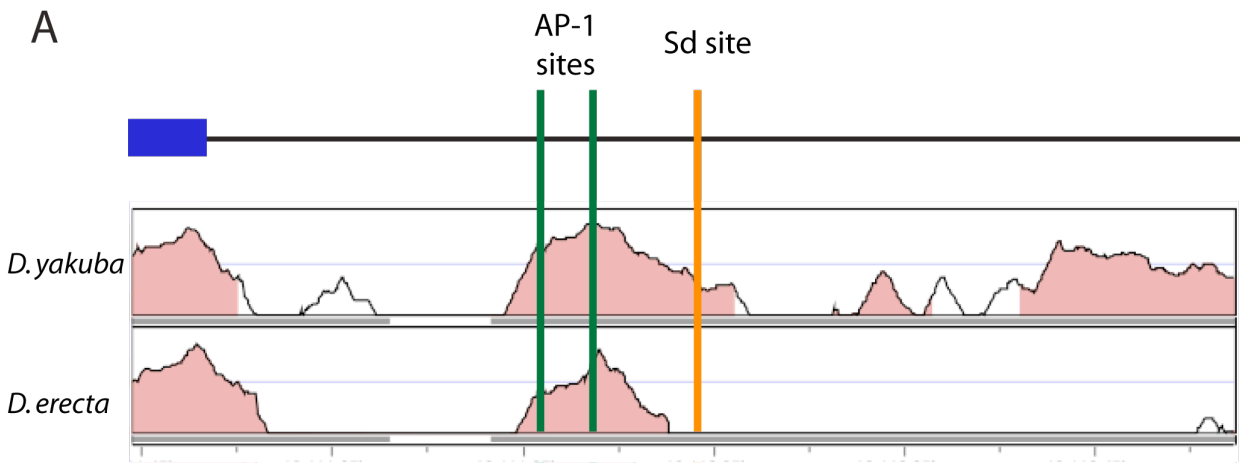

B

AP-1 Consensus:	TGANTCA
D. melanogaster:	TCGTGAATCACTG
D. sechellia:	TCATGAATCACTG
D. yakuba:	TCATGAATCACTG
D. erecta:	GCGTGAATCAGTG

AP-1 Consensus:	TGANTCA
D. melanogaster:	ATGTGAATCATAG
D. sechellia:	TTGTGAATCATAG
D. yakuba:	ATGTGAATCATAG
D. erecta:	ATGTGAATCACAG

C

Yki/Sd Consensus:	CATTCCA
D. melanogaster:	TTCCATTC-AACC
D. sechellia:	TTCCATTT-AACC
D. yakuba:	TTCT - - - - - - - - -
D. erecta:	- - - - - - - - - - - -

Figure 2.8: *Upd3.3* Contains AP-1 and Sd Binding Sites
Vista Genome Browser was used to align the 1-kb *upd3.3* enhancer region with two other Drosophila species. The *upd3* locus is depicted at the top, where the blue box indicates exonic sequence. The red areas under the curve denote regions of >70% conservation. *Upd3.3* contains two evolutionarily conserved AP-1 binding sites (green lines), and one semi-conserved Sd binding site (orange line). Alignment of the binding site sequences with the consensus site is shown in B and C.

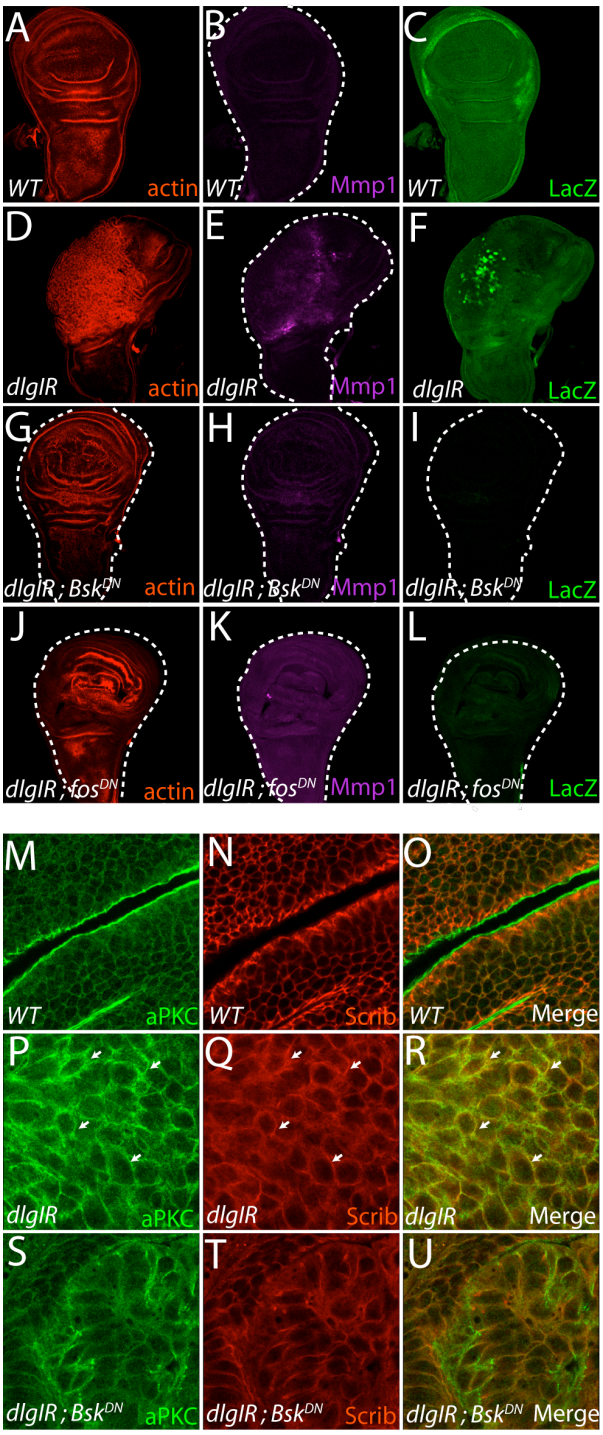

Figure 2.9: JNK-Dependent Transcription is Required for Neoplasia and *upd3.3* Activation Downstream of *dlg* Loss

Wild-type wing discs display normal architecture and actin levels (A), do not upregulate the JNK target, *Mmp1* (B), or activate *upd3.3LacZ* (C). Expression of *dlgIR* in the wing pouch promotes actin disorganization (D), *Mmp1* activation (E) and *upd3.3LacZ* transcription (F). Strikingly, co-

expression of either *Bsk*^{DN} or *fos*^{DN} with *dlgIR* restores normal disc architecture and actin organization (G,J), abrogates *Mmp1* expression (H,K), and blocks *upd3.3LacZ* activation (I,L). Normal discs segregate the apical marker aPKC (M) and the basolateral determinant Scrib (N) to establish normal apicobasal polarity (O). Knockdown of *dlg* leads to expansion of the apical domain (P) relative to the basolateral domain (Q) and co-localization of aPKC and Scrib (R, arrowheads). Inhibiting JNK signaling in *dlgIR*-expressing discs with *Bsk*^{DN} restores the separation of aPKC (S) and Scrib (T), suggesting that apicobasal polarity is rescued (U).

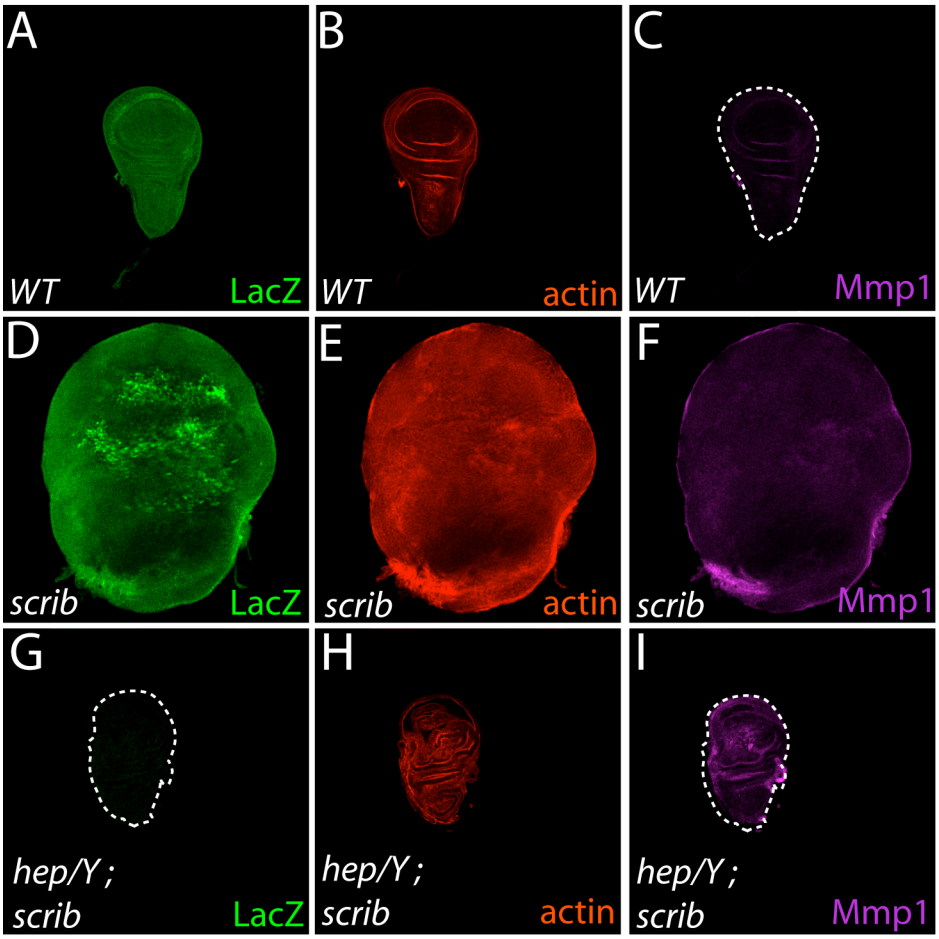

Figure 2.10: The JNK Kinase *Hep* is Required for Overgrowth, Architecture Defects, and *upd3.3LacZ* Activation in *scrib* Tissue
Homozygous *scrib* tissues have high *upd3.3LacZ* (D) and *Mmp1* expression (F) and form large tumors with disrupted architecture (E), relative to wild-type (A-C). Strikingly, loss of *hep* blocks *upd3.3LacZ* (G) and *Mmp1* upregulation (I), as well as tissue overgrowth (H).

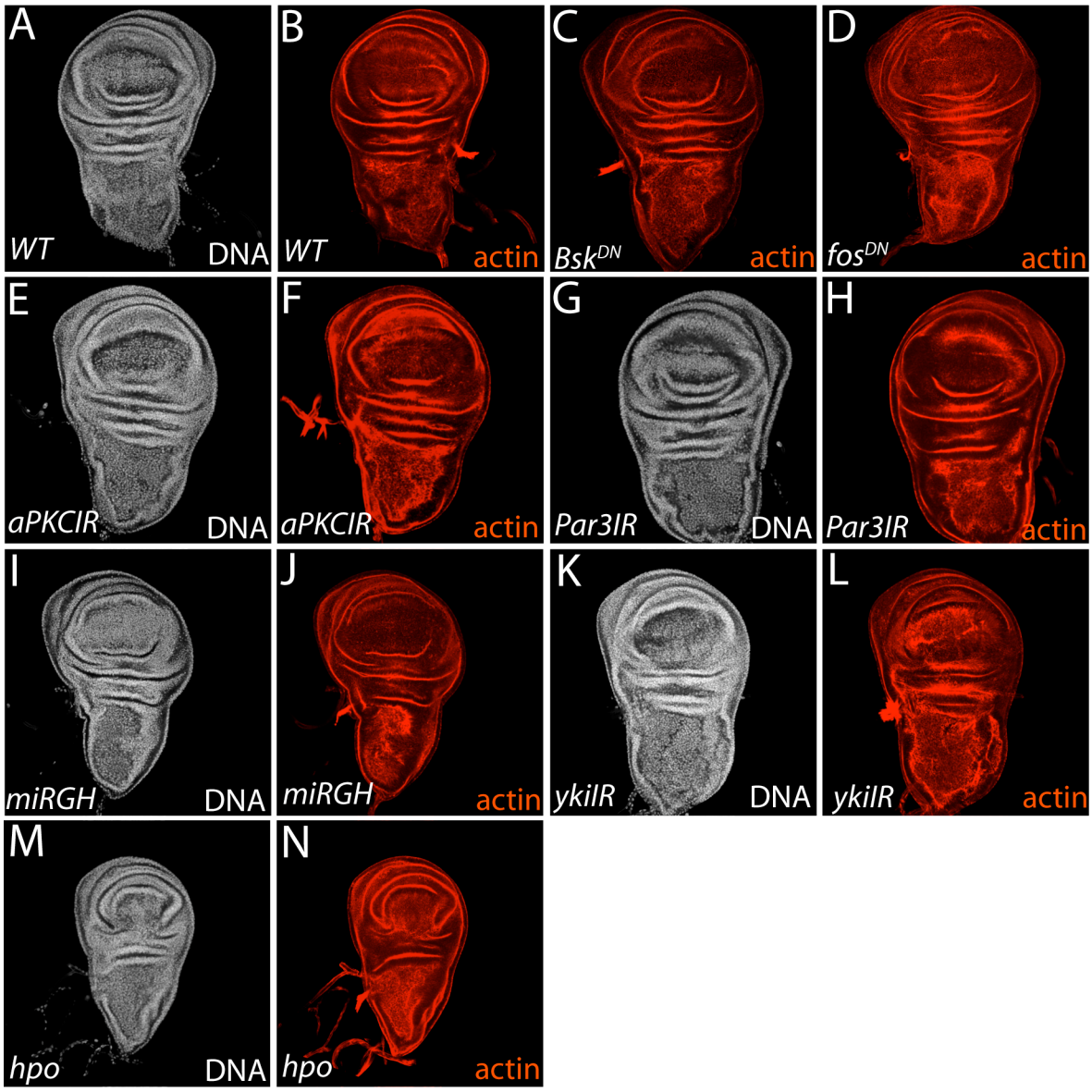

Figure 2.11: Knockdown of Apical Determinants or Inhibition of JNK/Hpo Signaling Does Not Significantly Affect Wild-Type Growth

Blocking JNK activity with Bsk^{DN} (C) or fos^{DN} (D) has no effect on normal growth or tissue architecture (B). Actin and DAPI stainings indicate that RNAi against the Par complex components *aPKC* (E,F) or *Baz* (G,H) does not affect tissue architecture or cell viability, relative to wild-type (A,B). Expression of *miRGH* has no effect on normal tissue architecture or apoptosis (I,J). Knockdown of Yki activity with *ykiIR* or *hpo* expression causes mild architecture disruption (L,N), and drives apoptosis in small portions of the wing pouch (K,M), relative to wild-type (A,B).

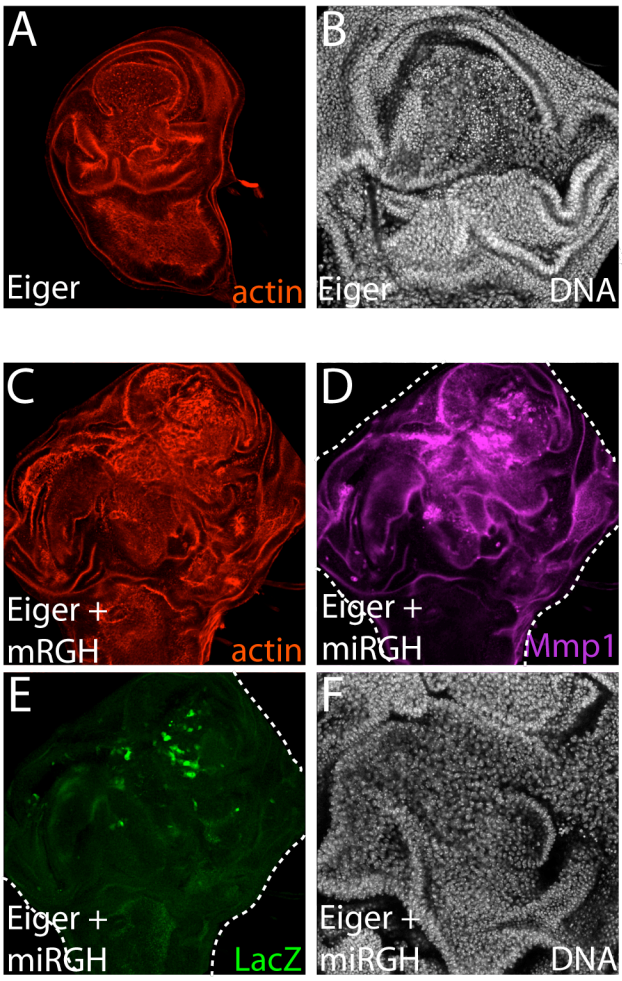

Figure 2.12: JNK Activation is Sufficient for *upd3.3LacZ* Activation and Overgrowth
Eiger expression disrupts tissue architecture (A) but drives apoptosis (B). Blocking apoptosis with *miRGH* (F) permits overgrowth (C), strong *Mmp1* expression (D) and *upd3.3LacZ* activation (E).

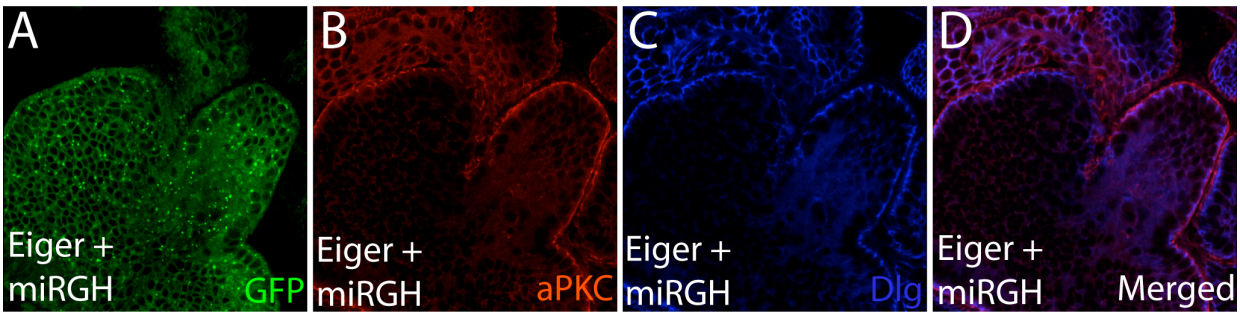

Figure 2.13: Ectopic JNK Activation Does Not Disrupt Polarity
Cells expressing Eiger and *miRGH*, marked with GFP (A), display proper localization of the apical determinant aPKC (B) and the basal determinant, Dlg (B), indicating that apicobasal polarity is normal (D).

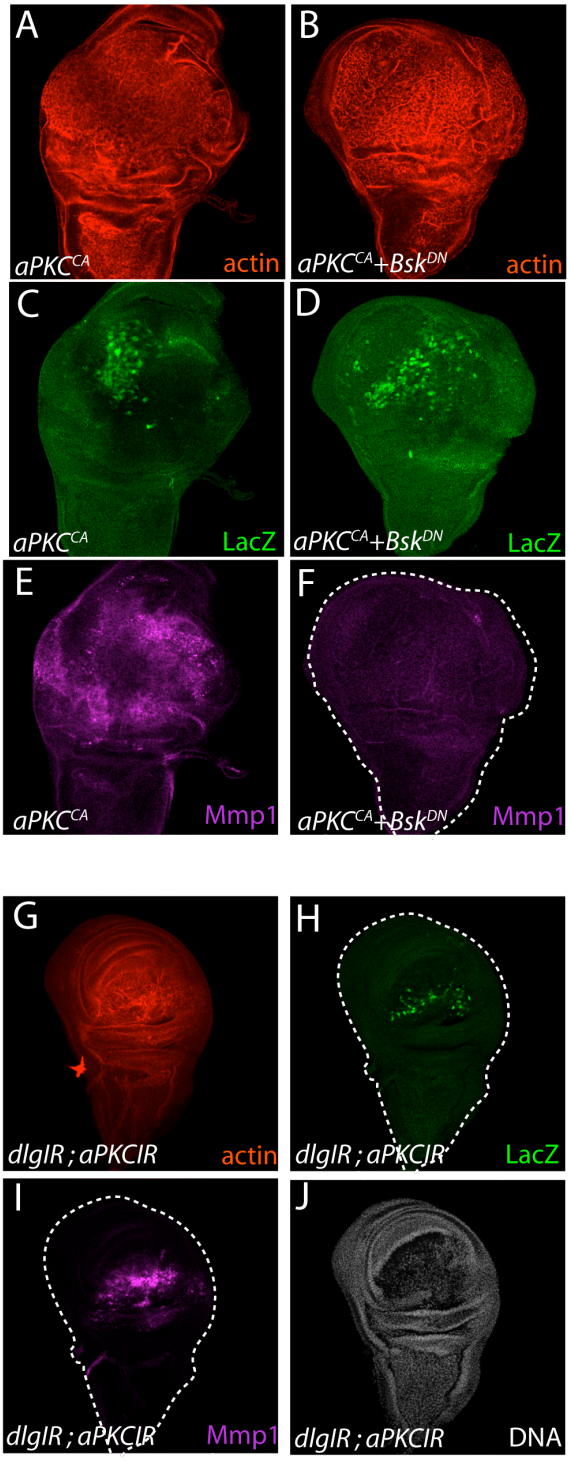

Figure 2.14: aPKC Activity is Sufficient, but Not Required, for *upd3.3LacZ* Activation
Expression of a constitutively active form of aPKC ($aPKC^{\Delta N}$) drives overgrowth (A) and *upd3.3LacZ* activation (C), but also *Mmp1* upregulation (E). Co-expression of $aPKC^{\Delta N}$ and Bsk^{DN} does not block overgrowth (B) or *upd3.3LacZ* upregulation, but prevents expression of the JNK target *Mmp1* (F). Co-expression of *dlgIR* and *aPKCIR* prevents overgrowth (G), but

does not block activation of *upd3.3LacZ* (H) or *Mmp1* (I). DAPI staining reveals that co-expression of *aPKCIR* and *dlgIR* does not drive apoptosis (J). See Figure 2.9 for the controls.

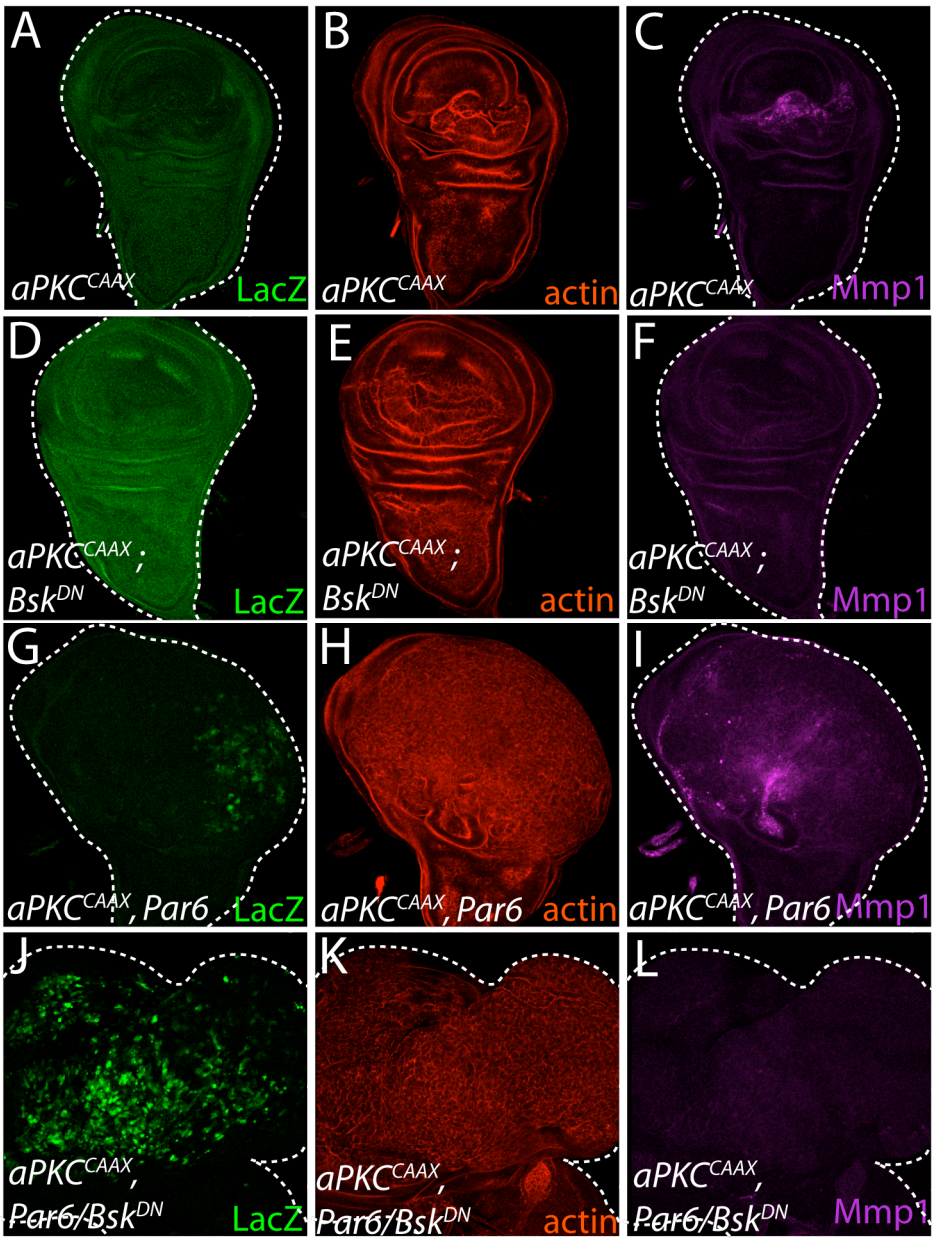

Figure 2.15: Co-expression of *aPKC^{CAAX}* and *Par6* Drives Overgrowth and *upd3.3LacZ* Activation in a JNK-Independent Manner

Expression of *aPKC^{CAAX}* alone does not activate *upd3.3LacZ* (A), but induces only mild overgrowth (B) and *Mmp1* upregulation (C), in a JNK-dependent manner (D-F). In contrast, expression of *aPKC^{CAAX}* and *Par6* drives strong overgrowth (H), *upd3.3LacZ* activation (G), and *Mmp1* expression (I) in the wing pouch. Co-expression of *Bsk^{DN}* does not suppress overgrowth (K) or *upd3.3LacZ* activation (J), though *Mmp1* upregulation is abrogated (L).

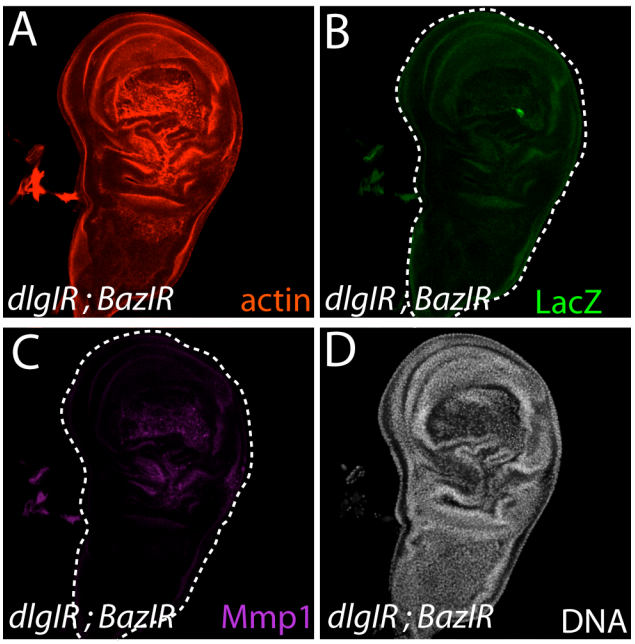

Figure 2.16: *Baz* is Necessary for Overgrowth, but Not *upd3.3LacZ* Expression or JNK Activation upon *dlg* Knockdown
Reducing *Baz* expression prevents overgrowth (A) of *dlgIR*-expressing tissue, without driving cell death (D), and reduces, but does not eliminate, *upd3.3LacZ* activation (B) and *Mmp1* expression (C). See Figure 2.9 for the controls.

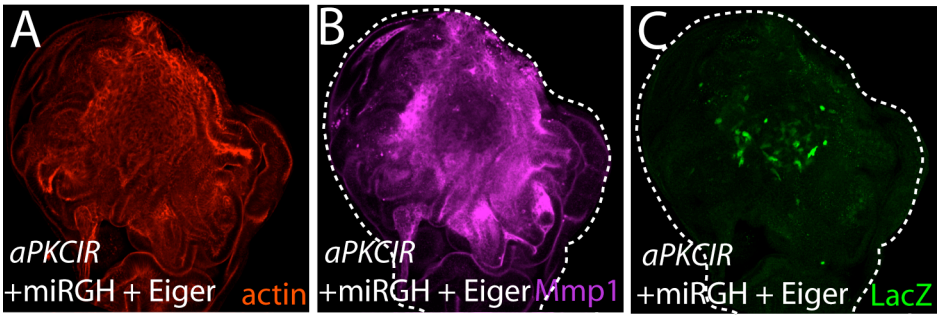

Figure 2.17: In the Absence of Apoptosis, JNK drives Growth and *upd3.3LacZ* Activation Independently of *aPKC*
Expressing *aPKCIR* does not prevent overgrowth (A), *Mmp1* expression (B), or *upd3.3LacZ* upregulation (C) in *eiger/miRGH*-expressing tissues. See Figure 2.12 for the controls.

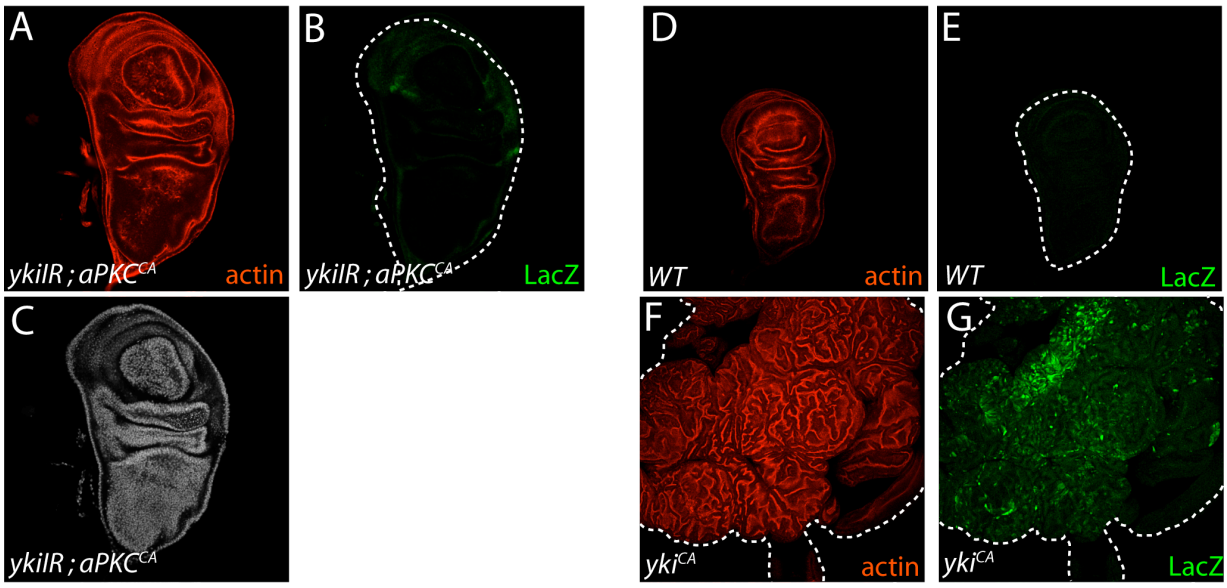

Figure 2.18: Yki is Necessary and Sufficient for *upd3.3LacZ* Activation and Overgrowth Downstream of aPKC

Expression of *ykiIR* blocks $aPKC^{\Delta N}$-mediated overgrowth (A) and *upd3.3LacZ* activation (B). Some of the $aPKC^{\Delta N}$/*ykiIR*-expressing cells undergo apoptosis, but the wing pouch remains largely intact (C). See Figure 2.14 for the controls. Expression of a constitutively active form of Yki drives dramatic tissue overgrowth (F) and *upd3.3LacZ* activation (G), relative to wild-type (D,E).

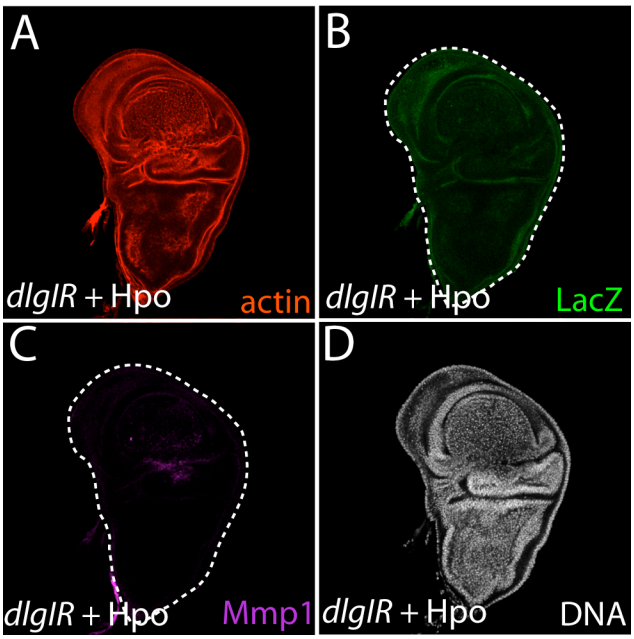

Figure 2.19: Canonical Hpo Signaling is Required for *upd3.3LacZ* Expression and Overgrowth upon Knockdown of *dlg*
Expressing the negative Yki regulator Hpo prevents tumor formation (A), *upd3.3LacZ* activation (B), and reduces *Mmp1* (C) upon knockdown of *dlg*. However, these discs exhibit some cell death in the wing pouch (D). See Figure 2.9 for the controls.

Flybase ID	Gene Name	WT RPKM	Scrib RPKM	Fold Change	P-value	Notes
FBgn0042173	CG18853	0.000	100.438	Inf	3.50E-28	DNA photolyase
FBgn0036324	CG12520	0.000	37.586	Inf	4.37E-06	Unknown
FBgn0035544	CG15021	0.000	53.659	Inf	0.000660484	Unknown
FBgn0030385	Ir11a	0.000	19.678	Inf	0.008729785	Ion Receptor
FBgn0051326	CG31326	0.000	13.987	Inf	0.039155018	Peptidase
FBgn0038840	CG5621	0.509	204.281	401.060	3.08E-26	NMDA receptor
FBgn0036690	**CG14059**	**39.009**	**14611.178**	**374.562**	**1.61E-55**	**dilp8-Develop. Delay**
FBgn0263219	Dscam4	10.469	3920.814	374.527	3.47E-40	Axon guidance/cell adhesion
FBgn0037766	Teh1	2.950	944.149	320.002	3.16E-68	Na-channel
FBgn0029994	**CG2254**	**7.592**	**1893.030**	**249.355**	**8.19E-86**	**Metabolism/Oxidative stress**
FBgn0259226	CG42326	35.979	8429.971	234.301	1.51E-07	Small GTPase-like
FBgn0069973	**CG40485**	**3.557**	**717.350**	**201.657**	**8.32E-29**	**Oxidoreductase-Metabolism**
FBgn0033501	CG12911	26.681	5138.476	192.589	8.98E-08	Unknown
FBgn0259994	CG42492	6.894	1279.005	185.536	3.68E-37	Otopetrin
FBgn0033574	**Spn47C**	**41.630**	**7668.545**	**184.209**	**5.02E-215**	**Oxidative stress**
FBgn0035798	frac	0.820	148.408	181.063	0.011751508	ECM
FBgn0263029	CG43324	0.255	37.437	146.998	3.46E-05	Unknown
FBgn0032040	CG13386	1.482	181.395	122.391	2.54E-21	Unknown
FBgn0001258	**ImpL3**	**332.690**	**37109.125**	**111.543**	**3.87E-18**	**LDH- Warburg effect**
FBgn0033598	Cpr47Eb	5.891	618.774	105.044	1.43E-12	Cuticle
FBgn0036381	CG8745	19.457	1528.372	78.550	1.12E-42	Amino Acid Transporter
FBgn0037447	Neurochondrin	34.866	2562.826	73.505	1.63E-37	Neuronal
FBgn0033593	**Listericin**	**1.116**	**77.910**	**69.800**	**0.000105761**	**Immune response**
FBgn0033302	**Cyp6a14**	**1.635**	**112.861**	**69.020**	**5.67E-08**	**Cytochrome-Metabolism**

Flybase ID	Gene Name	WT RPKM	Scrib RPKM	Fold Change	P-value	Notes
FBgn0040842	CG15212	88.842	0.000	0.000	3.59E-18	Unknown
FBgn0032116	CG3759	59.444	0.000	0.000	1.22E-09	Iron transporter
FBgn0034224	CG6520	12.690	0.000	0.000	0.003916093	Unknown
FBgn0000659	fkh	3.223	0.000	0.000	0.014691178	Transcription Factor-Cell Fate
FBgn0037498	CG10029	13.043	0.000	0.000	0.018793547	Oxidoreductase activity
FBgn0003375	Sgs5	8.240	0.000	0.000	0.02936059	Unknown
FBgn0051683	CG31683	4.558	0.000	0.000	0.036906885	Phospholipase activity
FBgn0051157	CG31157	166.997	0.265	0.002	5.24E-23	Unknown
FBgn0052248	CG32248	82.570	0.317	0.004	1.55E-05	Unknown
FBgn0034462	CG15905	2946.047	18.037	0.006	2.25E-24	Unknown
FBgn0001217	Hsc70-2	626.973	3.969	0.006	9.52E-24	Chaperone
FBgn0051025	Ppi1	38.587	0.265	0.007	0.001235014	Phosphatase activity
FBgn0037548	CG7900	346.021	2.442	0.007	2.68E-74	Amidase
FBgn0085276	CG34247	93.100	0.697	0.007	1.76E-05	Unknown
FBgn0001254	ImpE2	64986.207	604.198	0.009	6.88E-14	Unknown
FBgn0052475	mthl8	28.252	0.265	0.009	1.21E-17	G protein coupled receptor
FBgn0050428	CG30428	856.187	8.101	0.009	1.13E-65	Unknown
FBgn0051029	CG31029	69.596	0.795	0.011	9.41E-10	Unknown
FBgn0030542	CG12481	104.377	1.278	0.012	2.58E-15	Unknown
FBgn0029761	SK	2076.746	26.647	0.013	5.44E-08	Potassium channel

FBgn0037870	CG18577	19.560	0.265	0.014	0.002434745	Unknown
FBgn0039678	Obp99a	591.971	8.255	0.014	3.64E-31	Odorant receptor
FBgn0036677	CG13023	293.883	4.167	0.014	1.00E-24	Unknown
FBgn0039795	Spn100A	1469.586	22.129	0.015	1.45E-06	Serine peptidase
FBgn0036986	CG5282	55.830	0.878	0.016	7.98E-10	Peptidase

Table 2.1: *scrib* Transcriptome
Tables of the top 25 most highly up- and down-regulated genes in *scrib* tissues. The normalized expression level for each gene is quantified as 'Reads per kilobase gene length per million reads' (RPKM), and fold change refers to expression level in *scrib* tissue relative to wild-type. Descriptions of the genes are listed on the right-most column, and genes of particular interest in the neoplastic phenotype are in bold. The entire list of genes differentially expressed in *scrib* tissues can be found at: http://mcb.berkeley.edu/labs/bilder/brandon/Table2.1_Scrib.xlsx

Flybase ID	Gene Name	WT FPKM	Scrib FPKM	Fold Change	P-value	Notes
FBgn0042173	CG18853	0.000	39.603	Inf	7.79E-14	DNA photolyase
FBgn0050486	CG30486	0.000	43.168	Inf	8.67E-05	Unknown
FBgn0036324	CG12520	0.000	5.787	Inf	0.038355801	Unknown
FBgn0051865	Ada1-1	0.000	20.970	Inf	0.046836932	Transcription Factor
FBgn0262483	CG43073	0.255	313.310	1230.233	0.017741816	Protein Trafficking
FBgn0052581	CG32581	1.214	629.635	518.786	5.08E-22	Unknown
FBgn0262532	CR43086	0.255	130.623	512.898	0.000214403	Unknown
FBgn0030313	CG11697	4.192	1693.778	404.086	1.88E-59	Unknown
FBgn0031703	CG12512	1.015	290.302	286.121	6.40E-28	Fatty Acid CoA-ligase
FBgn0050488	CG30488	0.255	69.232	271.842	1.12E-09	Unknown
FBgn0033592	CG13215	0.862	218.843	254.023	5.08E-22	Unknown
FBgn0036690	**CG14059**	**39.009**	**6475.042**	**165.990**	**2.44E-42**	**dlip8- Develop. Delay**
FBgn0000278	CecB	0.310	48.797	157.259	0.003082768	Unknown
FBgn0032285	CG17108	7.031	1091.315	155.218	1.55E-05	Unknown
FBgn0035649	CG10483	2.246	298.361	132.834	1.78E-12	Unknown
FBgn0013277	**Hsp70Ba**	**14.836**	**1879.360**	**126.672**	**0.000721487**	**Stress response**
FBgn0259226	CG42326	35.979	3837.850	106.669	2.42E-05	Small GTPase-like
FBgn0026593	CG5707	2.390	218.329	91.368	3.90E-07	Unknown
FBgn0030105	CG15369	0.959	64.875	67.649	2.33E-05	Peptidase inhibitor
FBgn0050485	CG30485	4.715	313.926	66.584	3.49E-30	Unknown
FBgn0052475	mthl8	28.252	1768.005	62.581	1.38E-103	G protein coupled receptor
FBgn0259710	CG42364	0.973	55.960	57.527	0.000359449	Unknown
FBgn0033501	CG12911	26.681	1316.061	49.326	6.74E-05	Unknown
FBgn0058469	CR40469	255.921	12324.516	48.158	2.43E-08	Unknown
FBgn0000079	Amy-p	0.862	40.291	46.768	0.002137665	Amylase

Flybase ID	Gene Name	WT FPKM	Scrib FPKM	Fold Change	P-value	Notes
FBgn0039217	CG13627	146.498	0.000	0.000	4.73E-14	Unknown
FBgn0051157	CG31157	166.997	0.000	0.000	2.76E-13	Unknown
FBgn0040842	CG15212	88.842	0.000	0.000	1.09E-09	Unknown
FBgn0039795	Spn100A	1469.586	0.000	0.000	5.12E-08	Peptidase inhibitor
FBgn0036986	CG5282	55.830	0.000	0.000	1.78E-06	Peptidase
FBgn0260435	CR42530	25.085	0.000	0.000	0.000261886	Unknown
FBgn0023496	**Lip1**	**28.369**	**0.000**	**0.000**	**0.009065098**	**Lipase- Metabolism**
FBgn0035791	CG8539	14.856	0.000	0.000	0.017320074	Peptidase
FBgn0037870	CG18577	19.560	0.000	0.000	0.042813023	Unknown
FBgn0058005	CG40005	33.583	0.000	0.000	0.046463955	GTP binding
FBgn0001254	ImpE2	64986.207	36.791	0.001	6.09E-16	Unknown
FBgn0035625	Blimp-1	1908.403	1.540	0.001	0.000893488	Transcription factor
FBgn0034462	CG15905	2946.047	3.450	0.001	1.94E-20	Unknown
FBgn0024294	Spn43Aa	8431.815	25.856	0.003	2.20E-15	Peptidase inhibitor
FBgn0001217	Hsc70-2	626.973	2.495	0.004	8.44E-16	Chaperone
FBgn0035522	CG1273	2123.623	11.945	0.006	7.19E-07	Unknown
FBgn0043550	Tsp68C	102.226	0.584	0.006	0.018961353	Tetraspanin
FBgn0036677	CG13023	293.883	1.752	0.006	2.61E-16	Unknown
FBgn0037665	CG16733	1404.130	8.708	0.006	7.08E-09	Sulfotransferase
FBgn0085276	CG34247	93.100	0.584	0.006	0.004366397	Unknown
FBgn0000448	Hr46	776.790	4.990	0.006	0.026943887	Nuclear hormone receptor
FBgn0053302	Cpr31A	142.504	0.955	0.007	1.45E-11	Cuticle
FBgn0032869	CG17470	63.197	0.584	0.009	1.94E-08	Unknown
FBgn0033866	CG6280	584.694	6.000	0.010	1.82E-28	Unknown

FBgn0030491	CG15753	54.464	0.584	0.011	2.15E-06	Receptor scaffold

Table 2.2: *dlg* Transcriptome

Tables of the top 25 most highly up- and down-regulated genes in *dlg* mutant tissues. The normalized expression level for each gene is quantified as 'Reads per kilobase gene length per million reads' (RPKM), and fold change refers to expression level in *dlg* tissue relative to wild-type. Descriptions of the genes are listed on the right-most column, and genes of particular interest in the neoplastic phenotype are in bold. The entire list of genes differentially expressed in *dlg* tissues can be found at: http://mcb.berkeley.edu/labs/bilder/brandon/Table2.2_Dlg.xlsx

	Total Reads	Mapped Reads	Coverage	Non-aligned reads	Low Complexity Reads
white	145,780,859	114,771,877 (78.73%)	191X	29,933,911 (20.53%)	1,075,071 (0.74%)
scrib	153,244,798	117,055,137 (76.38%)	195X	32,136,301 (20.97%)	4,053,397 (2.64%)
dlg	68,300,718	48,851,804 (71.52%)	81X	18,758,908 (27.47%)	690,006 (1.01%)

Table 2.3: RNA-Seq Statistics
Table of the total number of 50-bp single-end sequencing reads for *white* (n=3), *scrib* (n=3), and *dlg* (n=2). Over 25 million reads were obtained per replicate. The coverage size is based on a 30 MB Drosophila transcriptome. Reads were considered 'non-aligned' if they had >2 mismatches relative to the reference genome, and 'low complexity' reads had multiple matches within the genome, reflecting sequencing reads from repeated DNA elements. The percentages refer to the relative number of reads for each category compared to the total number of reads.

	Total features	Genes with Mapped Reads	Differentially Expressed	Up-regulated	Down-regulated
white	15,494	11,025	N/A	N/A	N/A
scrib	15,494	10,870	1,181	676	505
dlg	15,494	11,270	828	440	388

Table 2.4: Number of Differentially Expressed Genes in *scrib* and *dlg* Tissues
Of the 15,494 total features in the Drosophila genome (version 5.25.62), ~70% of them have mapped reads in the transcriptome dataset. Unmapped features include genes not expressed in the wing disc as well as miRNA and rRNAs, which lack poly-A tails and were thus excluded during the mRNA purification prior to library construction. Of the mapped features, 1,181 (10.8%) and 828 (7.3%) were differentially expressed in *scrib* and *dlg* mutants, respectively.

Chapter 3

Coordination of apicobasal polarity determinants and chromatin-modifiers in epithelial tumor suppression

ABSTRACT

Forward genetic screens have implicated three major classes of genes –apicobasal polarity regulators, endocytic components, and chromatin-modifiers- as coordinators of epithelial architecture and proliferation in Drosophila. However, the relationship among these functionally diverse genes in tumor suppression remains unknown. Here, we provide evidence for the interaction of two such factors: the Scrib module, a core basal membrane determinant, and the Polycomb Group (PcG) complex, an epigenetic transcriptional repressor. Previous data demonstrated that the *unpaired* (*upd*) genes, which encode JAK-STAT pathway ligands, are direct PcG targets whose transcriptional upregulation triggers overgrowth when either the Scrib module or PcG genes are mutated [122]. Strikingly, we find that the Scrib module and PcG complex regulate *upd3* expression at a common *cis*-regulatory region. Functional assays indicate that growth of Scrib module mutant tissue is sensitive to PcG activity, and expression of PcG components is downregulated in polarity-deficient tumors. Transcriptome analysis of Scrib module and PcG deficient tissues show that these tumor suppressors co-regulate only a subset of PcG targets; Scrib module mutant tissues do not reflect a global loss of PcG function. Instead, our data suggest that a mild decrease in PcG activity upon Scrib module loss potentiates select targets for activation by polarity-responsive signaling pathways, including Jun kinase and Yorkie. Taken together, our data link the Scrib module and PcG function in tumor suppression through the regulation of mitogenic gene expression.

INTRODUCTION

Though DNA mutations play key roles in cancer progression, defective epigenetic regulation is also frequently observed in human tumors [123]. DNA methylation levels are reduced in colon cancer cells and alterations of histone modification patterns have been reported in several tumor types [124, 125]. Although these changes can affect specific genes, effectively substituting for mutations, they also alter global gene expression patterns, thereby broadly and coordinately influencing cell fate and differentiation. For example, the Polycomb Group (PcG) genes, epigenetic transcriptional silencers, normally repress pro-differentiation factors to insure stem cell maintenance; increased expression of PcG complex members is often associated with advanced tumor malignancy, perhaps through promoting a 'cancer stem cell' identity [126]. In other cases, however, PcG function may suppress tumor formation; mutations in PcG components lead to the expansion of hematopoietic stem cell populations [127]. Understanding the role of PcG and other epigenetic factors in tumorigenesis will require identifying the relevant target genes and the pathways regulating target selection. However, studying the function and targets of PcGs in cancer is difficult due to the multiplicity of PcG family members in mammals and heterogeneity of human tumor samples.

Much of our understanding of PcG function comes from work performed in Drosophila, where they were originally identified [128, 129]. In Drosophila, the PcG proteins form two evolutionarily conserved complexes, Polycomb Repressive Complex (PRC) 1 and 2. To silence gene expression, DNA binding proteins first recruit PRC2 to specific target genes. Once localized to the chromatin, the PRC2 subunit Enhancer of Zeste (E(z)) tri-methylates lysine 27 of histone H3. This epigenetic mark is subsequently recognized and bound by Polycomb (Pc), which recruits the remaining PRC1 members to suppress transcription [130, 131]. While PcG is traditionally known for maintaining cellular identity by repressing Hox gene expression, they target hundreds of other genes important for other decisions throughout development [132].

The recent and surprising discovery of PcG as potent Drosophila TSGs provides an opportunity to investigate the general role of PcG in organ growth and oncogenesis [122]. Similar to loss of Scrib module function, diminished PcG activity leads to dramatic overproliferation, polarity disruption, and a failure of the tissue to differentiate. The observation that PcG components are tumor suppressors indicates that PcG activity controls cell proliferation through transcriptional repression of downstream targets. Our previous work identified the *unpaired* (*upd*) genes as *bona fide* PcG targets whose derepression drives *PcG* mutant overgrowth [122]. Interestingly, in Chapter 2, I showed that the *upd*s are similarly upregulated in Scrib module mutant epithelia, and drive overproliferation through ectopic JAK-STAT activation. The revelation that PcG and Scrib module proteins share common downstream targets in tumor suppression raises the intriguing possibility that these distinct TSG classes act coordinately in a single pathway to control cell proliferation, differentiation and motility.

In this chapter, I investigate the relationship between the Scrib module and PcG in suppressing tumor formation. I provide evidence for the polarity-regulating and chromatin-modifying TSGs acting in concert. Scrib module tumor growth is sensitive to PcG activity, and the polarity-responsive enhancer of *upd3* is upregulated upon PcG loss. We detect transcriptional downregulation of PcG genes in Scrib module mutant tissue, linking polarity loss to decreased PcG activity. However, our data do not support a role for global derepression of PcG targets upon Scrib module loss. Instead, our results suggest that decreased PcG primes

select targets for activation by polarity-responsive effector pathways. Taken together, our work couples disorganization at the plasma membrane to misregulation of a global transcription regulator, leading to gene expression changes that drive tumorigenesis.

RESULTS

Molecular mapping of *Psc/Su(z)2* alleles

P3C was identified as a novel tumor suppressor allele in an unbiased genetic screen in Drosophila eye tissue [122]. Although *P3C* eye and wing discs form tumors in the absence of cell competition, lethal phase analysis revealed that homozygous *P3C* animals die as embryos (data not shown). Genetic mapping linked the mutation to a region containing the neighboring homologous PcG members, *Posterior sex combs* (*Psc*) and *Suppressor of zeste 2* (*Su(z)2*). Because loss of *Psc* or *Su(z)2* alone has no effect on tissue growth, we reasoned that *P3C* was likely a deletion of both genes. To molecularly map the deficiency breakpoints, we performed PCR on genomic DNA isolated from homozygous *P3C* embryos as well as embryos that were homozygous for *1b8*, a previously studied, but unmapped, *Psc/Su(z)2* allele [133]. The *P3C* mutation excises both *Psc* and *Su(z)2* as well as *CG33798*, a gene that lies between *Psc* and *Su(z)2* and is not conserved outside of Drosophila (Figure 3.1A). Strikingly, the *1b8* mutation not only removes *Psc*, *Su(z)2*, and *CG33798*, but also *Multidrug resistance 49* (*Mdr49*), *CG44251, CG44250, CG13321, CG13323, CG13324*, and *Derailed 2* (*Drl-2*) (Figure 3.1B). From these data, we conclude that *P3C* is a novel null allele of *Psc/Su(z)2*, and is better suited for studying PcG function than the *1b8* deficiency, which deletes seven additional genes.

Upd3.3LacZ is activated in Polycomb mutant tumors

Our subsequent work demonstrated that the PcG complex restricts epithelial growth by directly suppressing transcription of the *upd* ligands, *bona fide* PcG targets. Intriguingly, the *upd*s are similarly upregulated in *scrib* and *dlg* tissues, raising the possibility that the Scrib module and PcGs might coordinate to restrict mitogenic gene expression. We reasoned that if the Scrib module and PcGs act in concert to control downstream transcription, they would repress common *cis*-regulatory regions. Interestingly, the *upd3>GFP* and *upd3LacZ* reporters are upregulated in wing discs mutant for the functionally overlapping PcG members *polyhomeotic proximal* (*ph-p*) and *polyhomeotic distal* (*ph-d*), indicating that the *upd3* enhancer is sensitive to PcG activity (Figure 3.2) [92]. To determine if the Scrib module and PcGs repress common regulatory regions, we assessed activity of the polarity-responsive *upd3.3LacZ* reporter upon loss of *ph-p/ph-d* function. Expression of transgenic RNAi against *ph-p* and *ph-d* (*phIR*) promotes dramatic overgrowth and *Mmp1* upregulation, phenocopying *ph-p/ph-d* loss (Figure 3.3). Strikingly, *phIR* expression significantly activates *upd3.3LacZ*, but not other *upd3LacZ* subfragments (Figure 3.3A,D, data not shown). This response is identical to that observed in polarity-deficient tissues, consistent with the Scrib module and PcG acting in concert at common downstream target genes.

Our previous data indicated that JNK signaling is required for *upd3.3LacZ* expression upon Scrib module loss. To determine if JNK is also necessary for enhancer activation in PcG mutant tissues, we co-expressed Bsk^{DN} and *phIR*. As observed in Scrib module mutant tissues, inhibiting JNK suppresses *upd3.3LacZ* expression (Figure 3.3D,G). We note that, unlike *scrib,* tissue size is slightly reduced but blocking JNK does not completely restore normal growth and architecture upon PcG loss (Figure 3.3). Nevertheless, these data show that the PcGs and the Scrib module regulate activation of a common enhancer in a JNK-dependent manner, consistent with these TSGs coordinating to suppress mitogenic gene expression.

PcG/Trx components genetically interact with the Scrib module

To assess the functional significance of PcG activity in the Scrib module mutant phenotype, we used the genetic interaction assay described previously to assess the effect of reduced PcG function on hypomorphic *dlg* (*dlg*^{h321}) tissue. As a positive control, we used *dlgIR* to further deplete *dlg* levels in the *dlg*^{hf321} wing discs. Though it slightly reduces wild-type tissue size, mild *dlg* knockdown strongly enhances the growth and architectural defects in a *dlg*^{hf321} background (Figure 3.4). In a similar manner, reducing *ph-p* or *Su(z)2* to levels that have no effect on normal growth, significantly increases the size of *dlg*^{hf321} tissue (Figure 3.4). From these data, we conclude that *dlg* tumor growth is sensitive to PcG function, consistent with the Scrib module and PcG complex acting in a common regulatory pathway to modulate tissue growth.

We reasoned that if reduced PcG function contributes to overgrowth upon polarity loss, promoting PcG activity would decrease the size of Scrib module mutant tumors. To enhance PcG function in polarity-deficient tissues, we downregulated activity of the Trithorax (Trx) complex, a transcriptional activator that counters PcG-mediated repression [128]. Strikingly, expression of a dominant-negative form of the Trx component *Brahma* (*Brm*^{DN}) reduces the growth of *dlgIR*-expressing tissue (Figure 3.8B) [134]. Further, *upd3.3LacZ* expression is notably diminished in these tissues, indicative of restored PcG-mediated enhancer silencing (Figure 3.8C). We attribute the basal *Brm*-independent enhancer activity to JNK-mediated transcription, consistent with our previous demonstration that JNK signaling is sufficient to activate *upd3.3* (Figure 3.8D). Together, these data indicate that reduced PcG function upon Scrib module loss facilitates increased activation of polarity-responsive enhancers, promoting higher levels of mitogenic gene expression and tumor growth.

Scrib module and PcGs regulate common targets

Taken together, the above data suggest that the Scrib module and PcG complex act in concert to control tissue growth through the regulation of *upd3* transcription. To determine if these two TSG classes cooperate at additional targets to suppress neoplasia, we performed gene expression profiling of *Psc/Su(z)2* wing discs by RNA-Seq (Material and Methods). We identified 1256 genes that are differentially expressed at least twofold relative to wild-type (FDR<0.05), with 486 and 770 up- and down-regulated, respectively (Table 3.2). Given the canonical role of PcG as a transcriptional silencer, we focused on the upregulated genes as likely direct mediators of the neoplastic phenotype. The canonical PcG targets, the Hox genes *Abdominal-B* (*Abd-B*) and *Abdominal-A* (*Abd-A*), are upregulated >400-fold in *Psc/Su(z)2* tumors (Table 3.1). As expected from the known role of PcG activity in maintaining cell identity, the most highly enriched GO categories among the overexpressed targets are Embryonic Development and Regionalization (Figure 3.5) [132].

If the Scrib module and PcGs coordinately regulate PcG target transcription to suppress neoplasia, we would expect significant overlap of their gene expression profiles. Interestingly, comparing the Scrib module and PcG mutant transcriptomes revealed that nearly half of the genes upregulated upon polarity loss are overexpressed in PcG mutant tissues (Figure 3.6A). To identify PcG targets derepressed in the tumors, we juxtaposed the upregulated genes with loci identified in Pc binding profiles of thorasic imaginal discs [135]. Of the 639 direct PcG targets present in our transcriptome dataset, only 85 are significantly overexpressed in PcG mutant wing discs; 31 are derepressed in Scrib module tissue (Figure 3.7). Strikingly, however, 65% (20/31)

of the targets upregulated upon Scrib module loss are derepressed upon PcG loss- a highly significant enrichment (Figure 3.6B-C). Taken together, these data identify a subset of PcG targets that the Scrib module and PcGs co-regulate to prevent tumor formation.

PcGs expression and activity is downregulated in Scrib module tumors

We investigated one molecular mechanism that could link polarity maintenance to PcG activity. A prior publication demonstrated that JNK signaling induced by tissue wounding downregulates PcG expression, facilitating de-differentiation and regeneration [136]. Because JNK is activated upon polarity loss, we assessed PcG transcript levels in Scrib module mutant tissues. Strikingly, expression of the core PcG components, *ph-p*, *ph-d*, and *Su(z)2* is significantly reduced in *scrib* and *dlg* tumors (Figure 3.8). Significantly, the transcript levels measured upon Scrib module loss are nearly identical to those observed upon ectopic JNK activation [136]. These data demonstrate that loss of Scrib module activity decreases PcG expression, suggesting a mechanism linking polarity loss to the transcriptional derepression of PcG targets. Taken together, these data provide a molecular and functional link between polarity maintenance at the plasma membrane and the function of a global repressor of gene transcription.

DISCUSSION

Through this work, we provide evidence that the polarity-regulating and chromatin-modifying TSGs coordinately modulate transcription of select PcG targets to suppress epithelial tumor formation. We identify a specific *cis*-regulatory element at the *upd3* locus that is responsive to Scrib module and PcG activity. Further, functional assays demonstrate that growth of Scrib module mutant tumors is sensitive to PcG activity: knockdown of PcG components increases *dlg* tissue size, while blocking Trx activity suppresses overgrowth. Finally, gene expression data indicate that PcG components are transcriptionally downregulated in Scrib module mutant tissues, providing a molecular mechanism linking cell polarity regulators to PcG activity. However, transcriptome overlap of Scrib module and PcG mutant tissues do not reflect global derepression of PcG targets upon Scrib module loss. Instead, our data suggest that decreased PcG activity upon Scrib module loss potentiates activation of select target genes by polarity-responsive signaling pathways, such as JNK or Hippo. Taken together, our data support a model in which Scrib module proteins and the PcG complex coordinately silence select oncogenic targets to suppress tumor formation.

Interaction between the Scrib module and the PcGs

The Scrib module and PcG mutant phenotypes share a number of similarities, including disruption of epithelial organization, massive tissue overgrowth, and lethality upon transplant into a host. Strikingly, we also found significant overlap of their gene expression profiles- nearly half of the polarity-activated genes were also overexpressed in PcG mutant tissues. Furthermore, when we limited our analysis to putative direct PcG target genes, we found that 65% (20/31) of polarity-responsive targets are upregulated upon PcG loss. This significant enrichment provides evidence for co-regulation of select PcG targets by the Scrib module and PcG complex. However, 65 PcG targets, including the canonical target Hox genes *Abd-B* and *Abd-A*, are upregulated only in PcG mutant, and not in Scrib module mutant tissue. Further, we did not detect changes in total H3K27me3 levels in *scrib* discs (data not shown). These data rule out a global derepression of PcG targets in Scrib module mutant tissues, and suggest co-regulation of certain targets by these two distinct TSG classes.

How are the specific polarity-responsive PcG targets upregulated? Our functional and molecular experiments, which indicate a quantitative reduction of PcG function in Scrib module tissue, suggest a 'threshold model' in which downregulation of PcG activity synergizes with activation of polarity-responsive effector pathways, such as JNK and aPKC, to drive gene expression. In agreement with this view, many of the polarity-responsive PcG targets are activated by JNK, including the *upd*s, *Ets at 21C (Ets21C)*, an immune response gene, and *puckered* (*puc*), the JNK phosphatase [137, 138]. According to this model, the moderate decrease in PcG expression observed in Scrib module mutant tissue is not sufficient for global derepression of PcG targets, such as the Hox genes. Similarly, mild activation of polarity-responsive signaling pathways, such as JNK or aPKC, is insufficient to stimulate polarity- and PcG-responsive enhancers, as evidenced by the fact that expression of *eiger* or $aPKC^{CAAX}$ alone cannot activate *upd3.3LacZ*, as shown in Chapter 2. However, at select targets, such as the *upd*s, reduced PcG activity synergizes with JNK and aPKC signaling to drive transcription upon Scrib module loss. At these loci, reduced PcG activity may provide a permissive chromatin environment for JNK- and aPKC-dependent transcription factors to promote target upregulation.

Taken together, our data provide a model through which the Scrib module and PcGs interact to regulate transcription of specific mitogenic genes to suppress tumor formation.

Transcriptional profile of PcG mutant tissues

A common view of PcG activity is that its presence is necessary to prevent target gene expression. In this model, suggested by the paradigm of the Hox genes, loss of PcG expression is sufficient to derepress each direct target. Our analysis of the transcriptional profile of PcG mutant tissues revealed hundreds of misregulated target genes; however, only 13% (85/639) of direct PcG targets were upregulated in the tumors. This observation indicates that loss of PcG function alone is not sufficient to drive expression of many targets. It is likely that, for these loci, in addition to PcG derepression, specific activator proteins are necessary as well. Indeed, although *upd3* expression is highly elevated in PcG mutant tissue, activation of *upd3.3LacZ* upon *ph-p/ph-d* knockdown is JNK-dependent, and many upregulated PcG targets are downstream of JNK signaling, as discussed above. Our data provide support for studies which have shown that many canonical PcG targets, such as *engrailed* (*en*), exist in a 'void' state; they lack PcG binding and remain transcriptionally silent upon PcG knockdown [139]. Indeed, *en* expression is significantly downregulated in both Scrib module and PcG mutant tumors. Taken together, these data demonstrate that loss of PcG activity leads to the formation of an 'active' chromatin environment at target genes, but does not upregulate expression on its own.

Regulation of mitogenic gene expression

The observation that mitogenic target genes such as *upd* are controlled by multiple inputs- JNK, Hpo, and PcG- reflects their importance in the proper regulation of tissue growth. The tight control of JAK-STAT signaling ensures normal developmental cell proliferation, while preventing ectopic activity, which causes hyperplastic tumor formation [122]. However, upon loss of a single basolateral junctional scaffold component, *upd* transcription and JAK-STAT signaling are strongly activated. Why might transcription of these potent mitogenic targets be triggered by polarity loss? In Chapter 2, we suggested that polarity loss stimulates the same signaling events elicited upon tissue damage. Linking transcriptional control of mitogenic targets and PcG activity to polarity regulators allows the tissue to connect disturbances in tissue integrity to the activation of broader gene expression programs that promote cell proliferation and de-differentiation. Each of these responses is critical for regenerative growth and compensatory proliferation. By tying apicobasal polarity to the function of a single chromatin regulator, epithelial tissues trigger widespread transcriptional changes necessary for wound repair in a single step. However, as observed upon loss of Scrib module or PcG function, if these signals are unabated, they can lead to tumor formation. Therefore, these data linking apicobasal polarity to PcG activity provide further support to the model of cancer as a 'wound that never heals'.

MATERIALS AND METHODS

Fly Stocks

All flies were reared at 25°C. In addition to the stocks described in Chapter 2, Materials and Methods, the following additional flies were used: *FRT42 P3C* (*Psc/Su(z)2*), *FRT42 1b8* (*Psc/Su(z)2*), *isoFRT42*, *FRT42 XL26* (*Psc/Su(z)2*) [140], *UbxFLP; FRT42cL/CTG, FRT 19A* ph^{505}*/FM7c, cell-lethal ub-GFP FRT19A /FM6/Dp3560; UbxFLP/CyO*, *UAS-phIR* (*50028;* VDRC), *UAS-ph-pIR* (*10679*; VDRC), *UAS-Su(z)2IR* (*100096*; VDRC), *UAS-*Brm^{K804R} [134]

mRNA Purification, Sequencing, and Data Analysis

Iso42 (control) and *Psc/Su(z)2 [XL26]* mutant wing discs were generated using the *FLP/cell-lethal* system with *UbxFLP* (see stock list above). cDNA libraries for RNA-Seq were generated exactly as described in Chapter 2.

The libraries were sequenced by 50-bp single-end reads on the HighSeq2000 platform (Illumina). The reads were aligned to the *Drosophila melanogaster* reference genome (version 5.25.62) using Bowtie, allowing a maximum of two mismatches [120]. Downstream bioinformatic analysis of the sequencing reads was performed using Bowtie and DeSeq (UNION mode) as described in Chapter 2. Table 3.1 contains the sequencing and mapping statistics for each genotype, and Table 3.3 contains the number of differentially expressed genes [121]. Hyperbolic probability was used to calculate the P-values for the transcriptome overlap.

Mapping *Psc/Su(z)2* alleles

1b8 and *P3C* embryos were dechorionated in 50% bleach and washed in 1XPBS. Five homozygous mutant larvae and their cooresponding heterozygous siblings were collected and homogenized in 25 uL of Squishing Buffer (10mM Tris pH8.0, 1mM EDTA, 25mM NaCl) and 0.2uL of Proteinase K (Thermo-Scientific). PCR was performed using *Taq* polyermase (NEB) on 1 uL of embryonic extract in a 25uL PCR reaction. The presence or absence of product in the mutant samples was used to map the deletion breakpoints. Primers are available upon request.

Immunohistochemistry and Imaging

The same dissection, fixation, and staining protocols described in Chapter 2, Materials and Methods were used. Unless noted in the figure, the transgenes were expressed under the control of the wing pouch driver, *ms1096*. All of the antibodies used were listed in Chapter 2, Materials and Methods. Images were taken with the Leica LCS or Zeiss LSM700, and processed in Adobe Illustrator CS2 (12.0.1).

Fluorescence Activated Cell Sorting Analysis

The FACS sample preparation protocol was the same as described in Chapter 2, Material and Methods. Briefly, at least 10 wing imaginal discs of each genotype were dissected in 1XPBS and washed to remove trachea and fat body. The same flow cytometer (EPICS XL flow cytometer (Beckman-Coulter)) and gate settings were used, as described in Chapter 2, Materials and Methods. At least 3 biological replicates were obtained per genotype, and a two-tailed Student's T-test was used to calculate the P-value.

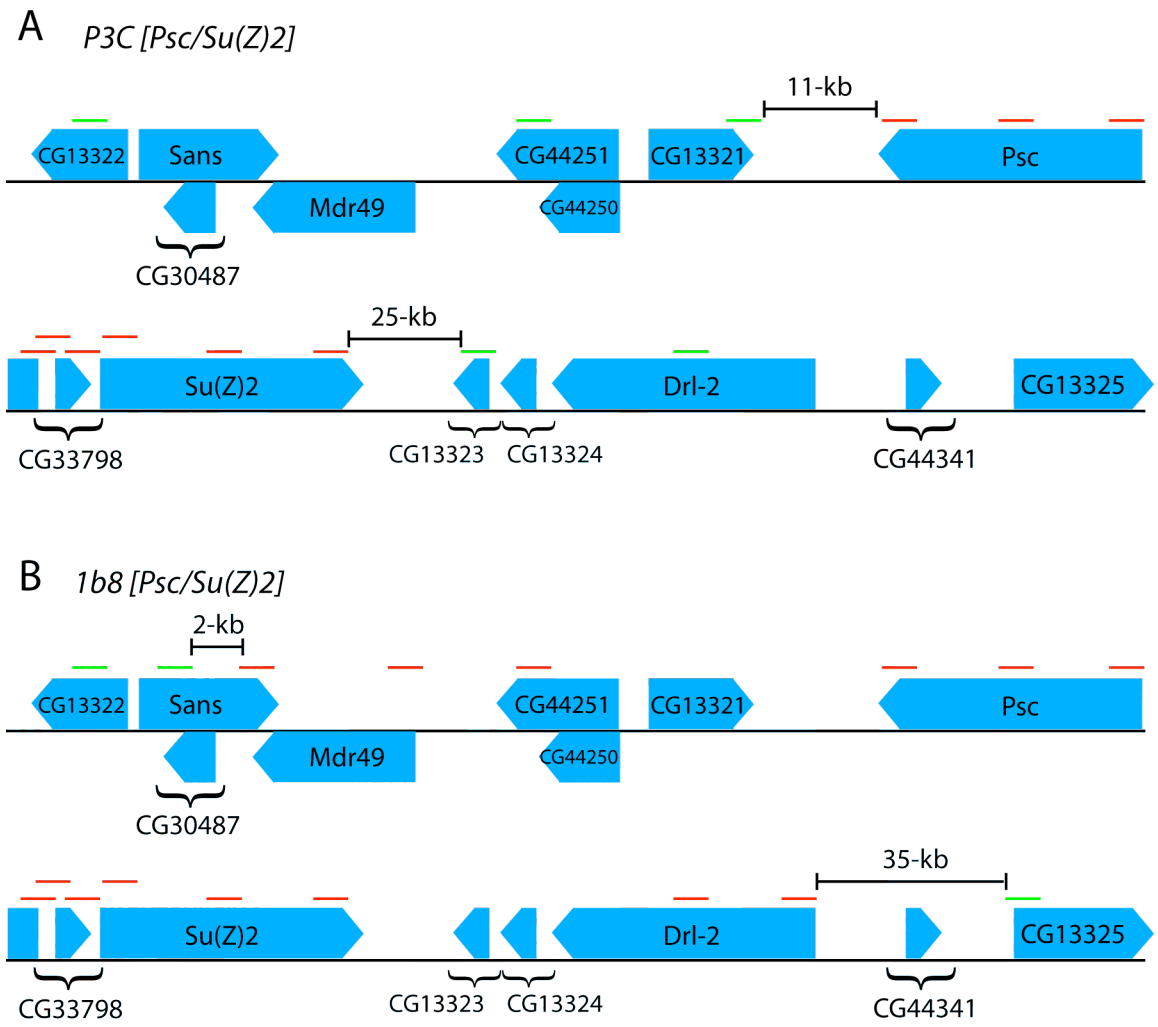

Figure 3.1: Molecular Mapping of the *P3C* and *1b8* Alleles
P3C deletes the neighboring homologous PcG components *Psc* and *Su(z)2*, as well as *CG33798* (A). However, *1b8* removes not only *Psc*, *Su(z)2* and *CG33798* but also *Multidrug resistance 49* (*Mdr49*), *CG44251, CG44250, CG13321, CG13323, CG13324*, and *Derailed 2* (*Drl-2*) (B). A red line above the schematic indicates the lack of PCR product; green line indicates the presence of product.

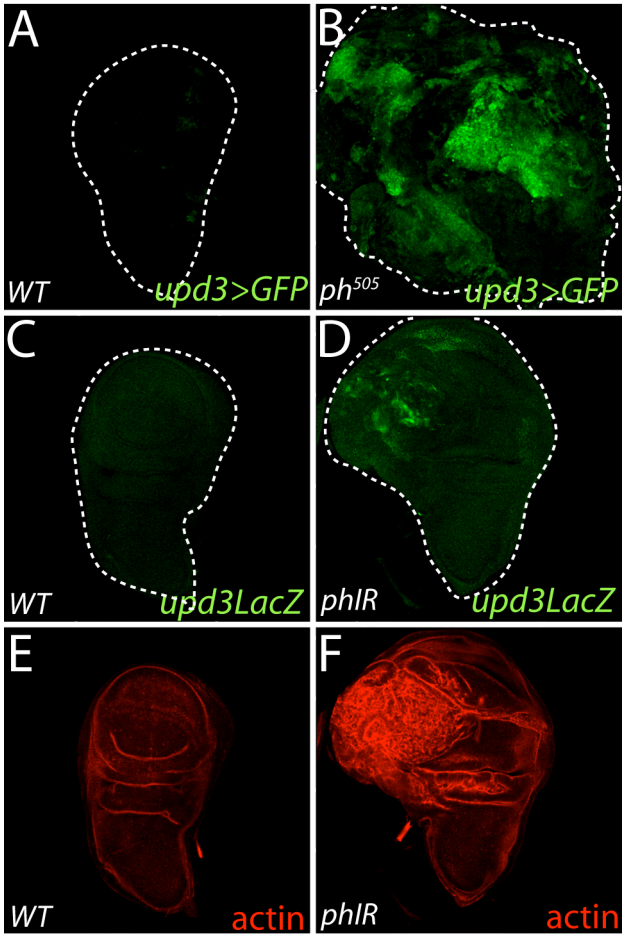

Figure 3.2: *Upd3>GFP* and *upd3LacZ* are Sensitive to PcG Activity
The *upd3>GFP* reporter is strongly activated in *ph* mutant discs (B), relative to wild-type (A). Similarly, knockdown of *ph-p*/*ph-d* in the wing pouch leads to upregulation of *upd3LacZ* (D) and overgrowth (F) relative to wild-type (C,E). Note that *upd3LacZ* expression is only observed where *phIR* is expressed by *ms1096GAL4*.

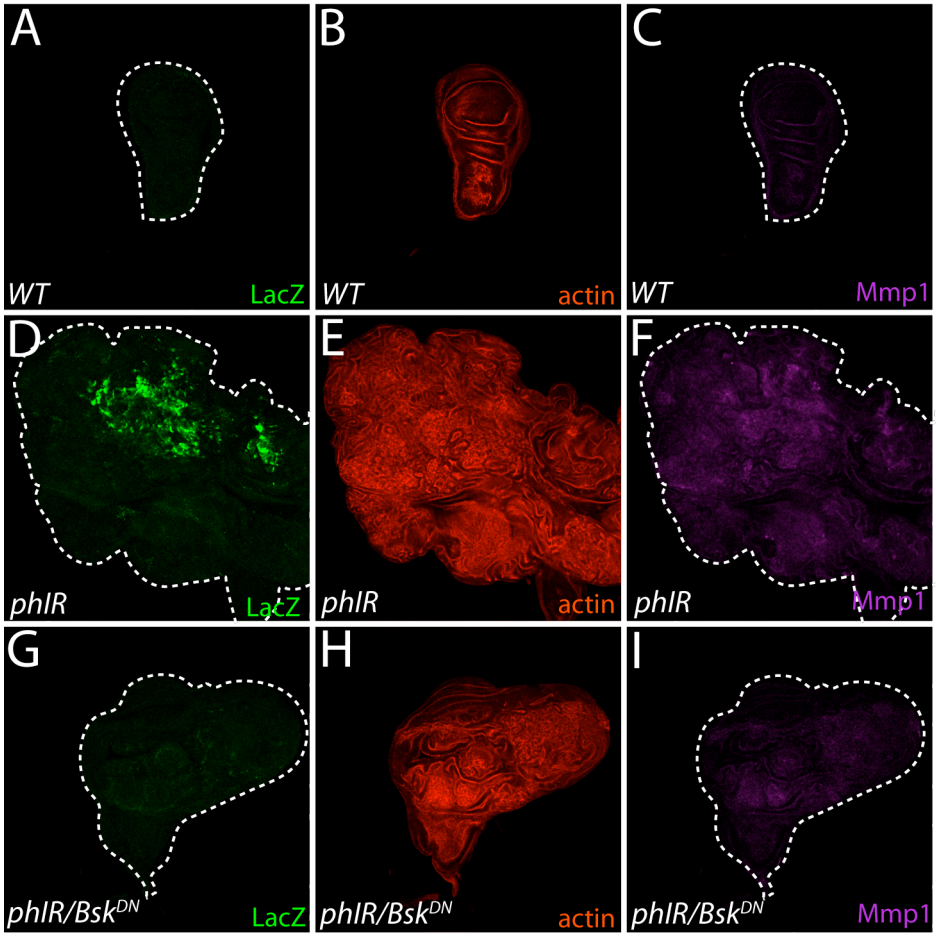

Figure 3.3: *Upd3.3LacZ* is Activated upon PcG Loss, in a JNK-Dependent Manner
Wild-type discs display normal architecture (B), and do not express *upd3.3LacZ* (A) or *Mmp1* (C). Expression of RNAi against the PcG components *ph-p* and *ph-d* leads to massive overgrowth and architecture defects (E), *upd3.3LacZ* activation (D), and mild *Mmp1* expression (F). Co-expression of Bsk^{DN}, suppresses *upd3.3LacZ* activation (G) and *Mmp1* upregulation (I), but is unable to completely restore normal growth and architecture (H).

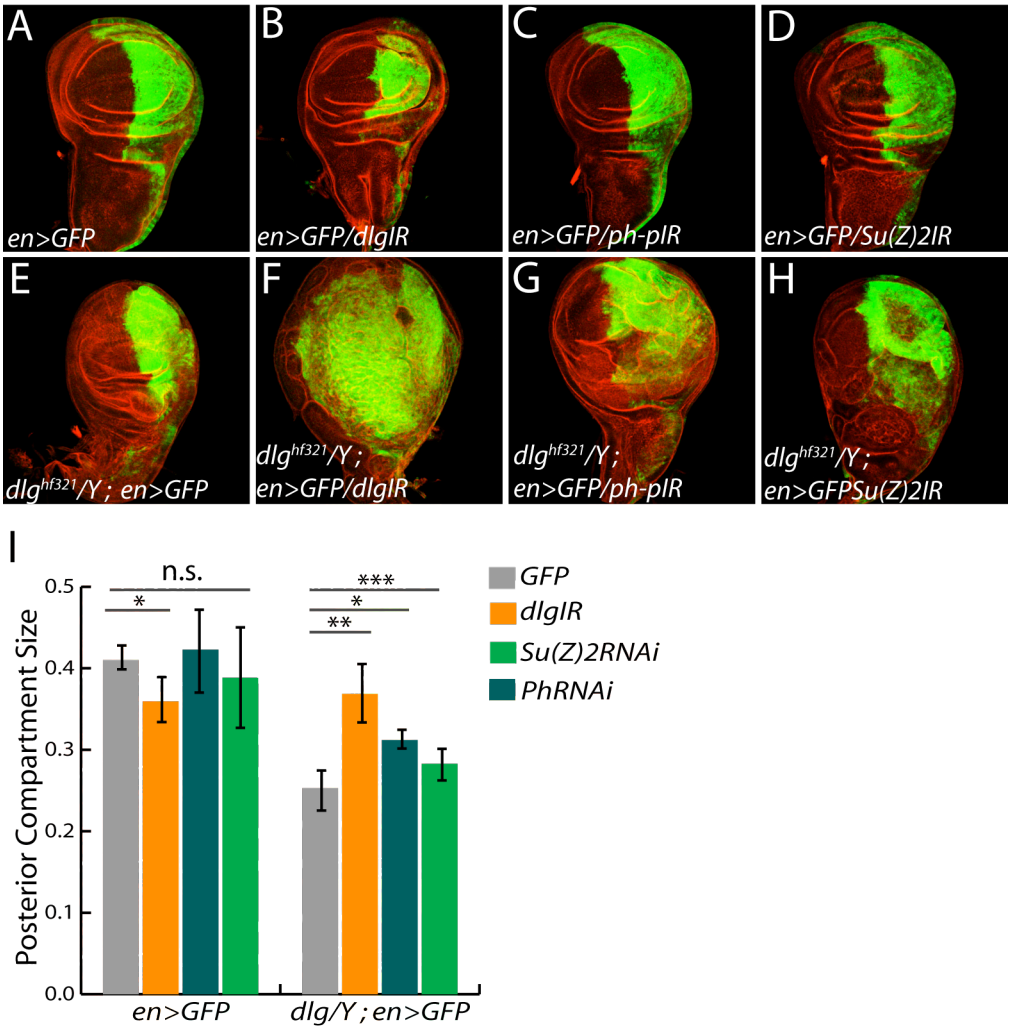

Figure 3.4: Growth of *dlg* Tissue is Sensitive to Levels of PcG Activity
Expression of *dlgIR* slightly reduces normal growth (A,B), but strongly enhances the overgrowth and architecture defects of *dlg* tissue (E,F,I). Likewise, knockdown of *ph-p* or *Su(z)2* to levels that have little effect on wild-type growth (C,D), increase the posterior compartment size of *dlg* tissue (G,H,I). Quantification is shown in I. (*$p < 0.05$; **$p < 0.0001$; ***$p < 0.00001$)

GO Categories: Upregulated Genes	P-value
Embryonic Development	1.62e-11
Regionalization	4.34e-9
Multicellular Organ Development	3.36e-8
Immune System Process	3.62e-7
Nervous System Development	1.99e-6
Defense Response	1.33e-5
Gut Development	1.77e-5
Regulation of Transcription	1.77e-5
Response to Stimulus	0.000210
Macromolecule Metabolic Process	0.000241

Figure 3.5: GO Term Analysis of Genes Upregulated in *Psc/Su(z)2* Tissues
GOstat analysis of targets upregulated in PcG mutant tumors reveals enrichment of genes involved in differentiation, as well as immune/stress response.

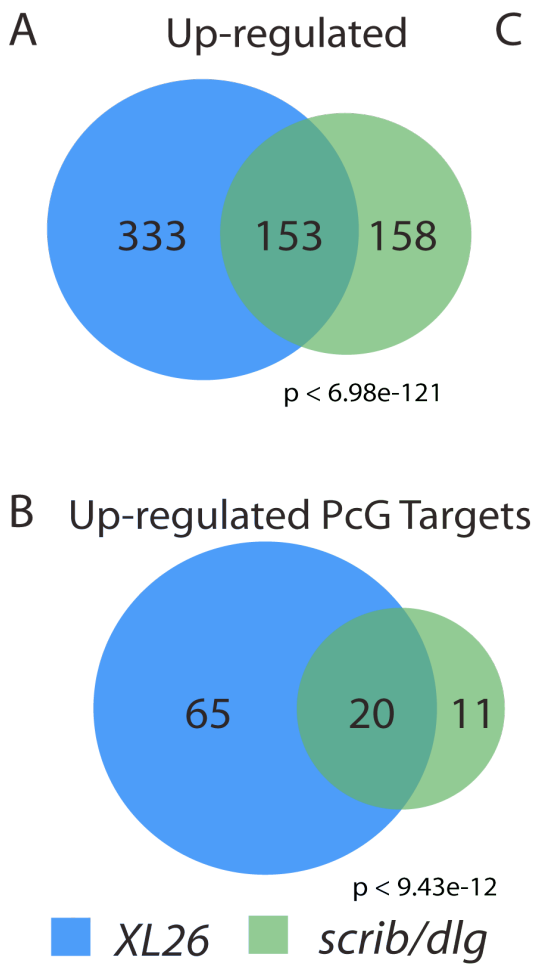

C

Gene	Description
lz	Hemocyte differentiation; eye development
ImpL3	Lactate dehydrogenase
upd2	JAK-STAT ligand; cell proliferation
Scr	Segment identity
Ets21C	Immune/stress response
upd3	JAK-STAT ligand; cell proliferation
chinmo	JAK-STAT target; growth & stem cell division
Poxm	Mesoderm development
nAcRBeta-21C	Neurotransmitter-gated ion channel
Rcd2	Centriole duplication
gol	Mesoderm development
os	JAK-STAT ligand; cell proliferation
CG3835	FAD-linked dehydrogenase
unpg	Tracheal branching
CG7800	Unknown function
CG10200	Unknown function
rempA	Cilia/flagella assembly
scb	Integrin
CG17129	Unknown function
puc	JNK phosphatase

Figure 3.6: Transcriptome Overlap of Scrib Module and PcG Mutant Tissues
Comparison of genes upregulated in *Psc/Su(z)2* and Scrib module mutant tissues demonstrates significant overlap (A). Differentially expressed genes are misregulated at least 2-fold relative to wild-type (FDR < 0.05). Analysis of PcG targets derepressed in PcG and Scrib module mutant tissues reveals 20 common targets, a statistically significant overlap (B). Each of the targets, along with a brief description, is listed in C.

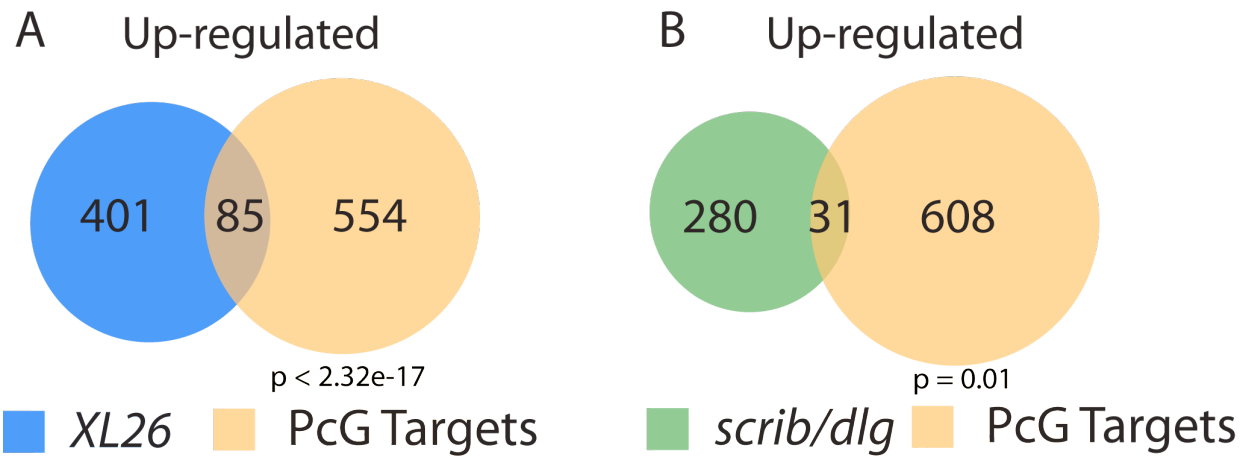

Figure 3.7: PcG Targets Upregulated in *Psc/Su(z)2* and Scrib Module Mutant Tissues
Of the 639 PcG target genes present in the transcriptome dataset, 85 are upregulated in PcG mutant tissues (A), while 31 are upregulated in Scrib module mutant tissues (B). Each overlap is statistically significant.

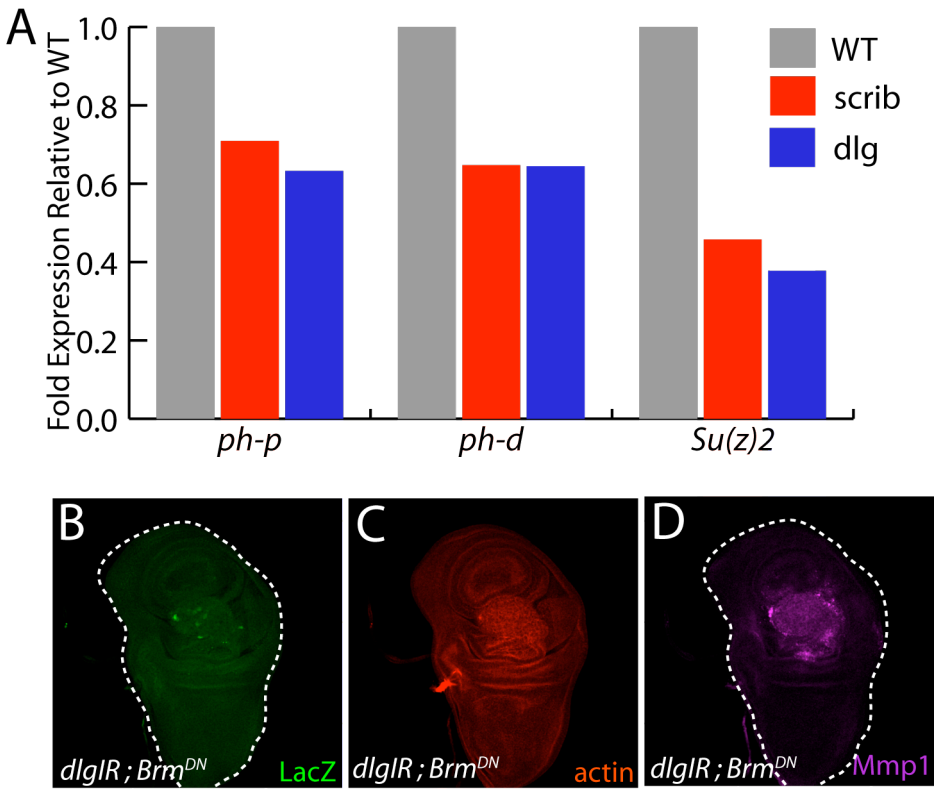

Figure 3.8: PcGs are Transcriptionally Downregulated upon Polarity Loss
The PcGs *ph-p*, *ph-d*, and *Su(z)2* are significantly downregulated in both *scrib* and *dlg* tissues (A). Expression of Brm^{DN} to reduce Trx complex function reduces both *upd3.3LacZ* activation (B), and *dlg-IR*-mediated overgrowth (C), but not *Mmp1* expression (D).

Flybase ID	Gene Name	WT RPKM	Psc/Su(z)2 RPKM	Fold Change	P-value	Notes
FBgn0014143	**croc**	**0.000**	**476.277**	**Inf**	**9.55E-15**	**Transcription Factor-Development**
FBgn0019809	gcm2	0.000	133.126	Inf	1.75E-08	**Transcription Factor-Fate Specification**
FBgn0051157	CG31157	0.000	25.952	Inf	2.04E-07	Unknown
FBgn0033592	CG13215	0.000	6.540	Inf	0.004139555	Unknown
FBgn0033065	**Cyp6w1**	**0.000**	**41.632**	**Inf**	**0.004954457**	**Cytochrome/ Oxidoreductase-**
FBgn0262476	CG43066	0.000	14.284	Inf	0.011003986	Neurotransmitter transporter
FBgn0030544	CG13403	0.000	145.123	Inf	0.011140134	Unknown
FBgn0020617	**Rx**	**0.000**	**36.818**	**Inf**	**0.015875121**	**Hox- Fate Specification**
FBgn0019650	**toy**	**0.000**	**34.341**	**Inf**	**0.017767432**	**Hox- Fate Specification**
FBgn0040318	**HGTX**	**0.000**	**114.009**	**Inf**	**0.017917925**	**Hox- Fate Specification**
FBgn0083951	CG34115	0.000	15.174	Inf	0.030062652	Unknown
FBgn0036324	CG12520	0.000	8.441	Inf	0.048071444	Unknown
FBgn0039683	**dmrt99B**	**0.322**	**1430.362**	**4436.897**	**4.35E-55**	**Immune response**
FBgn0039937	fd102C	0.322	532.296	1651.150	6.84E-31	Transcription Factor
FBgn0000606	**eve**	**0.322**	**364.758**	**1131.458**	**2.13E-21**	**Segmenation/patterning**
FBgn0051481	**pb**	**4.235**	**3035.309**	**716.705**	**8.65E-43**	**Hox- Fate Specification**
FBgn0015714	**Cyp6a17**	**4.690**	**2868.308**	**611.585**	**1.18E-23**	**Cytochrome/ Oxidoreductase**
FBgn0053965	CG33965	0.322	172.422	534.841	2.47E-05	Unknown
FBgn0263610	msa	2.667	1197.872	449.085	5.05E-54	Unknown
FBgn0000015	Abd-B	19.696	8763.958	444.960	1.44E-19	**Hox- Fate Specification**
FBgn0000014	abd-A	5.423	2364.281	435.969	9.79E-85	**Hox- Fate Specification**
FBgn0004795	retn	10.126	3844.940	379.701	1.05E-101	Neuronal development
FBgn0001325	**Kr**	**1.011**	**366.689**	**362.592**	**0.01238963**	**Segmentation/patterning**
FBgn0036690	**CG14059**	**28.431**	**8613.299**	**302.952**	**1.60E-30**	**dilp8- Dev. delay**
FBgn0263511	**Vsx1**	**0.645**	**163.821**	**254.081**	**6.37E-05**	**Hox- Fate Specification**

Table 3.1: *Psc/Su(z)2* Transcriptome
Table of the top 25 most highly upregulated genes in *Psc/Su(z)2* mutant tissues. We focused on the overexpressed genes, given the role of the PcGs as transcriptional repressors. The normalized expression level for each gene is quantified as 'Reads per Kilobase gene length per million reads' (RPKM), and fold change refers to expression level in *Psc/Su(z)2* tissue relative to wild-type. Descriptions of the genes are listed on the right-most column, and genes of particular interest in the tumorigenic phenotype are in bold. The entire list of genes differentially expressed in *Psc/Su(z)2* tissues can be found at: http://mcb.berkeley.edu/labs/bilder/brandon/Table3.1_PscSuZ2.xlsx

	Total Reads	Mapped Reads	Coverage	Non-aligned reads	Low Complexity Reads
iso42	123,348,015	72,297,417 (58.61%)	120X	49,848,410 (40.41%)	1,202,188 (0.97%)
Psc/Su(z)2	117,522,850	88,158,960 (75.01%)	146X	25,180,364 (21.43%)	4,183,526 (3.56%)

Table 3.2: RNA-Seq Sequencing Statistics
Table of combined number of 50-bp single-end sequencing reads for *iso42* (n=2), and *Psc/Su(z)2* (n=2). Over 40 million reads were obtained per replicate. The coverage size is based on a 30 MB Drosophila transcriptome. Reads were considered 'non-aligned' if they had >2 mismatches relative to the reference genome, and 'low complexity' reads had multiple matches within the genome, reflecting sequencing reads from repeated DNA elements. Percentages listed refer to the number of reads for each category relative to the total number of reads.

	Total features	Genes with Mapped Reads	Differentially Expressed	Up-regulated	Down-regulated
iso42	15,494	10,152	N/A	N/A	N/A
Psc/Su(z)2	15,494	9,683	1,256	486	770

Table 3.3: Number of Differentially Expressed Genes in *Psc/Su(z)2* Tissues
Of the 15,494 features in the Drosophila genome (version 5.25.62), 62% of them have mapped reads in the transcriptome dataset. Unmapped features include genes not expressed in the wing disc, as well as miRNA and rRNAs, which lack poly-A tails and were thus excluded during the mRNA purification prior to library construction. Of the mapped features, 1,256 (12.9%) were differentially expressed in *Psc/Su(z)2* mutants.

REFERENCES

1. Tyler S: **Epithelium--the primary building block for metazoan complexity.** *Integr. Comp. Biol.* 2003, **43**:55–63.
2. Fahey B, Degnan BM: **Origin of animal epithelia: insights from the sponge genome**. *Evolution & Development* 2010, **12**:601–617.
3. Bryant DM, Mostov KE: **From cells to organs: building polarized tissue**. *Nat Rev Mol Cell Biol* 2008, **9**:887–901.
4. Barnes AP, Polleux F: **Establishment of Axon-Dendrite Polarity in Developing Neurons**. *Annu. Rev. Neurosci.* 2009, **32**:347–381.
5. Yeaman C, Grindstaff KK, Nelson WJ: **New perspectives on mechanisms involved in generating epithelial cell polarity.** *Physiol. Rev.* 1999, **79**:73–98.
6. Müller HAJ, Bossinger O: **Molecular networks controlling epithelial cell polarity in development**. *Mechanisms of Development* 2003, **120**:1231–1256.
7. Tepass U, Tanentzapf G, Ward R, Fehon R: **Epithelial cell polarity and cell junctions in Drosophila.** *Annu. Rev. Genet.* 2001, **35**:747–784.
8. Bilder D: **Epithelial polarity and proliferation control: links from the Drosophila neoplastic tumor suppressors**. *Genes & Development* 2004, **18**:1909–1925.
9. Mellman I, Nelson WJ: **Coordinated protein sorting, targeting and distribution in polarized cells**. *Nat Rev Mol Cell Biol* 2008, **9**:833–845.
10. Li R, Gundersen GG: **Beyond polymer polarity: how the cytoskeleton builds a polarized cell**. *Nat Rev Mol Cell Biol* 2008, **9**:860–873.
11. Knust E: **Composition and Formation of Intercellular Junctions in Epithelial Cells**. *Science* 2002, **298**:1955–1959.
12. Tepass U: **The Apical Polarity Protein Network in DrosophilaEpithelial Cells: Regulation of Polarity, Junctions, Morphogenesis, Cell Growth, and Survival**. *Annu. Rev. Cell Dev. Biol.* 2012, **28**:655–685.
13. Gibson MC, Perrimon N: **Apicobasal polarization: epithelial form and function**. *Current Opinion in Cell Biology* 2003, **15**:747–752.
14. Bulgakova NA, Knust E: **The Crumbs complex: from epithelial-cell polarity to retinal degeneration**. *J. Cell. Sci.* 2009, **122**:2587–2596.
15. Tepass U, Theres C, Knust E: **crumbs encodes an EGF-like protein expressed on apical membranes of Drosophila epithelial cells and required for organization of epithelia**. *Cell* 1990, **61**:787–799.
16. Wodarz A, Ramrath A, Grimm A, Knust E: **Drosophila atypical protein kinase C associates with Bazooka and controls polarity of epithelia and neuroblasts**. *The Journal of Cell Biology* 2000, **150**:1361–1374.
17. Lehman K, Rossi G, Adamo JE, Brennwald P: **Yeast homologues of tomosyn and lethal giant larvae function in exocytosis and are associated with the plasma membrane SNARE, Sec9.** *The Journal of Cell Biology* 1999, **146**:125–140.
18. Betschinger J, Mechtler K, Knoblich JA: **The Par complex directs asymmetric cell division by phosphorylating the cytoskeletal protein Lgl**. *Nature* 2003, **422**:326–330.
19. Bilder D, Perrimon N: **Localization of apical epithelial determinants by the basolateral PDZ protein Scribble**. *Nature* 2000, **403**:676–680.
20. Santoni M-J, Pontarotti P, Birnbaum D, Borg J-P: **The LAP family: a phylogenetic point of view**. *Trends in Genetics* 2002, **18**:494–497.

21. Pearson HB, Perez-Mancera PA, Dow LE, Ryan A, Tennstedt P, Bogani D, Elsum I, Greenfield A, Tuveson DA, Simon R, Humbert PO: **SCRIB expression is deregulated in human prostate cancer, and its deficiency in mice promotes prostate neoplasia**. *J. Clin. Invest.* 2011, **121**:4257–4267.
22. Martin-Belmonte F, Gassama A, Datta A, Yu W, Rescher U, Gerke V, Mostov K: **PTEN-Mediated Apical Segregation of Phosphoinositides Controls Epithelial Morphogenesis through Cdc42**. *Cell* 2007, **128**:383–397.
23. Whiteman EL, Fan S, Harder JL, Walton KD, Liu CJ, Soofi A, Fogg VC, Hershenson MB, Dressler GR, Deutsch GH, Gumucio DL, Margolis B: **Crumbs3 is Essential for Proper Epithelial Development and Viability**. *Molecular and Cellular Biology* 2013.
24. Dow LE, Brumby AM, Muratore R, Coombe ML, Sedelies KA, Trapani JA, Russell SM, Richardson HE, Humbert PO: **hScrib is a functional homologue of the Drosophila tumour suppressor Scribble**. *Oncogene* 2003, **22**:9225–9230.
25. Grifoni D, Garoia F, Schimanski CC, Schmitz G, Laurenti E, Galle PR, Pession A, Cavicchi S, Strand D: **The human protein Hugl-1 substitutes for Drosophila Lethal giant larvae tumour suppressor function in vivo**. *Oncogene* 2004, **23**:8688–8694.
26. Thomas U, Phannavong B, Müller B, Garner CC, Gundelfinger ED: **Functional expression of rat synapse-associated proteins SAP97 and SAP102 in Drosophila dlg-1 mutants: effects on tumor suppression and synaptic bouton structure**. *Mechanisms of Development* 1997, **62**:161–174.
27. Ogawa K, Medline A, Farber E: **Sequential analysis of hepatic carcinogenesis: the comparative architecture of preneoplastic, malignant, prenatal, postnatal and regenerating liver.** *Br. J. Cancer* 1979, **40**:782–790.
28. Huang L, Muthuswamy SK: **Polarity protein alterations in carcinoma: a focus on emerging roles for polarity regulators**. *Current Opinion in Genetics & Development* 2010, **20**:41–50.
29. Atwood SX, Li M, Lee A, Tang JY, Oro AE: **GLI activation by atypical protein kinase C ι/λ regulates the growth of basal cell carcinomas**. *Nature* 2013, **494**:484–488.
30. Nakagawa S, Huibregtse JM: **Human Scribble (Vartul) Is Targeted for Ubiquitin-Mediated Degradation by the High-Risk Papillomavirus E6 Proteins and the E6AP Ubiquitin-Protein Ligase**. *Molecular and Cellular Biology* 2000, **20**:8244–8253.
31. Zeitler J: **Domains controlling cell polarity and proliferation in the Drosophila tumor suppressor Scribble**. *The Journal of Cell Biology* 2004, **167**:1137–1146.
32. Hariharan IK, Bilder D: **Regulation of Imaginal Disc Growth by Tumor-Suppressor Genes in Drosophila**. *Annu. Rev. Genet.* 2006, **40**:335–361.
33. Brumby AM, Richardson HE: **scribble mutants cooperate with oncogenic Ras or Notch to cause neoplastic overgrowth in Drosophila**. *The EMBO Journal* 2003, **22**:5769–5779.
34. Nakajima Y-I, Meyer EJ, Kroesen A, McKinney SA, Gibson MC: **Epithelial junctions maintain tissue architecture by directing planar spindle orientation**. *Nature* 2013, **500**:359–362.
35. Bissell MJ, Rizki A, Mian IS: **Tissue architecture: the ultimate regulator of breast epithelial function**. *Current Opinion in Cell Biology* 2003, **15**:753–762.
36. Woodhouse E, Hersperger E, Shearn A: **Growth, metastasis, and invasiveness of Drosophila tumors caused by mutations in specific tumor suppressor genes.** *Dev. Genes Evol.* 1998, **207**:542–550.
37. Khan SJ, Bajpai A, Alam MA, Gupta RP, Harsh S, Pandey RK, Goel-Bhattacharya S, Nigam

A, Mishra A, Sinha P: **Epithelial neoplasia in Drosophila entails switch to primitive cell states**. *Proceedings of the National Academy of Sciences* 2013, **110**:E2163–E2172.
38. Pastor-Pareja JC, Wu M, Xu T: **An innate immune response of blood cells to tumors and tissue damage in Drosophila**. *Disease Models & Mechanisms* 2008, **1**:144–154.
39. Dunn GP, Bruce AT, Ikeda H, Old LJ, Schreiber RD: **Cancer immunoediting: from immunosurveillance to tumor escape.** *Nat. Immunol.* 2002, **3**:991–998.
40. Swann JB, Smyth MJ: **Immune surveillance of tumors**. *J. Clin. Invest.* 2007, **117**:1137–1146.
41. Cordero JB, Macagno JP, Stefanatos RK, Strathdee KE, Cagan RL, Vidal M: **Oncogenic Ras Diverts a Host TNF Tumor Suppressor Activity into Tumor Promoter**. *Developmental Cell* 2010, **18**:999–1011.
42. Swann JB, Vesely MD, Silva A, Sharkey J, Akira S, Schreiber RD, Smyth MJ: **Demonstration of inflammation-induced cancer and cancer immunoediting during primary tumorigenesis**. *Proceedings of the National Academy of Sciences* 2008, **105**:652–656.
43. Suzuki H, Asakawa A, Amitani H, Nakamura N, Inui A: **Cancer cachexia—pathophysiology and management**. *J Gastroenterol* 2013, **48**:574–594.
44. Willoughby LF, Schlosser T, Manning SA, Parisot JP, Street IP, Richardson HE, Humbert PO, Brumby AM: **An in vivo large-scale chemical screening platform using Drosophila for anti-cancer drug discovery**. *Disease Models & Mechanisms* 2013, **6**:521–529.
45. Dar AC, Das TK, Shokat KM, Cagan RL: **Chemical genetic discovery of targets and anti-targets for cancer polypharmacology**. *Nature* 2012, **486**:80–84.
46. DeBerardinis RJ, Cheng T: **Q's next: the diverse functions of glutamine in metabolism, cell biology and cancer**. *Oncogene* 2009, **29**:313–324.
47. Bin Zhao, Tumaneng K, Guan K-L: **The Hippo pathway in organ size control, tissue regeneration and stem cell self-renewal**. *Nature Publishing Group* 2011, **13**:877–883.
48. Kyriakis JM, Avruch J: **Mammalian MAPK Signal Transduction Pathways Activated by Stress and Inflammation: A 10-Year Update**. *Physiol. Rev.* 2012, **92**:689–737.
49. Ríos-Barrera LD, Riesgo-Escovar JR: **Regulating cell morphogenesis: The drosophila jun N-terminal kinase pathway**. *genesis* 2012, **51**:147–162.
50. Weston CR, Davis RJ: **The JNK signal transduction pathway**. *Current Opinion in Genetics & Development* 2002, **12**:14–21.
51. Sabapathy K: *Role of the JNK Pathway in Human Diseases*. 1st edition. Elsevier Inc; 2012, **106**:145–169.
52. Sluss HK, Han Z, Barrett T, Davis RJ, Ip YT: **A JNK signal transduction pathway that mediates morphogenesis and an immune response in Drosophila.** *Genes & Development* 1996, **10**:2745–2758.
53. Igaki T: **Correcting developmental errors by apoptosis: lessons from Drosophila JNK signaling**. *Apoptosis* 2009, **14**:1021–1028.
54. Igaki T, Pagliarini RA, Xu T: **Loss of Cell Polarity Drives Tumor Growth and Invasion through JNK Activation in Drosophila**. *Current Biology* 2006, **16**:1139–1146.
55. Uhlirova M, Jasper H, Bohmann D: **Non-cell-autonomous induction of tissue overgrowth by JNK/Ras cooperation in a Drosophila tumor model.** *Proceedings of the National Academy of Sciences* 2005, **102**:13123–13128.
56. Hui L, Zatloukal K, Scheuch H, Stepniak E, Wagner EF: **Proliferation of human HCC cells and chemically induced mouse liver cancers requires JNK1-dependent p21 downregulation**. *J. Clin. Invest.* 2008, **118**:3943–3953.

57. Cellurale C, Sabio G, Kennedy NJ, Das M, Barlow M, Sandy P, Jacks T, Davis RJ: **Requirement of c-Jun NH2-Terminal Kinase for Ras-Initiated Tumor Formation**. *Molecular and Cellular Biology* 2011, **31**:1565–1576.
58. Uhlirova M, Bohmann D: **JNK-and Fos-regulated Mmp1 expression cooperates with Ras to induce invasive tumors in Drosophila**. *The EMBO Journal* 2006, **25**:5294–5304.
59. Wu M, Pastor-Pareja JC, Xu T: **Interaction between RasV12 and scribbled clones induces tumour growth and invasion**. *Nature* 2010, **463**:545–548.
60. Ohsawa S, Sato Y, Enomoto M, Nakamura M, Betsumiya A, Igaki T: **Mitochondrial defect drives non-autonomous tumour progression through Hippo signalling in Drosophila**. *Nature* 2012, **490**:547–551.
61. Sun G, Irvine KD: **Ajuba Family Proteins Link JNK to Hippo Signaling**. 2013, **6**:ra81–ra81.
62. Zhu M, Xin T, Weng S, Gao Y, Zhang Y, Li Q, Li M: **Activation of JNK signaling links lgl mutations to disruption of the cell polarity and epithelial organization in Drosophila imaginal discs**. *Cell Research* 2010:242–245.
63. Colombani J, Andersen DS, Leopold P: **Secreted Peptide Dilp8 Coordinates Drosophila Tissue Growth with Developmental Timing**. *Science* 2012, **336**:582–585.
64. Garelli A, Gontijo AM, Miguela V, Caparros E, Dominguez M: **Imaginal Discs Secrete Insulin-Like Peptide 8 to Mediate Plasticity of Growth and Maturation**. *Science* 2012, **336**:579–582.
65. Igaki T, Kanda H, Yamamoto-Goto Y, Kanuka H, Kuranaga E, Aigaki T, Miura M: **Eiger, a TNF superfamily ligand that triggers the Drosophila JNK pathway.** *The EMBO Journal* 2002, **21**:3009–3018.
66. Tepass U: **The Apical Polarity Protein Network in Drosophila Epithelial Cells: Regulation of Polarity, Junctions, Morphogenesis, Cell Growth, and Survival**. *http://dx.doi.org/10.1146/annurev-cellbio-092910-154033*.
67. Atwood SX, Prehoda KE: **aPKC Phosphorylates Miranda to Polarize Fate Determinants during Neuroblast Asymmetric Cell Division**. *Current Biology* 2009, **19**:723–729.
68. Smith CA, Lau KM, Rahmani Z, Dho SE, Brothers G, She YM, Berry DM, Bonneil E, Thibault P, Schweisguth F: **aPKC-mediated phosphorylation regulates asymmetric membrane localization of the cell fate determinant Numb**. *The EMBO Journal* 2007, **26**:468–480.
69. Lee C-Y, Robinson KJ, Doe CQ: **Lgl, Pins and aPKC regulate neuroblast self-renewal versus differentiation**. *Nature Publishing Group* 2005, **439**:594–598.
70. Leong GR, Goulding KR, Amin N, Richardson HE, Brumby AM: **scribble mutants promote aPKC and JNK-dependent epithelial neoplasia independently of Crumbs**. *BMC Biol* 2009, **7**:62.
71. Rolls MM: **Drosophila aPKC regulates cell polarity and cell proliferation in neuroblasts and epithelia**. *The Journal of Cell Biology* 2003, **163**:1089–1098.
72. Rogulja D, Irvine KD: **Regulation of Cell Proliferation by a Morphogen Gradient**. *Cell* 2005, **123**:449–461.
73. Sun G, Irvine KD: **Regulation of Hippo signaling by Jun kinase signaling during compensatory cell proliferation and regeneration, and in neoplastic tumors**. *Developmental Biology* 2011, **350**:139–151.
74. Doggett K, Grusche FA, Richardson HE, Brumby AM: **Loss of the Drosophila cell polarity regulator Scribbled promotes epithelial tissue overgrowth and cooperation with oncogenic**

Ras-Raf through impaired Hippo pathway signaling. *BMC Developmental Biology* 2011, **11**:57.
75. Grzeschik NA, Parsons LM, Allott ML, Harvey KF, Richardson HE: **Lgl, aPKC, and Crumbs Regulate the Salvador/Warts/Hippo Pathway through Two Distinct Mechanisms**. *Current Biology* 2010, **20**:573–581.
76. Robinson BS, Huang J, Hong Y, Moberg KH: **Crumbs Regulates Salvador/Warts/Hippo Signaling in Drosophila via the FERM-Domain Protein Expanded**. *Current Biology* 2010, **20**:582–590.
77. Drubin DG, Nelson WJ: **Origins of cell polarity.** *Cell* 1996, **84**:335–344.
78. Suzuki T: **The apical localization of SGLT1 glucose transporter is determined by the short amino acid sequence in its N-terminal domain**. *European Journal of Cell Biology* 2001, **80**:765–774.
79. Muthuswamy SK, Xue B: **Cell Polarity as a Regulator of Cancer Cell Behavior Plasticity**. *Annu. Rev. Cell Dev. Biol.* 2012, **28**:599–625.
80. Wodarz A, Näthke I: **Cell polarity in development and cancer.** *Nat Cell Biol* 2007, **9**:1016–1024.
81. Zhan L, Rosenberg A, Bergami KC, Yu M, Xuan Z, Jaffe AB, Allred C, Muthuswamy SK: **Deregulation of Scribble Promotes Mammary Tumorigenesis and Reveals a Role for Cell Polarity in Carcinoma**. *Cell* 2008, **135**:865–878.
82. Tanentzapf G, Tepass U: **Interactions between the crumbs, lethal giant larvae and bazooka pathways in epithelial polarization**. *Nat Cell Biol* 2002, **5**:46–52.
83. Beissbarth T, Speed TP: **GOstat: find statistically overrepresented Gene Ontologies within a group of genes**. *Bioinformatics* 2004, **20**:1464–1465.
84. Castillejo-López C, Häcker U: **The serine protease Sp7 is expressed in blood cells and regulates the melanization reaction in Drosophila**. *Biochemical and Biophysical Research Communications* 2005, **338**:1075–1082.
85. Fossett N, Hyman K, Gajewski K, Orkin SH, Schulz RA: **Combinatorial interactions of serpent, lozenge, and U-shaped regulate crystal cell lineage commitment during Drosophila hematopoiesis**. *Proceedings of the National Academy of Sciences* 2003, **100**:11451–11456.
86. Landis GN, Abdueva D, Skvortsov D, Yang J, Rabin BE, Carrick J, Tavaré S, Tower J: **Similar gene expression patterns characterize aging and oxidative stress in Drosophila melanogaster**. *Proceedings of the National Academy of Sciences* 2004, **101**:7663–7668.
87. Sohal RS, Agarwal A, Agarwal S, Orr WC: **Simultaneous overexpression of copper-and zinc-containing superoxide dismutase and catalase retards age-related oxidative damage and increases metabolic potential in Drosophila melanogaster**. *Journal of Biological Chemistry* 1995, **270**:15671–15674.
88. Duttaroy A, Paul A, Kundu M, Belton A: **A Sod2 null mutation confers severely reduced adult life span in Drosophila**. *Genetics* 2003, **165**:2295–2299.
89. Callus BA, Mathey-Prevot B: **SOCS36E, a novel Drosophila SOCS protein, suppresses JAK/STAT and EGF-R signalling in the imaginal wing disc.** *Oncogene* 2002, **21**:4812–4821.
90. Woods DF, Bryant PJ: **Molecular cloning of the lethal(1)discs large-1 oncogene of Drosophila.** *Developmental Biology* 1989, **134**:222–235.
91. Buchon N, Broderick NA, Chakrabarti S, Lemaitre B: **Invasive and indigenous microbiota impact intestinal stem cell activity through multiple pathways in Drosophila**. *Genes & Development* 2009, **23**:2333–2344.
92. Agaisse H, Petersen U-M, Boutros M, Mathey-Prevot B, Perrimon N: **Signaling Role of**

Hemocytes in Drosophila JAK/STAT-Dependent Response to Septic Injury. *Developmental Cell* 2003, **5**:441–450.
93. Jiang H, Grenley MO, Bravo M-J, Blumhagen RZ, Edgar BA: **EGFR/Ras/MAPK Signaling Mediates Adult Midgut Epithelial Homeostasis and Regeneration in Drosophila**. *Stem Cell* 2011, **8**:84–95.
94. Loots GG, Ovcharenko I, Pachter L, Dubchak I, Rubin EM: **rVista for Comparative Sequence-Based Discovery of Functional Transcription Factor Binding Sites**. *Genome Research* 2002, **12**:832–839.
95. Shaulian E, Karin M: **AP-1 in cell proliferation and survival.** *Oncogene* 2001, **20**:2390–2400.
96. Ciapponi L: **Drosophila Fos mediates ERK and JNK signals via distinct phosphorylation sites**. *Genes & Development* 2001, **15**:1540–1553.
97. Siegrist SE, Haque NS, Chen C-H, Hay BA, Hariharan IK: **Inactivation of Both foxo and reaper Promotes Long-Term Adult Neurogenesis in Drosophila**. *Current Biology* 2010, **20**:643–648.
98. Perez-Garijo A, Shlevkov E, Morata G: **The role of Dpp and Wg in compensatory proliferation and in the formation of hyperplastic overgrowths caused by apoptotic cells in the Drosophila wing disc**. *Development* 2009, **136**:1169–1177.
99. Wu S, Liu Y, Zheng Y, Dong J, Pan D: **The TEAD/TEF Family Protein Scalloped Mediates Transcriptional Output of the Hippo Growth-Regulatory Pathway**. *Developmental Cell* 2008, **14**:388–398.
100. Oh H, Irvine KD: **In vivo analysis of Yorkie phosphorylation sites**. 2009, **28**:1916–1927.
101. Meister M, Lagueux M: **Drosophilablood cells**. *Cellular Microbiology* 2003, **5**:573–580.
102. Moreira S, Stramer B, Evans I, Wood W, Martin P: **Prioritization of Competing Damage and Developmental Signals by Migrating Macrophages in the Drosophila Embryo**. *Current Biology* 2010, **20**:464–470.
103. Niethammer P, Grabher C, Look AT, Mitchison TJ: **A tissue-scale gradient of hydrogen peroxide mediates rapid wound detection in zebrafish**. *Nature* 2009, **459**:996–999.
104. Palanker L, Tennessen JM, Lam G, Thummel CS: **Drosophila HNF4 Regulates Lipid Mobilization and β-Oxidation**. *Cell Metabolism* 2009, **9**:228–239.
105. Okamoto N, Nakamori R, Murai T, Yamauchi Y, Masuda A, Nishimura T: **A secreted decoy of InR antagonizes insulin/IGF signaling to restrict body growth in Drosophila**. *Genes & Development* 2013, **27**:87–97.
106. Teleman AA, Hietakangas V, Sayadian AC, Cohen SM: **Nutritional Control of Protein Biosynthetic Capacity by Insulin via Myc in Drosophila**. *Cell Metabolism* 2008, **7**:21–32.
107. Miao P, Sheng S, Sun X, Liu J, Huang G: **Lactate dehydrogenase a in cancer: A promising target for diagnosis and therapy**. *IUBMB Life* 2013, **65**:904–910.
108. Lunt SY, Vander Heiden MG: **Aerobic Glycolysis: Meeting the Metabolic Requirements of Cell Proliferation**. *Annu. Rev. Cell Dev. Biol.* 2011, **27**:441–464.
109. Janic A, Mendizabal L, Llamazares S, Rossell D, Gonzalez C: **Ectopic Expression of Germline Genes Drives Malignant Brain Tumor Growth in Drosophila**. *Science* 2010, **330**:1824–1827.
110. Razzell W, Wood W, Martin P: **Swatting flies: modelling wound healing and inflammation in Drosophila**. *Disease Models & Mechanisms* 2011, **4**:569–574.
111. Dvorak HF: **Tumors: wounds that do not heal: similarities between tumor stroma generation and wound healing**. *The New England journal of medicine* 1986, **315**:1650–1659.

112. Riss J: **Cancers as Wounds that Do Not Heal: Differences and Similarities between Renal Regeneration/Repair and Renal Cell Carcinoma**. *Cancer Research* 2006, **66**:7216–7224.
113. Missirlis F, Rahlfs S, Dimopoulos N, Bauer H, Becker K, Hilliker A, Phillips JP, Jäckle H: **A putative glutathione peroxidase of Drosophila encodes a thioredoxin peroxidase that provides resistance against oxidative stress but fails to complement a lack of catalase activity.** *Biol. Chem.* 2003, **384**:463–472.
114. Missirlis F, Phillips JP, Jäckle H: **Cooperative action of antioxidant defense systems in Drosophila.** *Current Biology* 2001, **11**:1272–1277.
115. Bach EA, Vincent S, Zeidler MP, Perrimon N: **A sensitized genetic screen to identify novel regulators and components of the Drosophila janus kinase/signal transducer and activator of transcription pathway.** *Genetics* 2003, **165**:1149–1166.
116. Bach EA, Ekas LA, Ayala-Camargo A, Flaherty MS, Lee H, Perrimon N, Baeg G-H: **GFP reporters detect the activation of the Drosophila JAK/STAT pathway in vivo**. *Gene Expression Patterns* 2007, **7**:323–331.
117. Weber U, Paricio N, Mlodzik M: **Jun mediates Frizzled-induced R3/R4 cell fate distinction and planar polarity determination in the Drosophila eye.** *Development* 2000, **127**:3619–3629.
118. Emoto K, Parrish JZ, Jan LY, Jan Y-N: **The tumour suppressor Hippo acts with the NDR kinases in dendritic tiling and maintenance**. *Nature* 2006, **443**:210–213.
119. Dalton JE, Fear JM, Knott S, Baker BS, McIntyre LM, Arbeitman MN: **Male-specific Fruitless isoforms have different regulatory roles conferred by distinct zinc finger DNA binding domains**. *BMC Genomics* 2013, **14**:1–1.
120. Langmead B, Trapnell C, Pop M, Salzberg SL: **Ultrafast and memory-efficient alignment of short DNA sequences to the human genome**. *Genome Biology* 2009, **10**:R25.
121. Anders S, Huber W: **Differential expression analysis for sequence count data**. *Genome Biology* 2010, **11**:R106.
122. Classen A-K, Bunker BD, Harvey KF, Vaccari T, Bilder D: **A tumor suppressor activity of Drosophila Polycomb genes mediated by JAK-STAT signaling**. *Nat Genet* 2009, **41**:1150–1155.
123. Iacobuzio-Donahue CA: **Epigenetic Changes in Cancer**. *Annu. Rev. Pathol. Mech. Dis.* 2009, **4**:229–249.
124. Feinberg AP, Vogelstein B: **Hypomethylation distinguishes genes of some human cancers from their normal counterparts.** *Nature* 1983, **301**:89–92.
125. Fraga MF, Ballestar E, Villar-Garea A, Boix-Chornet M, Espada J, Schotta G, Bonaldi T, Haydon C, Ropero S, Petrie K, Iyer NG, Pérez-Rosado A, Calvo E, Lopez JA, Cano A, Calasanz MJ, Colomer D, Piris MÁ, Ahn N, Imhof A, Caldas C, Jenuwein T, Esteller M: **Loss of acetylation at Lys16 and trimethylation at Lys20 of histone H4 is a common hallmark of human cancer**. *Nat Genet* 2005, **37**:391–400.
126. Richly H, Aloia L, Di Croce L: **Roles of the Polycomb group proteins in stem cells and cancer**. *Cell Death and Disease* 2011, **2**:e204–7.
127. Cales C, Roman-Trufero M, Pavon L, Serrano I, Melgar T, Endoh M, Perez C, Koseki H, Vidal M: **Inactivation of the Polycomb Group Protein Ring1B Unveils an Antiproliferative Role in Hematopoietic Cell Expansion and Cooperation with Tumorigenesis Associated with Ink4a Deletion**. *Molecular and Cellular Biology* 2008, **28**:1018–1028.
128. Ringrose L, Paro R: **Epigenetic Regulation of Cellular Memory by the Polycomb and**

Trithorax Group Proteins. *Annu. Rev. Genet.* 2004, **38**:413–443.
129. Lewis EB: **A gene complex controlling segmentation in Drosophila.** *Nature* 1978, **276**:565–570.
130. Schwartz YB, Pirrotta V: **Polycomb silencing mechanisms and the management of genomic programmes**. *Nat Rev Genet* 2007, **8**:9–22.
131. Schuettengruber B, Chourrout D, Vervoort M, Leblanc B, Cavalli G: **Genome Regulation by Polycomb and Trithorax Proteins**. *Cell* 2007, **128**:735–745.
132. Schwartz YB, Pirrotta V: **Polycomb complexes and epigenetic states**. *Current Opinion in Cell Biology* 2008, **20**:266–273.
133. Wu CT, Howe M: **A genetic analysis of the Suppressor 2 of zeste complex of Drosophila melanogaster.** *Genetics* 1995, **140**:139–181.
134. Elfring LK, Daniel C, Papoulas O, Deuring R, Sarte M, Moseley S, Beek SJ, Waldrip WR, Daubresse G, DePace A: **Genetic analysis of brahma: the Drosophila homolog of the yeast chromatin remodeling factor SWI2/SNF2**. *Genetics* 1998, **148**:251–265.
135. Kwong C, Adryan B, Bell I, Meadows L, Russell S, Manak JR, White R: **Stability and Dynamics of Polycomb Target Sites in Drosophila Development**. *PLoS Genet* 2008, **4**:e1000178.
136. Lee N, Maurange C, Ringrose L, Paro R: **Suppression of Polycomb group proteins by JNK signalling induces transdetermination in Drosophila imaginal discs**. *Nature* 2005, **438**:234–237.
137. Park JM: **Targeting of TAK1 by the NF- B protein Relish regulates the JNK-mediated immune response in Drosophila**. *Genes & Development* 2004, **18**:584–594.
138. McEwen DG: **Puckered, a Drosophila MAPK phosphatase, ensures cell viability by antagonizing JNK-induced apoptosis**. *Development* 2005, **132**:3935–3946.
139. Schwartz YB, Kahn TG, Stenberg P, Ohno K, Bourgon R, Pirrotta V: **Alternative Epigenetic Chromatin States of Polycomb Target Genes**. *PLoS Genet* 2010, **6**:e1000805.
140. Li X, Han Y, Xi R: **Polycomb group genes Psc and Su(z)2 restrict follicle stem cell self-renewal and extrusion by controlling canonical and noncanonical Wnt signaling**. *Genes & Development* 2010, **24**:933–946.